

Department Biologie II
Institut für Anthropologie und Humangenetik
der Ludwig-Maximilians-Universität München

Characterization of new interaction partners of the DNA double-strand break repair protein DNA-PKcs



Dissertation der Fakultät für Biologie
der Ludwig-Maximilians-Universität München
zur Erlangung des Doktorgrades der Naturwissenschaften

vorgelegt von
Thomas Wechsler
aus Spalt

Mai 2005

Diese Arbeit wurde am Department of Microbiology and Immunology der University of California San Francisco unter Anleitung von Dr. Matthias Wabl durchgeführt.

Eingereicht am: 23.05.2005

Erstgutachterin: Prof. Dr. E. H. Weiß

Zweitgutachterin: Prof. Dr. F. Eckardt-Schupp

Tag der mündlichen Prüfung: 18.08.2005

Table of contents

Table of contents

Abbreviations

1.	Summary	1
2.	Introduction	2
2.1.	Double-strand break repair in eukaryotes	2
2.1.1.	Homology-directed DSB repair	2
2.1.2.	DSB repair by DNA end joining	6
2.2.	The role of DNA-PKcs in nonhomologous end joining	8
3.	Specific aim: Characterization of PP5 and Kub3 as new interaction partners of DNA-PKcs	15
3.1.	Protein phosphatase 5 (PP5)	16
3.2.	Ku70 binding protein 3 (Kub3)	18
4.	Results	20
4.1.	DNA-PKcs function specifically regulated by protein phosphatase 5 (PP5)	20
4.1.1.	Overexpression of PP5 decreases phosphorylation of DNA-PKcs, but not of ATM	20
4.1.2.	Dominant negative and decreased expression of PP5 increase phosphorylation of DNA-PKcs	22
4.1.3.	Hypo- and hyperphosphorylation of DNA-PKcs do not alter the use of microhomology based repair	23
4.1.4.	Both hypo- and hyperphosphorylation increase radiation sensitivity	26
4.2.	Ku70 binding protein 3 (Kub3) is a putative metalloprotease and interacts with DNA-PKcs	28
4.2.1.	Human Kub3 is a protein of 246 amino acid residues with a highly conserved metalloprotease domain	28
4.2.2.	A polyclonal antibody against the Kub3 C-terminus recognizes a 29 kd protein and variants of similar size	32
4.2.3.	Kub3 is localized in the nucleus	35
4.2.4.	Kub3 co-precipitates with DNA-PKcs	36
4.2.5.	Kub3 does not redistribute after DNA damage	39
4.2.6.	Kub3 overexpression leads to increased DNA-PKcs T2609 phosphorylation	39
4.2.7.	RNAi and double-strand break repair in <i>Drosophila melanogaster</i>	41
4.2.8.	RNAi of DSB repair proteins in drosophila S2 cells	43
4.2.9.	Decreased expression of Blm and Rad54 but not of Kub3 increases radiation sensitivity in S2 cells	45

Table of contents

4.2.10. Decreased expression of Kub3 can not suppress the knock-down of homology directed DSB repair proteins in S2 cells	47
5. Discussion	49
5.1. DNA-PKcs function specifically regulated by protein phosphatase 5 (PP5)	49
5.1.1. Interaction of PP5 with DNA-PKcs	49
5.1.2. A cell cycle checkpoint role for DNA-PKcs	50
5.1.3. Regulation of DNA-PKcs and ATM by protein phosphatases	50
5.2. Ku70 binding protein 3 (Kub3) is a putative metalloprotease and interacts with DNA-PKcs	53
5.2.1. Characterization of Kub3 protein	53
5.2.2. Interaction of Kub3 with DNA-PKcs	54
5.2.3. Function of Kub3 in DSB repair	55
5.2.4. Alternative functions of Kub3	57
6. Materials and Methods	59
6.1. Cell lines, cell Culture and irradiation Treatments	59
6.2. Retroviral constructs and transduction	60
6.3. Whole cell lysates	60
6.4. Nuclear extracts	60
6.5. Western blotting	60
6.6. Co-Immunoprecipitation	61
6.7. Immunofluorescence	61
6.8. λ protein phosphatase (λ -PPase) treatment	62
6.9. Dik van Gent Assay	62
6.10. Flow cytometry survival assay	62
6.11. siRNA inhibition in HeLa cells	63
6.12. DsRNA inhibition in drosophila S2 cells	63
6.13. Quantitative RT-PCR (Taqman)	64
6.14. Bioinformatics resources	65
6.15. Instruments	65
7. Acknowledgements	66
8. Literature	67

Table of contents

Abbreviations

Abbreviations

ATM	Ataxia telangiectasia mutated protein
ATR	ATM-Rad3-related protein
BLAST	Basic local alignment search tool
DNA-PKcs	DNA-dependent protein kinase catalytic subunit
DNA-PK	DNA-dependent protein kinase; includes DNA-PKcs, Ku70 and Ku80
DSB	Double-strand break repair
EST	Expressed sequence tag
HR	Homologous recombination with Holliday junctions
NHEJ	Nonhomologous end joining
HRP	Horseradish peroxidase
IR	Ionizing radiation
Kub3	Ku70 binding protein 3
λ -PPase	λ protein phosphatase
MMS	Methyl methanesulfonate
M/R/N	Mre11/Rad50/Nbs1
NCBI	National center for biotechnology information
PNK	Polynucleotide kinase
PP5	Protein phosphatase 5
RDS	Radioresistant DNA synthesis
RNAi	RNA inhibition
SCID	Severe combined immunodeficiency
SDSA	Synthesis-dependent strand annealing
siRNA	small inhibitory RNA
SSA	Single-strand annealing
TPR	Tetratricopeptide repeat

1. Summary

Unrepaired DNA double-strand breaks can lead to apoptosis or tumorigenesis. In mammals double-strand breaks are repaired mainly by nonhomologous end joining mediated by the DNA-PK complex. The core protein of this complex, DNA-PKcs, is a DNA-dependent serine/threonine kinase that phosphorylates protein targets as well as itself.

To identify new proteins, which contribute to double-strand break repair by non-homologous end joining, we previously performed a yeast two-hybrid screen with fragments of human DNA-PKcs as bait. From the identified putative interaction partners of DNA-PKcs we chose two for further characterization: Protein phosphatase 5 (PP5) and Ku70 binding protein 3 (Kub3).

With PP5 we have identified the first protein phosphatase with a function in double-strand break repair. We show that protein phosphatase 5 interacts with DNA-PKcs and dephosphorylates with surprising specificity at least two functional sites of it. Cells with either hypo or hyperphosphorylation of DNA-PKcs at these sites show increased radiation sensitivity.

For the characterization of Kub3 we describe its correct reading frame and a putative metalloprotease domain. Using a rabbit polyclonal antibody against human Kub3 we demonstrate that Kub3 is a nuclear protein which co-precipitates with DNA-PKcs. When Kub3 is overexpressed in HeLa cells, DNA-PKcs phosphorylation at T2609 is increased after ionizing radiation. However, when Kub3 is knocked down in drosophila cells by RNAi, cell survival after ionizing radiation is not affected.

In summary, with PP5 and Kub3 we have characterized two new interaction partners of DNA-PKcs. While PP5 clearly functions in double-strand break repair, further experiments are necessary to confirm such a role for Kub3.

2. Introduction

2.1. Double-strand break repair in eukaryotes

Unrepaired DNA double-strand breaks (DSB) either trigger apoptosis or lead to genomic rearrangements, which in turn can lead to cancer. To fix DSBs, eukaryotic cells have several competing DSB repair pathways, which can be divided into two groups (Allen et al., 2002).

The first group employs DNA sequence homology either on the same chromatid, the sister chromatid or the homologous chromosome. These pathways allow the reconstitution of genetic information that may have been lost through the double-strand break. The second group relies on DNA end joining of the open DNA strands with no regards to the loss of genetic information during this process. By joining open DNA ends together quickly, these pathways prevent nucleolytic end digestion, chromosomal breakage and apoptosis triggered by open DNA ends.

2.1.1. Homology directed DSB repair

Homology directed DSB repair can further be divided into three pathways:

1. Single-strand annealing (SSA).
2. Synthesis-dependent strand annealing (SDSA).
3. Homologous recombination with Holliday junctions (HR).

In the following sections we describe models for these three pathways and the proteins implicated.

The first pathway is the single-strand annealing pathway (SSA) (Lin et al., 1984). The model for SSA explains how a double-strand break between two copies of homologous sequences on one DNA strand leads to the collapse of those two copies into only one copy of the sequence (Fig. 1). The sequence homology used for SSA ranges from 29 bp to 1 kb with an optimum around 400 bp (Sugawara et al., 2000). The current model for SSA suggests a 5' end nucleolytic resection step and subsequent annealing of both double strands on the opposite side of the double-strand break. This is followed by a DNA sequence homology search between the two strands. After such a sequence homology has been found, the non-pairing flapping DNA ends are cut off, and subsequent DNA synthesis and DNA ligation fill the remaining nicks (Paques and Haber, 1999). Little is known about the proteins involved in SSA, but factors such as Ligase III, FEN-1 and DNA polymerase ϵ have been implicated (Gottlich et al., 1998). It seems that SSA also requires a subset of the genes involved in homologous recombination such as Rad52, but not Rad51, Rad55, Rad57 and Blm (Ivanov et al., 1996; Preston et al., 2002). However, it is unclear if this pathway is of any biological relevance. The requirement of two adjacent copies of a similar sequence may seem artificial, but on the other hand the vast stretches of repetitive DNA in mammalian genomes could serve as a substrate for this pathway.

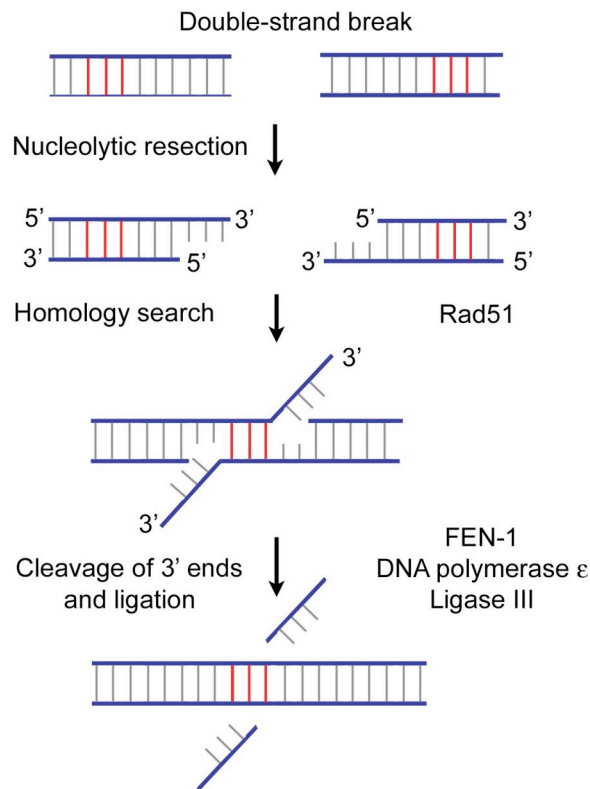


Figure 1. DSB repair by single-strand annealing (SSA)

In this model, after a DSB the 5' ends of the broken DNA strands are resected first. Then both strands are used to search for long homologous sequences (red) which can anneal, eventually. Afterwards, the nonhomologous 3' ends are cleaved and the remaining gaps are filled by DNA synthesis and ligation. The factors implicated in the respective steps of SSA are listed.

The second (SDSA) and third pathways (HR) are similar in the first steps of the repair process (Fig. 2.). After a DSB occurs, the ends of both DNA strands are resected, which results in ssDNA overhangs. This nucleolytic resection is presumably carried out by the Mre11/Rad50/Nbs1 (M/R/N) complex (West, 2003). Then, the 3' end of the first single strand of DNA associates with the recombinase Rad51 and invades the second copy of the gene (Sung, 1994); (Baumann et al., 1996). Apart from Rad51, the single strand invasion step also requires Rad52, Rad54 and RPA (Benson et al., 1998; Petukhova et al., 1999; Sung, 1997).

At this point the SDSA and the HR models diverge (Fig. 2.). In the synthesis-dependent annealing pathway (SDSA), the invaded gene copy serves as a template for short stretches of DNA synthesis (Nassif et al., 1994). The newly synthesized strand then dissociates from its template and tries to re-anneal with the broken complementary strand on the damaged chromatid (McVey et al., 2004b). After multiple cycles of this reaction, the new strand can eventually bridge the DSB and repair is finished by DNA synthesis and DNA ligation (McVey et al., 2004b).

Introduction – Double-strand break repair in eukaryotes

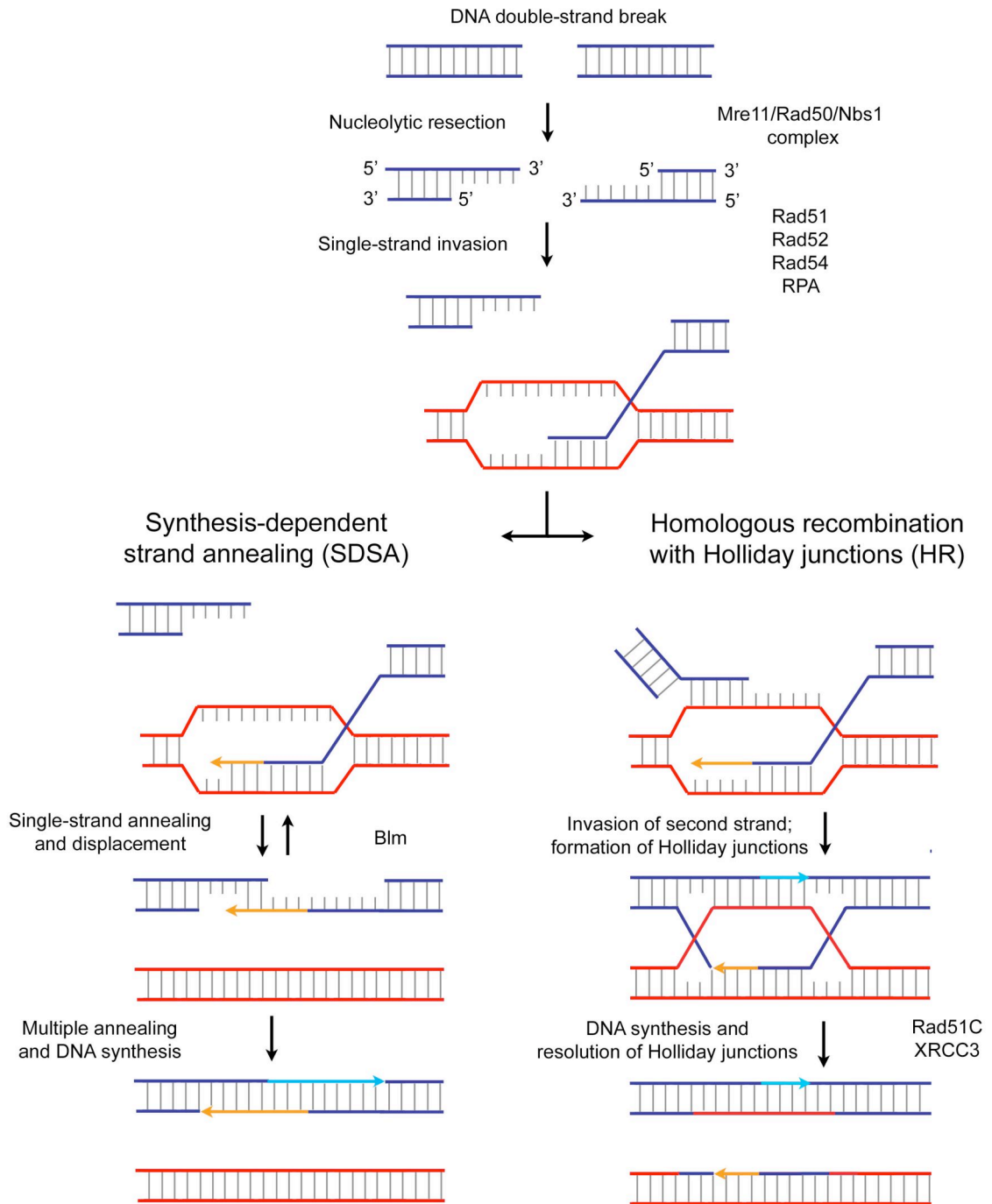


Figure 2. Homology-directed repair (modified after (McVey et al., 2004b); (West, 2003))

After a DSB occurs in the acceptor strand (blue), it can be repaired by SDSA or HR using the homologous donor strand (red). According to this model both pathways share the initial steps of the process and then continue to repair the DNA differently. In summary, SDSA occurs by one single-strand invasion step and one single-strand annealing step while in HR two single-strand invasion steps are necessary. In both cases DNA synthesis (bright blue/orange) is required for the process. The factors implicated in the respective steps of SDSA and HR are listed.

The SDSA pathway was characterized first in *Drosophila melanogaster* using P-element excision repair (Nassif et al., 1994). For this pathway the drosophila ortholog of the mammalian Blm protein, which is encoded by the Mus309 locus, is essential (Adams et al., 2003; Kusano et al., 2001). Also, flies bearing a mutation in Mus309 have increased sensitivity towards methyl methanesulfonate (MMS) and ionizing radiation (IR) (Boyd and Harris, 1981; Kooistra et al., 1999). McVey and colleagues recently suggested a model where Blm displaces the DNA strand after DNA synthesis and is therefore needed to initiate multiple annealing cycles (McVey et al., 2004b).

While Blm acts downstream of the single-strand invasion step, several proteins involved in this initial step have an impact on SDSA as well. For example, Rad51 is needed for P-element excision repair by SDSA (McVey et al., 2004a); and the drosophila ortholog of Rad54 has a role in SDSA and DSB repair after IR (Kooistra et al., 1999; Kooistra et al., 1997). Interestingly, Rad54 mutant flies show higher radiation sensitivity than Mus309/Blm mutant flies, while double mutants show an additive effect (Kooistra et al., 1999).

The third pathway is the classic homologous recombination pathway (HR), also referred to as gene conversion with cross-over or Holliday junctions, respectively. After initial single-strand invasion, the prototypic break-repair model described by Frank Stahl and colleagues suggests that the second ssDNA also invades the donor locus (Fig. 2.) (Szostak et al., 1983). Subsequent chromatin acrobatics result in two cross-over structures or Holliday junctions. Branch migration combined with DNA synthesis lead to the continued exchange of sequences between both gene copies. Finally, the cross-over structures are resolved and the open gaps are filled and ligated (West, 2003).

In this well-characterized pathway many steps have been linked to the activity of several major DNA repair genes. As mentioned before, the initial single strand invasion is promoted by Rad51, Rad52, RPA and RAD54 (West, 2003). Other proteins that have been localized to sites of HR repair include BRCA1, BRCA2 and FANCD2 (Scully et al., 1997); (Chen et al., 1998b; Garcia-Higuera et al., 2001). The mammalian resolvase activity, for years the elusive holy grail of DNA repair, has been recently attributed to the RAD51 paralogs RAD51C and XRCC3 (Liu et al., 2004). Nevertheless, it is not clear what additional factors are needed for branch migration and resolution of Holliday junctions (Liu et al., 2004).

2.1.2. DSB repair by DNA end joining

DNA end joining can be divided into microhomology based end joining and non-homologous end joining. The microhomology based end joining pathway also termed B-NHEJ (as in backup NHEJ), occurs mostly in the absence of the more faithful NHEJ, also termed D-NHEJ (as in DNA-PKcs dependent NHEJ) (Verkaik et al., 2002). For this work we refer to D-NHEJ as NHEJ and to B-NHEJ as microhomology based repair. Microhomology based repair uses DNA sequence microhomologies of 1-8 bp to bring open DNA-ends together and to ligate them (Kabotyanski et al., 1998). Similar to the SSA pathway, this leads to the collapse of two microhomology sequences into one.

To date there are no proteins implicated in this pathway. However, microhomology based repair seems to function independently of NHEJ factors like Ku, DNA-PKcs and Ligase IV (Wang et al., 2003; Chen et al., 2005; Wang et al., 2001). As a hallmark feature of microhomology based repair small deletions can be found at the joined sites (Feldmann et al., 2000). Its status as a distinct pathway is heavily debated as it may merely represent low efficiency SSA or the remaining activity of other NHEJ components (Verkaik et al., 2002; Lieber et al., 2004).

NHEJ is mediated by the DNA-PK complex, which is composed of the proteins DNA-dependent protein kinase catalytic subunit (DNA-PKcs); the heterodimer Ku70/80; XRCC4; and Ligase IV (Smith and Jackson, 1999). DNA-PKcs belongs to the family of phosphatidylinositol-3 (PI-3) like kinases and is therefore related to the ataxia-telangiectasia mutated (ATM) and ATM-Rad3-related (ATR) kinases (Kastan and Lim, 2000; O'Driscoll et al., 2004). Both play important roles in the DNA damage response (Durocher and Jackson, 2001). The importance of the serine/ threonine kinase activity of DNA-PKcs for NHEJ was demonstrated in severe combined immunodeficient (SCID) mice, in which mutated DNA-PKcs lacks this activity and thus fails to repair DSBs induced by the immunoglobulin and T-cell receptor gene rearrangement processes (Blunt et al., 1995; Lieber et al., 1988; Schuler et al., 1986). As a consequence, T and B-cell development are impaired, and radiation sensitivity is increased (Fulop and Phillips, 1990). In cell lines, the lack of other DNA-PK complex components like Ku70, Ku80 and Ligase IV results in increased radiation sensitivity and inability to carry out DNA end joining reactions (Andreeva and Kutuzov, 1999; Errami et al., 1996; Grawunder et al., 1998). Mice deficient in Ku70 or Ku80 have a SCID phenotype and show abnormalities during brain development (Gu et al., 1997; Gu et al., 2000; Nussenzweig et al., 1996). Ligase IV knock-out mice and XRCC4 minus mice are embryonic lethal (Frank et al., 1998); however, cell lines derived from early embryonic cells also show increased radiation sensitivity (Frank et al., 1998).

Besides V(D)J rearrangement, another B cell specific recombination process, the immunoglobulin class switch, depends on NHEJ rather than HR (Essers et al., 1997). However, while all the components of the DNA-PK complex are clearly needed for V(D)J rearrangement, their requirement for successful immunoglobulin class switch is less clear (Wang and Wabl, 2004). Because animals with defects in NHEJ have no B cells, they first need to be reconstituted with pre-arranged light and heavy immunoglobulin

chain genes. The variable region of the heavy chain then can be switched from IgM to all other isotypes. Using such approaches, it could be shown that Ku70 and Ku80 are indispensable for immunoglobulin class switch (Casellas et al., 1998; Manis et al., 1998). In contrast, DNA-PKcs knock-out mice retain the ability to switch to IgG1 (Manis et al., 2002). Furthermore, mice carrying the DNA-PKcs SCID mutation even shown normal levels of all immunoglobulin isotypes (Bosma et al., 2002). Presumably, the leakiness of the SCID mutation accounts for these differences (Rooney et al., 2002). There is also evidence for the involvement of XRCC4/Ligase IV in immunoglobulin class switch (Pan-Hammarstrom et al., 2005).

2.2. The role of DNA-PKcs in nonhomologous end joining

In recent years our understanding of how NHEJ works and how it is intertwined with proteins of the cellular damage response, has grown remarkably. In the following section the current model for NHEJ is laid out in some detail.

Step I: Ku binding

Upon DNA damage the highly abundant Ku heterodimer, consisting of the DNA helicases Ku70 and Ku80 binds to open DNA ends (Fig. 3A) (Mimori and Hardin, 1986). It has been estimated that the Ku protein is so abundant that if it were evenly distributed in the cell, single molecules would be only 4-6 diameters apart from each other (Lieber et al., 2003). This way the Ku protein ensures a quick detection of DSBs and protects the open DNA ends from nucleolytic attack (Downs and Jackson, 2004). Structural data showed that the Ku heterodimer forms a ring and encloses the dsDNA like a bead on a thread (Fig. 3B) (Walker et al., 2001). Because purified Ku binds DNA *in vitro*, it is clear that additional loading factors may not be needed *in vivo* (Walker et al., 2001). Ku70 and Ku80 proteins are very unstable if they are not part of the heterodimer. Therefore, decreased Ku70 protein expression automatically leads to decreased Ku80 protein expression and vice versa (Andreeva and Kutuzov, 1999; Errami et al., 1996).

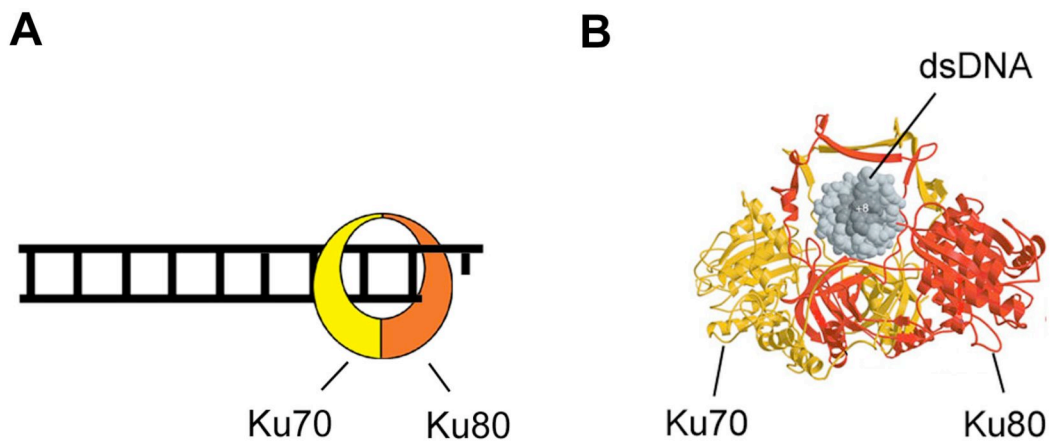


Figure 3. DSB binding by Ku

(A) Schematic model of the Ku70/80 heterodimer bound to open DNA ends. This occurs at both open DNA strands of the DNA double-strand break site. (B) Crystal structure of Ku bound to dsDNA (Walker et al., 2001).

Step II: DNA-PKcs autophosphorylation

After the Ku protein associates with DNA, it recruits DNA-PKcs to the damaged site. Upon DNA binding DNA-PKcs changes its conformation, which triggers its kinase activity and leads to autophosphorylation (Fig. 4) (Boskovic et al., 2003; Rivera-Calzada et al., 2005). This autophosphorylation seems to occur in trans and implies that DNA-PKcs molecules are bound to both DNA ends in proximity (Rivera-Calzada et al., 2005).

Several DNA-PKcs autophosphorylation sites have been identified to date and current models suggest the existence of at least three distinct functional clusters of such sites. The first cluster, also termed ABCDE, includes the potential autophosphorylation sites T2609 (A), T2620 / S2624 (B), T2638 (C), T2647 (D) and S2612 (E) (Douglas et al., 2002). In vivo, phosphorylation of the T2609 site is essential for both cell survival and DSB repair after IR (Chan et al., 2002). Also, DNA-PKcs pT2609 co-localizes at DNA damage foci with the DSB repair proteins H2AX and 53BP1 (Chan et al., 2002). In reconstitution experiments with DNA-PKcs deficient hamster cells, expression of DNA-PKcs mutated in all ABCDE sites led to increased radiation sensitivity and decreased NHEJ activity (Ding et al., 2003). Experiments reconstituting NHEJ activity in vitro showed that DNA bound DNA-PKcs can control the access of other factors to the open DNA strand (Reddy et al., 2004). This function of DNA-PKcs seemed to be regulated by phosphorylation in the ABCDE cluster (Reddy et al., 2004). In summary, the ABCDE cluster is important for the end joining activity of DNA-PKcs.

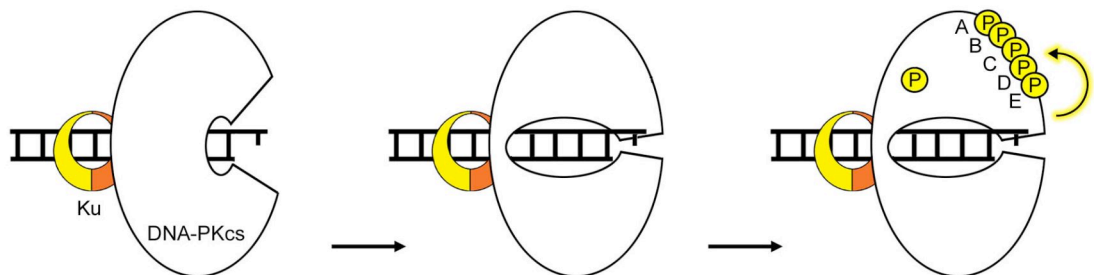


Figure 4. Autophosphorylation of DNA-PKcs

Binding to Ku and dsDNA induces a conformational change in the DNA-PKcs protein. This triggers its kinase activity thus leading to autophosphorylation (yellow arrow) at several sites. The ABCDE cluster of six adjacent autophosphorylation sites (T2609 (A), T2620 / S2624 (B), T2638 (C), T2647 (D) and S2612 (E) is depicted. The other single phosphorylation site represents S2056.

Hypothetically, another cluster of autophosphorylation sites is responsible for kinase disassembly, because mutations in the ABCDE cluster do not abolish such activity (Ding et al., 2003; Merkle et al., 2002). Recently, another autophosphorylation site, upstream of the ABCDE cluster has been identified at S2056 (Chen et al., 2005). DNA-PKcs autophosphorylation at S2056 is independent of ATM and is important for NHEJ efficiency. Interestingly, S2056 phosphorylation occurs in irradiated cells mainly in G1 but not in S phase. Moreover, in response to replication-associated DSBs, phosphorylation of S2056 was increased and further seemed to be dependent on DNA-polymerase α or δ activity (Chen et al., 2005).

Step III: DNA damage response

The cellular DNA damage response ensures that apart from the activation of DNA repair pathways the cell reacts appropriately to the insult (Zhou and Elledge, 2000). For this, the cell cycle is halted at checkpoints, and in the case of extensive DNA damage, apoptosis is induced (Zhou and Elledge, 2000). The first response to DNA damage is phosphorylation of the DNA damage response gene ATM at S1981 (Fig. 5) (Bakkenist and Kastan, 2003). Presumably triggered by changes in chromatin structure, ATM dimers autophosphorylate in trans and monomerize.

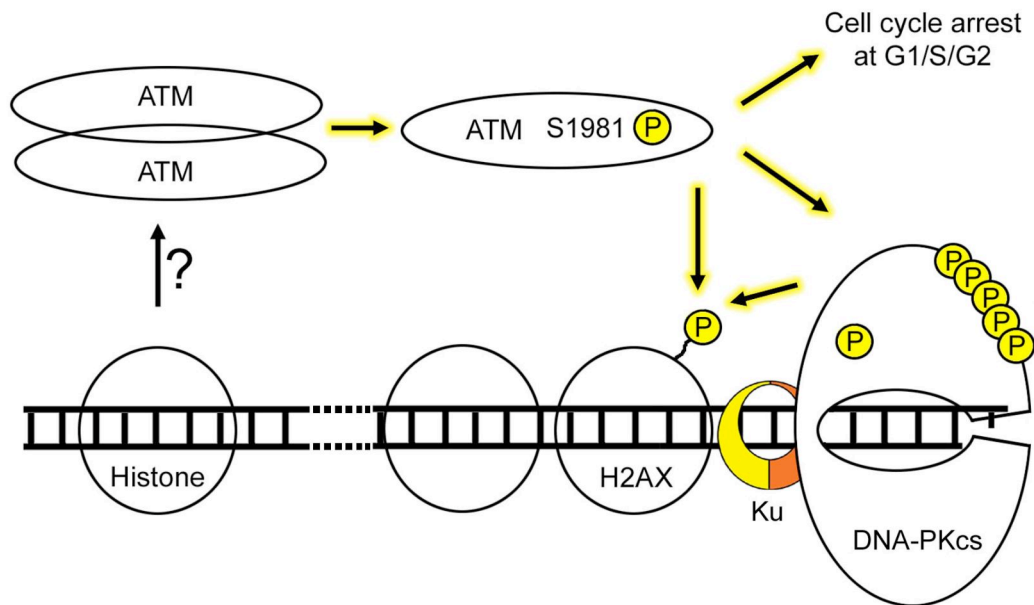


Figure 5. NHEJ and the damage response

Schematic representation of functional interactions between NHEJ components and proteins of the cellular damage response. DNA damage triggers changes in chromatin structure which results in ATM monomerization and ATM autophosphorylation at S1981. The dashed line in the DNA strand indicates that chromatin changes caused by the DSB may signal DNA damage over long distances. Enzymatically active ATM then targets G1/S/G2 checkpoint proteins and DSB repair proteins like H2AX and DNA-PKcs. Phosphorylation steps are depicted by yellow arrows. It is important to note that all events happen on both end of the DSB.

This event further increases ATM kinase activity and ATM then targets checkpoint proteins like p53, NBS1 and Chk2, which halt the cell cycle at G1, S or G2, respectively (Abraham, 2001; Bakkenist and Kastan, 2003). Interestingly, ATM also participates in the actual DNA repair process by phosphorylating H2AX together with DNA-PKcs (Stiff et al., 2004). Phosphorylated H2AX (γ -H2AX) is a marker for damaged DNA regions, and it has been suggested that γ -H2AX concentrates DNA repair proteins and prepares the chromatin for subsequent DNA repair events (Fernandez-Capetillo et al., 2004). Recently, it was shown that ATM can also phosphorylate DNA-PKcs at T2609 (Chan et al., 2002).

Step IV: DNA end processing

Depending on the underlying cause, DSBs can look very differently. For this reason they require specific end processing before the final DNA ligation reaction can occur (Lieber et al., 2003). Several factors have been implicated in this process (Fig. 6):

DSB breaks caused by IR are either blunt or staggered with either 5' or 3' overhanging ends. These ends can be processed by the M/R/N complex consisting of the endonuclease Mre11, Rad50 and NBS1 (van den Bosch et al., 2003). The nucleolytic resection activity of the M/R/N complex has also been implicated in the HR pathway of DSB repair (West, 2003).

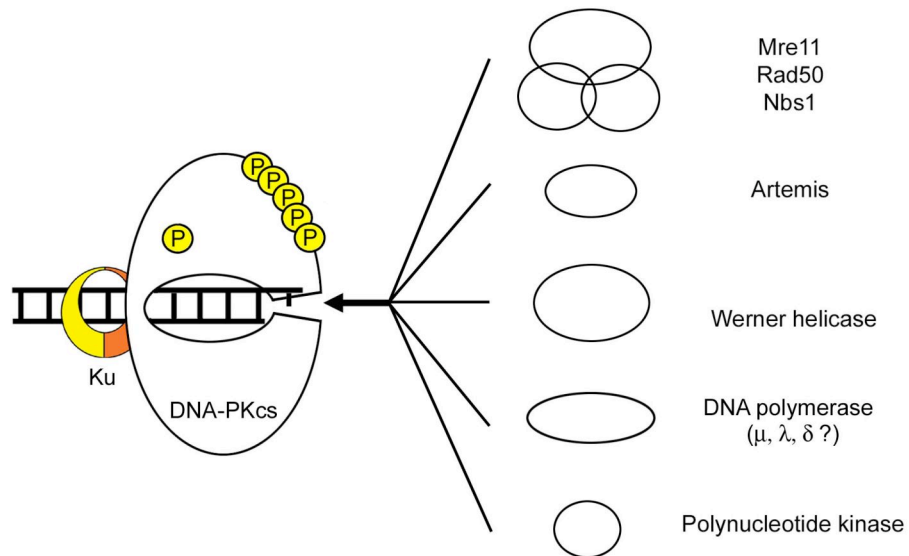


Figure 6. DSB end processing

Several proteins implicated in DNA end processing are depicted. Mre11, Rad50 and NBS1 form a complex with nucleolytic activity. The exonuclease Artemis acquires endonuclease activity when bound to DNA-PKcs. The Werner protein possesses helicase and exonuclease activity. Several DNA polymerases are implicated in NHEJ, but their exact role is unclear. Poly-nucleotide kinase phosphorylates the terminal 3' OH of the DNA, which is essential for ligation. As shown in the model, phosphorylated DNA-PKcs may actually control the access of these processing proteins to the DNA.

More extensive DNA processing may require that the DNA is unwound by DNA helicases. For example, the Werner helicase interacts with DNA-PKcs, is regulated by DNA-PKcs phosphorylation and might participate in DNA end processing (Li and Comai, 2002; Yannone et al., 2001).

The formation of DSB at stalled replication forks requires DNA polymerase activity and several DNA polymerases like α and δ have been implicated in this reaction (Chen et al., 2005; Pospiech et al., 2001). But also DNA damage due to IR exposure might require DNA polymerase activity, and it was shown that DNA polymerase μ forms a complex with Ku and XRCC4/Ligase IV and co-localizes with γ -H2AX foci (Mahajan et al., 2002).

During V(D)J rearrangement the recombination activating proteins 1 and 2 (RAG 1/2) cause DSB with hairpins (McBlane et al., 1995; Schatz et al., 1989). These hairpins have to be opened first in order to ligate both DNA strands together and to complete the rearrangement of the immunoglobulin variable region (Schlissel, 2002). After a long quest for the elusive factor, it was found that in complex with DNA-PKcs the exonuclease Artemis acquires also endonuclease activity and is therefore able to open these hairpin structures (Ma et al., 2002). In agreement with this role, loss of function mutations in Artemis or DNA-PKcs result in a SCID phenotype with no T or B cells (Schuler et al., 1986) (Noordzij et al., 2003).

In order to ligate open DNA ends together, DNA ligases require a 3' end phosphate group. If this phosphate group is lost by the DNA damage or end processing, the polynucleotide kinase (PNK) can phosphorylate the 3' end and allow DNA ligation (Chappell et al., 2002).

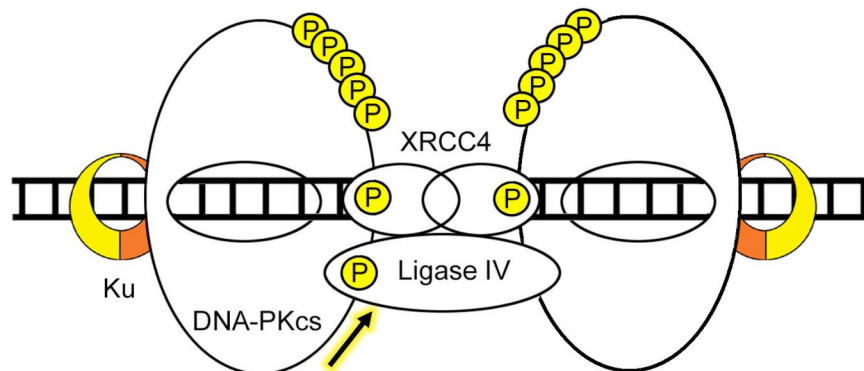


Figure 7. End ligation by the XRCC4/Ligase IV complex

Schematic representation of the ligation reaction carried out by the XRCC4/Ligase IV complex. Both DNA strands bound to Ku/DNA-PKcs are brought together and then ligated. Ligase IV phosphorylation by DNA-PKcs is depicted by a yellow arrow.

Step V: DNA end ligation

The DNA ligation step of NHEJ is carried out by the XRCC4/Ligase IV complex (Grawunder et al., 1997). It has been suggested that two molecules of XRCC4 are associated with one molecule of Ligase IV (Fig. 7) (Grawunder et al., 1997). While XRCC4 is the structural protein that may hold the open DNA ends together, Ligase IV provides the catalytic activity to close the gap (Grawunder et al., 1998; Junop et al., 2000). Both proteins are phosphoproteins; for Ligase IV it was shown that it is a phosphorylation target of DNA-PKcs, while XRCC4 phosphorylation depends on other protein kinases (Wang et al., 2004).

Step VI: Dissociation of the DNA-PKcs complex

This NHEJ step is the least understood step. Assuming that the Ku heterodimer stays on the DNA until the final ligation step, the question is how it gets unloaded from the DNA (Fig. 8). The first possibility is that the dimer can be separated by an additional factor, presumably at the expense of ATP. In the alternative case, Ku could be cleaved by a protease (Downs and Jackson, 2004). In fact, a Ku70 derived polypeptide that binds and inhibits the proapoptotic factor BAX has been recently identified (Sawada et al., 2003). However, the search for the responsible protease has so far been unsuccessful.

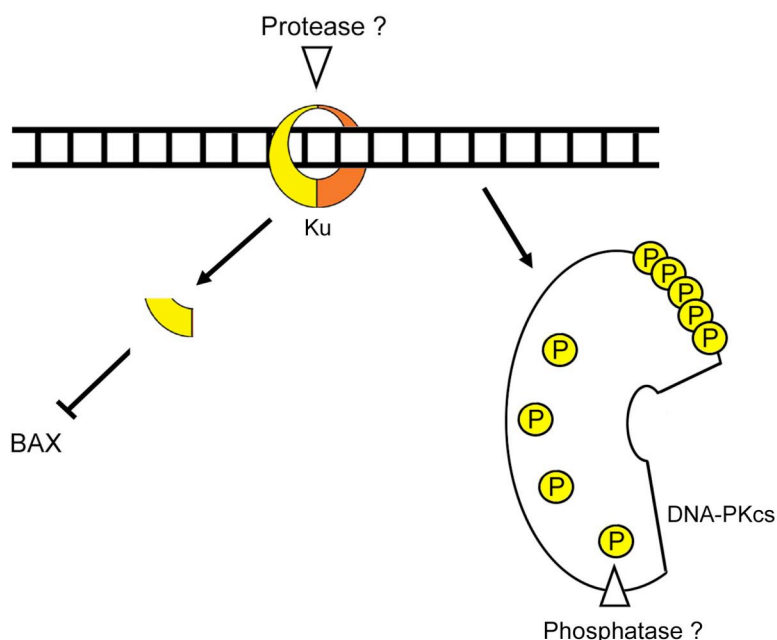


Figure 8. Dissociation of the NHEJ complex

Schematic representation of steps following DNA end ligation. The Ku70/80 heterodimer presumably gets cleaved by an unknown protease. A Ku70 derived polypeptide binds the proapoptotic factor BAX and inhibits its function. Hyperphosphorylated DNA-PKcs dissociates from the Ku protein and dsDNA and gets dephosphorylated by an unknown protein phosphatase. Additional phosphorylation sites represent unknown sites responsible for kinase disassembly.

For DNA-PKcs it is clear that hyperphosphorylation leads to its dissociation from Ku and DNA (Merkle et al., 2002). However, it is not clear which DNA-PKcs phosphorylation sites in particular are responsible for this event, and they are yet to be identified. It is also unclear if phosphorylated DNA-PKcs gets dephosphorylated and can be reused, or if phosphorylated DNA-PKcs is to be degraded. Even though there is some evidence that dephosphorylation occurs, the corresponding phosphatase has been elusive so far (Douglas et al., 2001).

3. Specific aim: Characterization of PP5 and Kub3 as new interaction partners of DNA-PKcs

Despite the importance of DNA-PKcs for DSB repair after DNA damage, V(D)J rearrangement and class switch recombination, little is known about its interaction partners and phosphorylation targets. Apart from its complex partners Ku, XRCC4/Ligase IV, only Artemis and the Werner protein have recently been identified (Graeme C.M. Smith, 1999) (Ma et al., 2002; Yannone et al., 2001). Because of its large size of 465 kD one would expect that DNA-PKcs interacts with many proteins at the same time and thus could function as an organizer for DSB repair. That is why we set out to identify new interaction partners of DNA-PKcs. Because a previous yeast two-hybrid screen with full length DNA-PKcs only identified the DNA-PKcs interacting protein (KIP), we decided to use six fragments of DNA-PKcs of 3 kb cDNA length (Fig. 9) as bait (Xiantuo Wu, 1997). To identify potential binding partners, we used cDNA libraries from human activated B cells, human brain and from 18-81, a mouse cell line of B-cell origin (Burrows et al., 1981). From several multiple hits we identified in the screen, we decided to focus on the two proteins protein phosphatase 5 (PP5) and Ku70 binding protein 3 (Kub3) which we describe in more detail in the following sections.

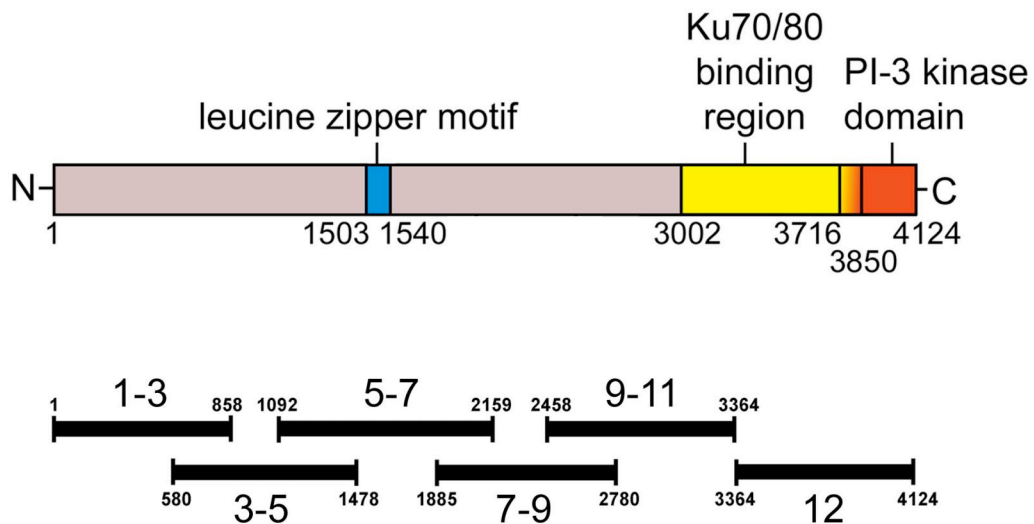


Figure 9. Yeast two-hybrid screen with human DNA-PKcs fragments

Upper panel: protein structure of DNA-PKcs with functional domains. Numbers represent amino acid residue positions in the full length human DNA-PKcs protein. Lower panel: six DNA-PKcs cDNA fragments of 3 kb length used in the yeast two-hybrid screen. Small numbers represent amino acid residue positions in the full length human DNA-PKcs protein.

3.2. Protein phosphatase 5 (PP5)

PP5 is a ubiquitously expressed serine/threonine protein phosphatase that is present in both cytoplasm and nucleus (Chen et al., 1994; Chinkers, 2001). It dephosphorylates the proapoptotic protein apoptosis signal-regulating kinase 1 (ASK1) and interacts with a variety of proteins including the heat shock protein 90 (Hsp90)/glucocorticoid receptor (GR) and Hsp90/heme-regulated inhibitor of protein synthesis (HRI) heterocomplexes (Morita et al., 2001) (Chen et al., 1996); (Shao et al., 2002); cell division cycle 16 and 27 homologs (CDC16/27) of the APC complex (Ollendorff and Donoghue, 1997); the A-subunit of protein phosphatase 2A (PP2A) (Lubert et al., 2001); the human blue-light photoreceptor hCRY2 (Zhao and Sancar, 1997); and the $G\alpha_{12}/G\alpha_{13}$ subunits of heterotrimeric G proteins (Yamaguchi et al., 2002). Furthermore, PP5 also regulates p53 function and dephosphorylates in vitro the protein tau, which is implicated in several neurodegenerative diseases like Alzheimer's disease (Liu et al., 2002; Zuo et al., 1998); (Brandt et al., 2005). PP5 is a protein of 499 aa in humans and has a predicted molecular weight of 58 kD (Chen et al., 1994). On the N-terminus PP5 has three tandem repeats forming a tetratricopeptide repeat (TPR) domain, which has been implicated in protein-protein interactions (Das et al., 1998). The catalytic domain is located in the middle of the protein and the carboxy-terminal 80 aa are required for the nuclear import of PP5 by an unknown mechanism (Chinkers, 2001); (Borthwick et al., 2001).

Five cDNA clones identified in our yeast two-hybrid screen PP5. Of those, four encoded mouse PP5 from the 18-81 cDNA library and one encoded human PP5 from the human activated B-cell library (Fig. 10A). Four clones were able to interact with the 9-11 region of DNA-PKcs and one clone with the 7-9 region (Fig. 10B). Interestingly, this interaction region covers the two DNA-PKcs autophosphorylation sites T2609 and S2056 (Fig. 10B) (Chan et al., 2002; Chen et al., 2005). Because none of the five isolated PP5 cDNA clones started downstream of the TPR motif, it is possible that this domain is essential for the DNA-PKcs/PP5 interaction. To test this possibility in vitro, GST-tagged DNA-PKcs fragments were used to pull down the His-tagged PP5 TPR (Fig. 10C) (Wechsler et al., 2004). These DNA-PKcs polypeptides contained either the T2609 (aa 2500-2700) and related sites or the serine at position 2056 (S2056) (aa 1878-2261) (Fig. 10B). However, while the T2609 fragment retrieved the PP5-TPR domain very well, the S2056 fragment did not (Fig. 10C) (Wechsler et al., 2004). This suggests an interaction between the PP5-TPR domain and the DNA-PKcs region aa 2500-2700.

Because DNA-PKcs activity is dependent on its phosphorylation status, it is intriguing that cells incubated with okadaic acid have decreased DNA-PKcs kinase activity considering that PP5 is sensitive to this compound as well (Chen et al., 1994; Douglas et al., 2001). This suggested to us that dephosphorylation of DNA-PKcs might be necessary for its activity and that it is PP5 which can dephosphorylate DNA-PKcs and regulate its function in DSB repair. To test this hypothesis we decided to further study the interaction between DNA-PKcs and PP5 in vivo; and PP5 function with respect to DNA-PKcs phosphorylation at the sites T2609/S2056 and cell survival after irradiation with IR.

Specific aim

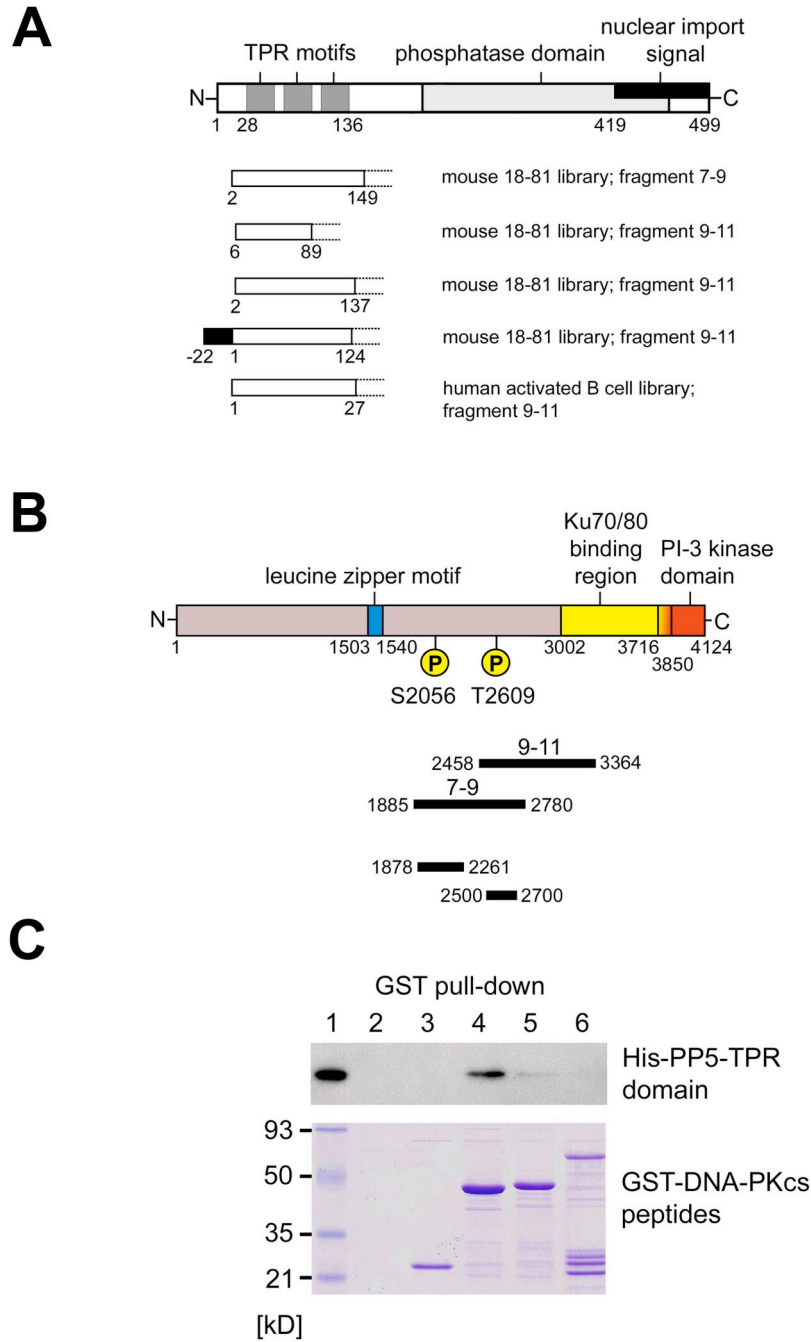


Figure 10. Binding of PP5 to DNA-PKcs

(A) Schematic representation of human PP5 and fragments isolated by yeast two-hybrid screen from the corresponding cDNA libraries. The dashed line indicates that the fragments are in fact longer, but sequencing ended at the amino acid residue indicated. (B) Schematic representation of human DNA-PKcs and fragments used in yeast two-hybrid (7-9 and 9-11) and GST pull down experiments. The numbers correspond to amino acid residues. (C) Pull down with GST-fusion and His-tagged proteins expressed in *E. coli*. Upper panel: His-tagged TPR domain of PP5 (lane 1; input) was co-immunoprecipitated with the GST-DNA-PKcs fragment 2500-2700 with wild type threonine (lane 4), or aspartic acid (lane 5) at position 2609; and fragment 1878-2267 (lane 6); beads only (lane 2), or GST only (lane 3) and visualized with anti His-HRP conjugated antibody. Lower panel: pull down input controls of GST-DNA-PKcs peptides were stained with Coomassie Blue.

3.1. Ku70 binding protein 3 (Kub3)

Kub3 has been originally identified in a yeast two-hybrid screen using human Ku70 as bait and a human liver cDNA library (Yang et al., 1999a). In these experiments the authors identified a 1.2 kb cDNA with an ORF that they deemed as partial Kub3 sequence (Genbank accession AF078164). Against this (His-tagged) 36 kD polypeptide they raised a rabbit polyclonal antibody, which recognized in human cell lines two proteins of 220 and ~300 kD, respectively. Because the ~300 kD protein could be co-precipitated with Ku70, the authors suggested that Kub3 might be part of the DNA-PK complex and might have a function in DSB repair (Yang et al., 1999a).

Further clues to the function of Kub3 came from studies on gene amplification in glioblastomas (Fischer et al., 2001). Fischer and colleagues identified a 130 bp sequence, which was amplified in the glioblastoma cell line TX3868, hence termed glioblastoma amplified sequence 16 (GAS16). When they further characterized GAS16, they discovered that it was located in an intronic sequence between two Kub3 exons. They also found evidence that GAS16 is part of an alternative splice variant of Kub3 expressed in fetal brain and glioblastomas. The size of the corresponding transcript was 4.2 kb, as compared to the regular 1.3-kb Kub3 transcript. When they tested primary glioblastoma tumors, they found an up to 39-fold increase of Kub3 mRNA in 12 out of 82 tumors (14%), presumably due to amplification of the Kub3 gene. However, there was no evidence for overexpression of the alternatively spliced mRNA. They also noted that human Kub3 is located at 12q13 and in close proximity to MDM2 and CDK4. Both genes are amplified in glioblastomas in 7% (MDM2) and 14% (CDK4) of the tumors and are important regulators of the tumor suppressor activity of p53 and the cell cycle, respectively (Fischer et al., 2001).

Another indication that Kub3 is an interaction partner of the DNA-PK complex came from our own yeast two-hybrid studies, where we identified Kub3 as an interaction partner of human DNA-PKcs fragments. Specifically, three independent clones encoding Kub3 from the mouse cDNA library 18-81 bound to the region 1-3 (one clone) and to the region 9-11 (two clones) of human DNA-PKcs (Fig. 16). Interestingly, one Kub3 cDNA clone binding to the DNA-PKcs fragment 9-11 was truncated at the N-terminus. This indicates that the first 85 amino acid residues of mouse Kub3 are dispensable for its interaction with DNA-PKcs.

Based on the previous data and assuming that Kub3 binds indeed to both Ku70 and DNA-PKcs, we considered the two following hypotheses for Kub3 function:

1) Kub3 is a component of the DNA-PK complex and is essential for DSB repair by nonhomologous end joining

In this case, loss of function mutations in Kub3, or decreased expression of the Kub3 protein, would increase the number of unrepaired DNA breaks after irradiation, decreasing the survival chance of the cell. Overexpression of Kub3 could also have adverse effects on NHEJ, similar to the way how overexpression of Ku70 or Ku80 leads to decreased DNA-PKcs activity (Kasten et al., 1999).

Specific aim

2) Kub3 is a negative regulator of the DNA-PK complex and of DSB repair by nonhomologous end joining

According to this hypothesis, Kub3 overexpression would lead to decreased NHEJ activity, thus leading to increased genomic instability. Because increased genomic instability drives tumorigenesis, this would explain the massive amplification of Kub3 in some glioblastomas.

To distinguish between these two working hypotheses, we decided to characterize the Kub3 protein and its interaction with DNA-PKcs. Furthermore, we planned to investigate its function with respect to DSB repair in mammalian and insect cells.

4. Results

4.1. DNA-PKcs function specifically regulated by protein phosphatase 5 (PP5)

4.1.1. Overexpression of PP5 decreases phosphorylation of DNA-PKcs, but not of ATM

Perhaps due to the short interaction time *in vivo*, we were unable to co-precipitate PP5 and DNA-PKcs (data not shown). Hence we decided to study the functional relevance of the PP5/DNA-PKcs interaction instead and stably overexpressed human wild type PP5 in HeLa cells, using a retroviral vector. We then compared the phosphorylation level of T2609 in transduced subclones with the one in untransduced HeLa cells, with or without irradiation. When the cells were irradiated, we monitored phosphorylation after 30, 60, 120, 240, and 410 min recovery time. To this end, we prepared nuclear extracts and analyzed them by Western blotting with a polyclonal rabbit antibody that specifically reacts with pT2609, but not with unphosphorylated T2609 (Fig. 11A, upper panel) (Chan et al., 2002). Under these conditions, the T2609 phosphorylation in the PP5 overexpressing subclones PP5.C4 and PP5.C13 was diminished, as compared to non-transduced HeLa cells, whether undamaged or damaged by irradiation. Furthermore, the dephosphorylation at T2609 occurred much faster in clones PP5.C4 and PP5.C13, with the pT2609 signal returning to undamaged levels at 410 min.

Besides the 450-kD band, which represents DNA-PKcs, we also noticed two other bands stained by the antibody, at 240 kD and 150 kD respectively; these bands might result from degradation of DNA-PKcs. The 240-kD fragment is probably due to the apoptotic cleavage at position 2708-2713 (Song et al., 1996); we do not know anything about the identity of the 150-kD band. At any rate, compared to HeLa control cells, the 240-kD band is less intense in the PP5.C4 and PP5.C13 subclones; and the 150-kD band appears later after damage.

Apart from T2609, another functional DNA-PKcs phosphorylation site at S2056 has been recently defined (Chen et al., 2005). In order to find out if this site is also regulated by PP5, we used a polyclonal rabbit antibody generated against this site, on the same nuclear extracts as before. While HeLa cells showed weak phosphorylation under undamaged conditions, it was absent in clones PP5.C4 and PP5.C13 and weaker in these clones at 30 min after irradiation (Fig. 11B). After 410 min the S2056 was almost completely dephosphorylated in PP5.C13, but not in HeLa and PP5.C4. Despite this difference, and the slight difference in the level of PP5 overexpression between subclones PP5.C4 and PP5.C13 (Fig. 11A), the observed similarities of the phosphorylation patterns seem to exclude a site-specific effect of the retroviral vector integration.

Therefore, we conclude that PP5 is the phosphatase that is responsible for removing the phosphate group from T2609 and S2056 of DNA-PKcs after irradiation damage. However, ATM can also phosphorylate DNA-PKcs at T2609 (but not at S2056) and may

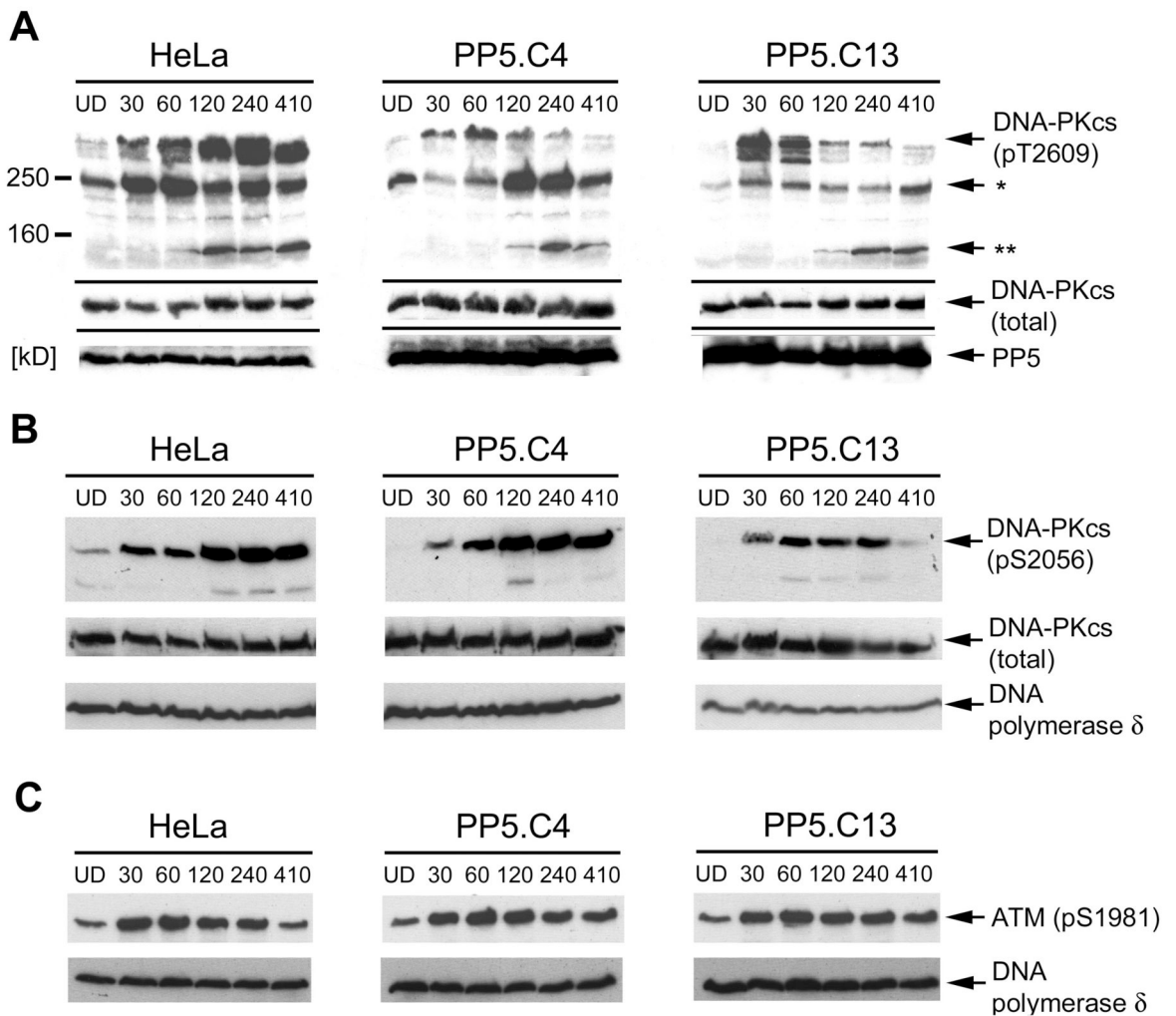


Figure 11. Phosphorylation status of DNA-PKcs after irradiation in PP5 overexpressing clones

HeLa cells, PP5.C4 and PP5.C13 subclones were irradiated with IR (11.5 Gy) and recovered for 30 - 410 min. The undamaged control (UD) is shown on the left. Nuclear extracts were prepared and 35 μ g of protein applied to a SDS gel. After Western blotting the membrane was stained with (A) rabbit antibody to DNA-PKcs pT2609, with (B) rabbit antibody to DNA-PKcs pS2056, or (C) rabbit antibody to ATM pS1981. For loading controls the same membranes were stripped and incubated with antibody to total DNA-PKcs or to DNA polymerase δ . PP5 overexpression was visualized by anti-PP5 antibody. * and ** denote phosphorylated DNA-PKcs degradation products.

be dephosphorylated by PP5 as well (Chan et al., 2002). Because this, in part, may contribute indirectly to the phosphorylation differences, we tested our subclones for ATM phosphorylation at the S1981 site (Bakkenist and Kastan, 2003). As we observed no obvious differences (Fig. 11C), it seems that PP5 is fairly specific for DNA-PKcs.

4.1.2. Dominant negative of PP5 increases phosphorylation of DNA-PKcs

The import of PP5 into the nucleus apparently is dependent on its terminal 80 aa residues (Borthwick et al., 2001). One of the transduced HeLa subclones, PP5.C7, expressed a protein that encodes the first 389 residues of PP5 fused to GFP (Fig. 12A), thus lacking the sequence required for nuclear import. The PP5.GFP fusion protein had a molecular weight of ~70 kD, accumulated in the cytoplasm (Fig. 12B), and could be detected by PP5 antibody (Fig. 12C). We reasoned that this fusion protein may act as a

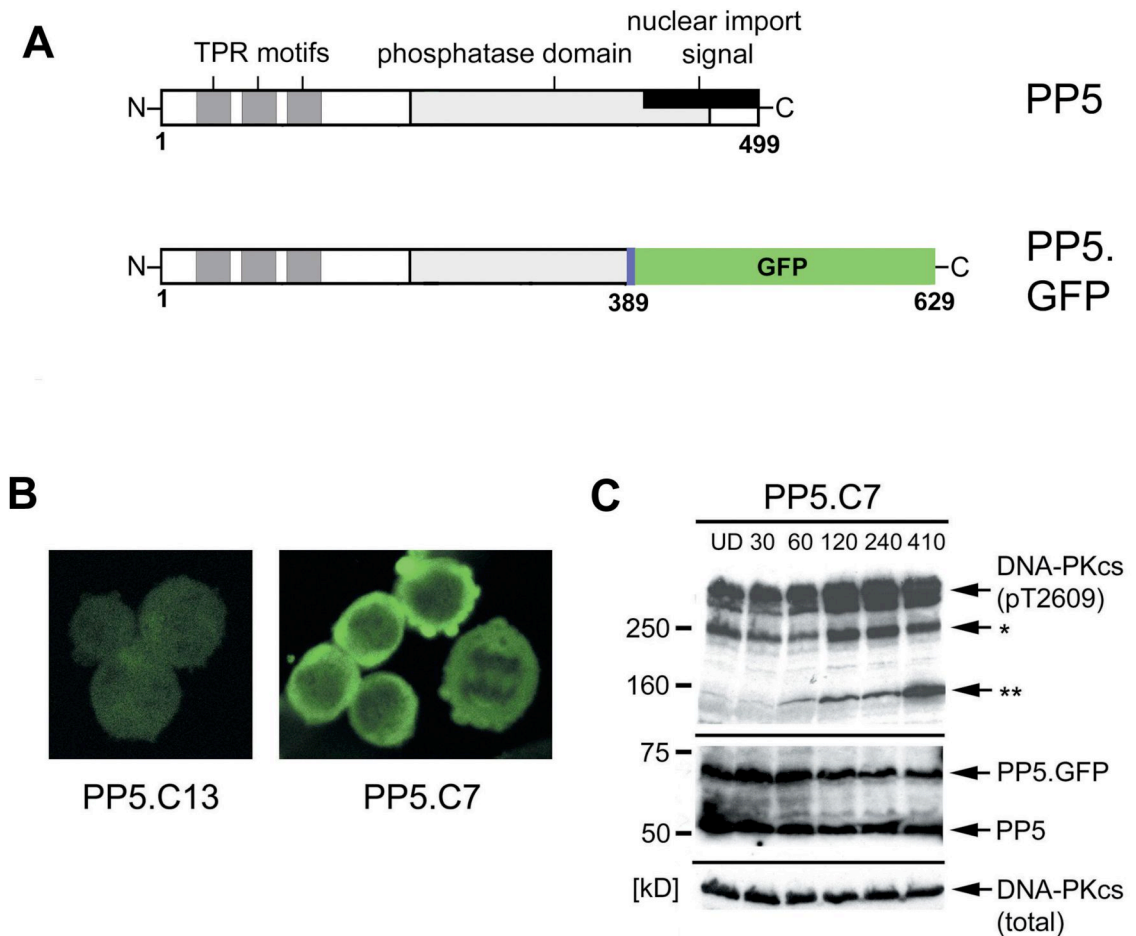


Figure 12. Effect of dominant negative PP5 on phosphorylation of DNA-PKcs

(A) Structure of the dominant negative PP5.GFP fusion protein compared to wildtype PP5 protein. (B) Cellular localization in unfixed cells of either GFP in subclone PP5.C13 (left picture) or PP5.GFP fusion protein in subclone PP5.C7 (right picture). (C) The PP5.C7 subclone expressing dominant negative PP5.GFP was irradiated with 11.5 Gy and recovered for 30 - 410 min. Nuclear extracts, Western blotting and staining with anti-pT2609 antibody were part of the experiment series shown in Fig. 11, the HeLa wild type cells of Fig. 11a. thus serve as control. * and ** denote phosphorylated DNA-PKcs degradation products.

dominant negative form. One possible way would be that PP5.GFP blocks the import mechanism while still binding to (some of) the proteins that are needed for this import; endogenous PP5 import would be competed out in this way. Another possibility came to mind when we considered the surprising finding that the fusion protein was not completely denatured by alcohol, as it still was fluorescent (not shown). Thus, it may be that the fusion protein does not fold correctly for the import, but still takes away the protein(s) required for it. Both before irradiation (undamaged) and after, in the subclone PP5.C7 DNA-PKcs was heavily phosphorylated at position T2609 at all time points (Fig. 12C). Even after 410 min, when the signal began to wane in the untransduced HeLa cells (Fig. 11A, which was part of the same experimental series and thus serves as a control), phosphorylation remained strong. Apart from confirming that PP5 provides the dephosphorylation activity the findings in clone PP5.C7 indicate that no other phosphatase can substitute for PP5 at T2609. In line with the phosphorylation patterns of ATM in the PP5 overexpressing subclones, no pronounced differences occurred in the PP5.C7 clone (data not shown). But obviously a possible regulation of ATM by PP5 needs a more detailed investigation.

4.1.3. Hypo- and hyperphosphorylation of DNA-PKcs do not alter the use of microhomology based repair

From the experiments described above, it seems to be clear that PP5 can dephosphorylate DNA-PKcs. But does this enzymatic activity have a biological consequence? DNA repair proteins are either involved in the DNA damage response (like ATM, ATR) or in the DNA repair process itself (like XRCC4, Ligase IV). Because the expression of DNA-PKcs with mutations in the major autophosphorylation cluster (including T2609) causes decreased NHEJ activity, we investigated if DNA-PKcs pT2609 phosphorylation is important for DNA double-strand break repair by NHEJ (Chan et al., 2002; Ding et al., 2003).

To do so we used an *in vivo* method termed the Dik van Gent assay (Verkaik et al., 2002). This method is based on the fact that, if no long homologous sequence is present, mammalian cells have two options to repair a transfected blunt end linearized indicator plasmid. The use of NHEJ leads to direct ligation of the DNA ends which results in an unaltered plasmid. Alternatively, the lesion can be repaired by using microhomologies flanking the DNA break (Fig. 13A). As a result two microhomologies are converted into one, which creates a unique *BstX* I restriction site in the repaired plasmid (Fig. 13A). The plasmid DNA flanking this site can then be PCR amplified, ³²P labeled and assayed for *BstX* I sensitivity. The ratio between *BstX* I resistant and sensitive PCR product hereby reflects the ratio between the use of NHEJ and microhomology based repair, respectively. This can be readily demonstrated in DNA-PKcs deficient Chinese hamster ovary cells (CHO-V3) containing an empty vector (V3-JM), or reconstituted with a DNA-PKcs expressing vector (V3-F18) (Chan et al., 2002). While the DNA-PKcs deficient cells show microhomology use in 95% of the ligated molecules, the reconstitution of DNA-PKcs can decrease this percentage to 54% (Fig. 13B).

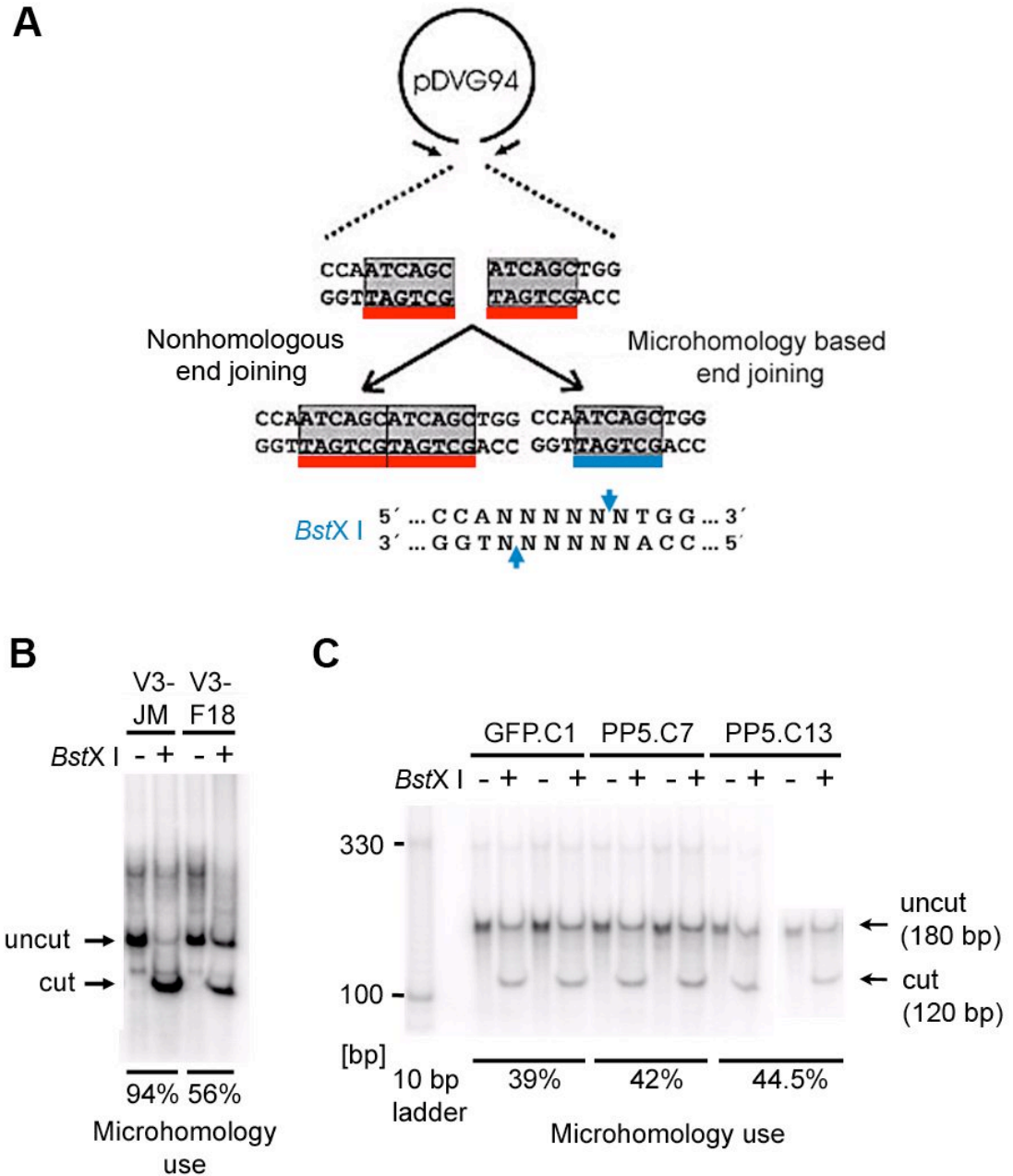


Figure 13. Use of microhomology based repair in HeLa and V3 cells measured by the Dik van Gent assay.

(A) The transfected plasmid pDVG94 contains a duplicated 6 bp microhomology DNA sequence. The repair of the linearized plasmid by microhomology based repair results in generation of a *BstX* I restriction site, while repair by NHEJ does not (modified after (Verkaik et al., 2002)). (B) ³²P labeled and PCR amplified pDVG94 DNA was recovered from DNA-PKcs deficient CHO-V3 cells transfected with either empty vector (V3-JM) or DNA-PKcs expressing vector (V3-F18) and *BstX* I digested. The depicted percentage of microhomology use hereby results from the ratio of uncut to cut PCR product. (C) HeLa subclones overexpressing GFP (GFP.C1), PP5 (PP5.C13) or dominant negative PP5.GFP (PP5.C7) were tested in duplicates for microhomology use.

When we tested the HeLa subclones overexpressing GFP, PP5, or dominant negative PP5.GFP, we did not see any difference in the use of microhomology based repair (~40%) between them (Fig. 13C). This interpretation of the results is not necessarily straightforward, as we found in parallel experiments with a GFP expressing vector that the transfection efficiency in HeLa was more than 10 fold lower than in the V3 cells (0.4% compared to 6%). Nevertheless, we found no evidence that DNA-PKcs pT2609 hypo- or hyperphosphorylation coincide with increased use of microhomology based repair. This seems surprising at first, considering that V3 cells reconstituted with DNA-PKcs mutants T2609A or S2056A show an increase in microhomology based repair (Chen et al., 2005). But in contrast to these cells, where autophosphorylation at T2609 and S2056 sites can not occur at all, this is still possible in our HeLa subclones. Only the timing and the extent to which DNA-PKcs is phosphorylated is different from wildtype cells and thus still allowing efficient DNA end joining. This is consistent with our observation that initiation of the DSB repair process measured by DNA-PKcs pT2609 foci formation was normal in all subclones (data not shown).

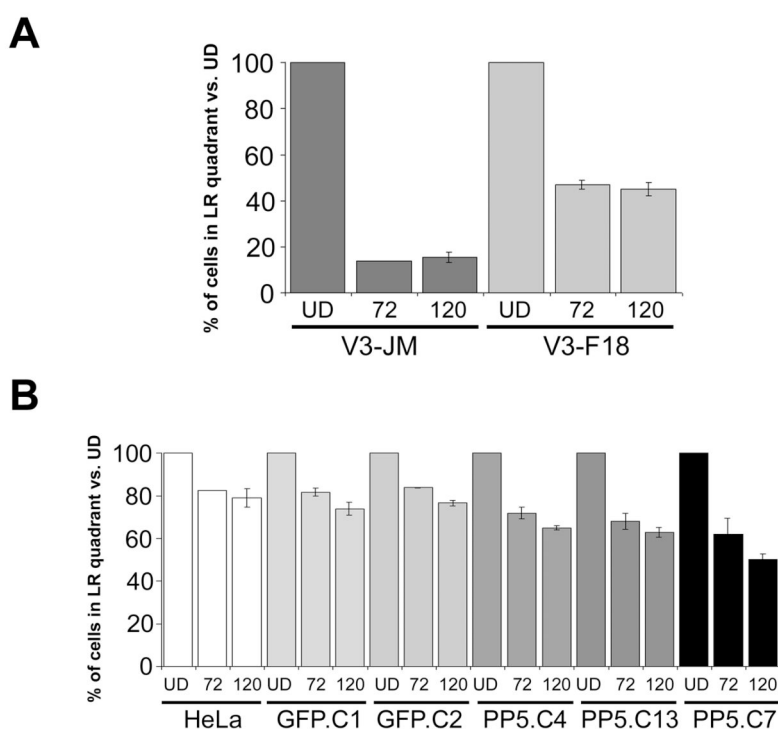


Figure 14. Survival of irradiated cell lines, assayed by flow cytometry

(A) DNA-PKcs deficient CHO-V3 cells transfected with either empty vector (V3-JM) or DNA-PKcs expressing vector (V3-F18) were irradiated with 4 Gy, seeded in triplicates and analyzed after 72 and 120 hr, respectively. For both cell lines the percentage of viable cells represented in the lower right quadrant of forward scatter and side scatter of flow cytometry (not shown) versus undamaged (UD) cells (which are set to 100%) is shown. (B) HeLa subclones analyzed for cell viability like in (A). Cells were irradiated with 4 Gy and analyzed after 72 hr and 120 hr.

4.1.4. Both hypo- and hyperphosphorylation increase radiation sensitivity

Because we have shown that all the transduced clones described above are proficient in DNA end joining, we wanted to investigate if they are deficient in the damage response and therefore show increased radiation sensitivity. To address this question, we used flow cytometry analysis, which allows quantitation of viable and dividing cells, as they appear in defined quadrants of the forward (FSC) and side scatter (SSC) profiles. We determined the number of these cells per 10,000 events in the cytometer after irradiation with either 4 or 11.5 Gy at 72 and 120 hr. Although the protocol does not provide absolute numbers of cell survivors, it does give ratios of live and dividing cells over all events that can be compared between cultures. To ensure that such an assay reasonably reflects cell viability, we compared DNA-PKcs deficient CHO-V3 cells containing an empty vector (V3-JM), or reconstituted with a DNA-PKcs expressing vector (V3-F18) 72 and 120 hr after irradiation with 4 Gy (Chan et al., 2002). As expected, the DNA-PKcs positive cells clearly had a higher number of viable and dividing cells per culture than the DNA-PKcs deficient culture at both time points (Fig. 14A).

Next we irradiated our transduced HeLa subclones and three different GFP only controls (GFP.C1, GFP.C2 and GFP.C3) with either 4 or 11.5 Gy. After irradiation with 4 Gy, there was no difference between the HeLa and the GFP controls (Fig. 14B). In contrast subclones PP5.C4 and PP5.C13 were more radiosensitive, while subclone PP5.C7 was most sensitive. To investigate the effects of a higher dose, we irradiated the cells with 11.5 Gy (Fig. 15A and B). The differences are easily seen in the FSC/SSC panels (Fig. 15A), which after 5 days showed a distinct population of viable and dividing cells for HeLa and GFP.C3, while this was not the case for the cells with aberrant PP5 expression. As another way to measure the viability of the transduced cells we determined their ability to express GFP, with similar results. When we determined by flow cytometry the numbers of GFP positive cells in the very same experiments, they were in line with the survival rates calculated by counts in the FSC/SSC (data not shown).

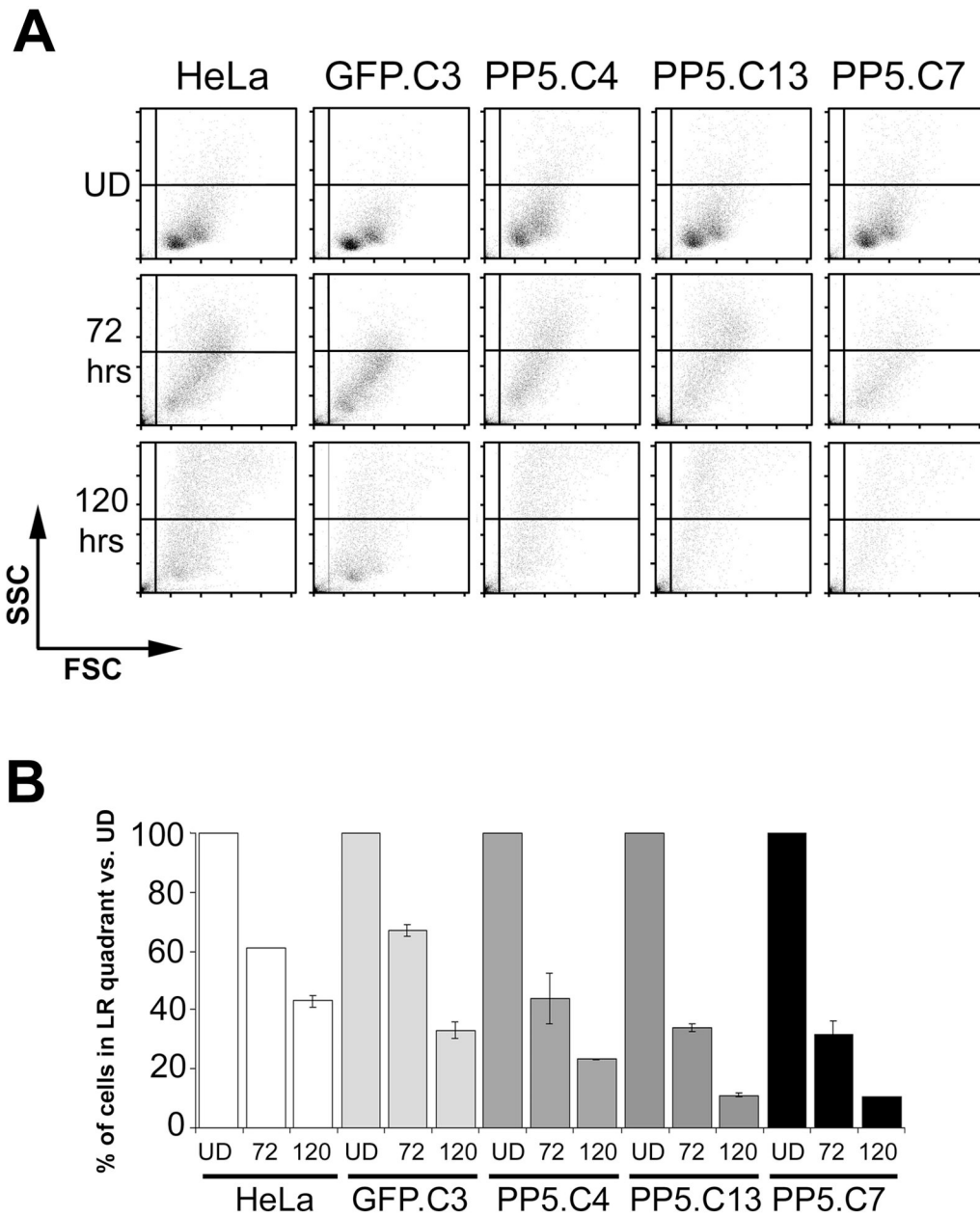


Figure 15. Survival of irradiated cell lines, assayed by flow cytometry

(A and B) HeLa subclones were irradiated with 11.5 Gy and analyzed after 72 hr and 120 hr. FSC, forward scatter; SSC side scatter. For all cell lines the percentage of viable cells represented in the lower right quadrant of FSC/SSC as shown in (A) was plotted compared to undamaged (UD) cultures.

4.2. Ku70 binding protein 3 (Kub3) is a putative metalloproteinase and interacts with DNA-PKcs

4.2.1. Human Kub3 is a protein of 246 amino acid residues with a highly conserved metalloprotease domain

In order to characterize the Kub3 protein we first determined the complete cDNA sequence of human Kub3. For this we searched the human expressed sequence tags (ESTs) from the NCBI Genbank for cDNAs that were homologous to the mouse coding sequences of the three yeast two-hybrid hits. All ORFs that we found were identical to the putative partial sequence posted by Yang and colleagues (Yang et al., 1999a). Since this ORF contained both an N-terminal methionine and a stop codon, we considered the possibility that the full length Kub3 protein is encoded by this 741 bp cDNA. Indeed, after extensive search in the NCBI and Celera databases, we did not find a Kub3 ORF that extended further to the N-terminus and had a methionine start codon. Therefore, we conclude that in the original yeast two-hybrid screen the identified Kub3 cDNA contained the upstream untranslated region and thus gave the wrong impression of a longer protein.

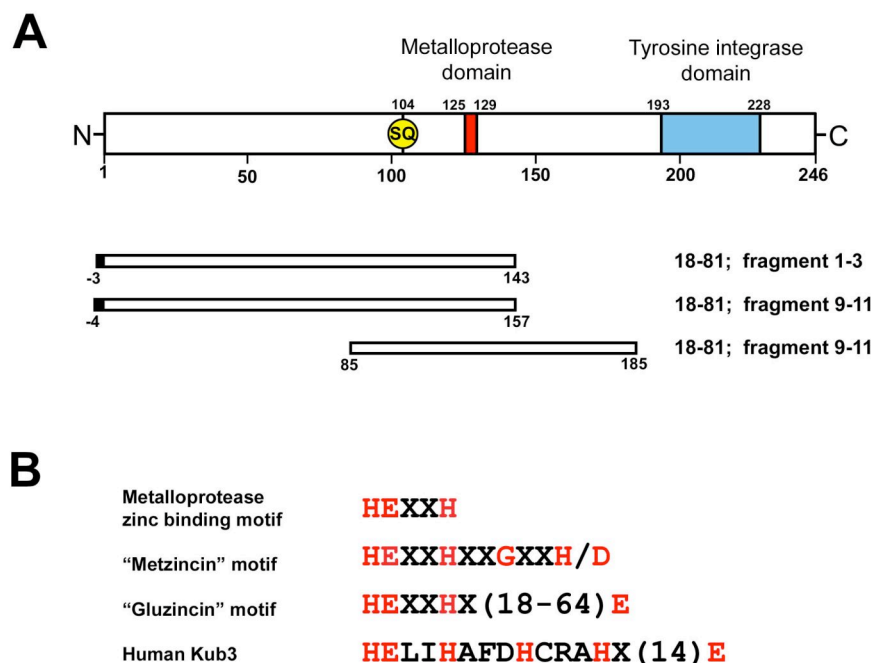


Figure 16. Protein structure of human Kub3

(A) Protein structure and two putative functional domains of the 246 aa Kub3 protein are depicted. The numbers refer to amino acid residues. The mouse cDNA clones encoding the Kub3 fragments that bound to the indicated human DNA-PKcs fragments are shown. The two consecutive amino acid residues serine/glutamine acid (SQ) represent a potential DNA-PKcs phosphorylation site. (B) The minimal consensus metalloproteases sequence HEXXH and conserved motifs of the metalloprotease subfamilies “metzincins” and “gluzincins” compared to the putative Kub3 metalloprotease region. The numbers in brackets refer to the number of unspecified residues X which lie between the H and E residues.

In fact this was also the case for two of our three yeast two-hybrid hits which contained two and three additional N-terminal amino acid residues, respectively (Fig. 16A). However, this does not rule out the existence of splice variants as suggested by Fischer and colleagues (Fischer et al., 2001).

In order to find clues for the function of Kub3 we conducted an extensive sequence analysis of the Kub3 protein. In the initial NCBI entry, an tyrosine integrase domain of Kub3 was mentioned but not further described. Tyrosine integrases are site specific DNA recombinases which can integrate and excise DNA involving an essential tyrosine residue (Esposito and Scocca, 1997). The well-characterized lambda integrase and the cre recombinase are both examples for tyrosine integrases (Esposito and Scocca, 1997). When we attempted to find the described domain in Kub3, the only hint in the amino acid sequence were several C-terminal tyrosine residues that are essential for tyrosine integrase domains when combined with upstream arginine residues. Even though there were several arginine residues upstream, only one combination of the arginine, at position 194, and the tyrosine at position 228 constituted the conserved distance necessary for integrase function (data not shown). However, when compared to the tyrosine integrase like cre recombinase sequence, several other conserved residues were missing (data not shown). Despite these differences we can not rule out that Kub3 possesses integrase activity.

Another NCBI entry for Kub3 suggested a zinc-metalloprotease function (Fig. 16A). Consistent with this, we identified two motifs, HCRAH and HEXXH, which both contained the two histidine residues in proximity that are essential for the zinc-binding of metalloproteases (Hooper, 1994). Although it is possible that the HCRAH motif has also enzymatic activity (Dr. Charles Craik, personal communication), we decided to focus on the more conserved HEXXH motif. The zinc-metalloproteases can be further divided into subfamilies with respect to other amino acid residues that participate in the binding of zinc. For the “metzincins”, which include matrix metalloproteases, a close downstream third histidine, a conserved glycine (in the HEXXHXXGXXH/D motif) and a methionine turn are characteristic (Bode et al., 1993). Although human Kub3 has two more histidine residues downstream of the HEXXH motif, the strictly conserved glycine is missing (Fig.16B). The members of the other subfamily, the “gluzincins”, have a conserved glutamic acid residue 18-64 positions downstream of the HEXXH motif (Hooper, 1994). In this context we found in Kub3 several glutamic acid residues, which were located 22, 37 or 70 positions downstream of the HEXXH catalytic site (Fig. 16B). This raised the possibility that Kub3 is a “gluzincin” metalloprotease.

Because functional protein domains tend to be highly conserved among species, we compared Kub3 protein sequences of several organisms from yeast to human (Fig.17). Remarkably, all Kub3 orthologs were in the range of 194-283 amino acid residues. Also, when we performed a protein Blast search in the non-redundant NCBI protein database with the putative metalloprotease region (106 aa-151 aa) of human Kub3 we only found proteins of similar size. When we aligned all ortholog sequences, the comparison showed the highest degree of conservation in the putative metalloprotease domain (Fig. 17).

Results - Kub3 interacts with DNA-PKcs

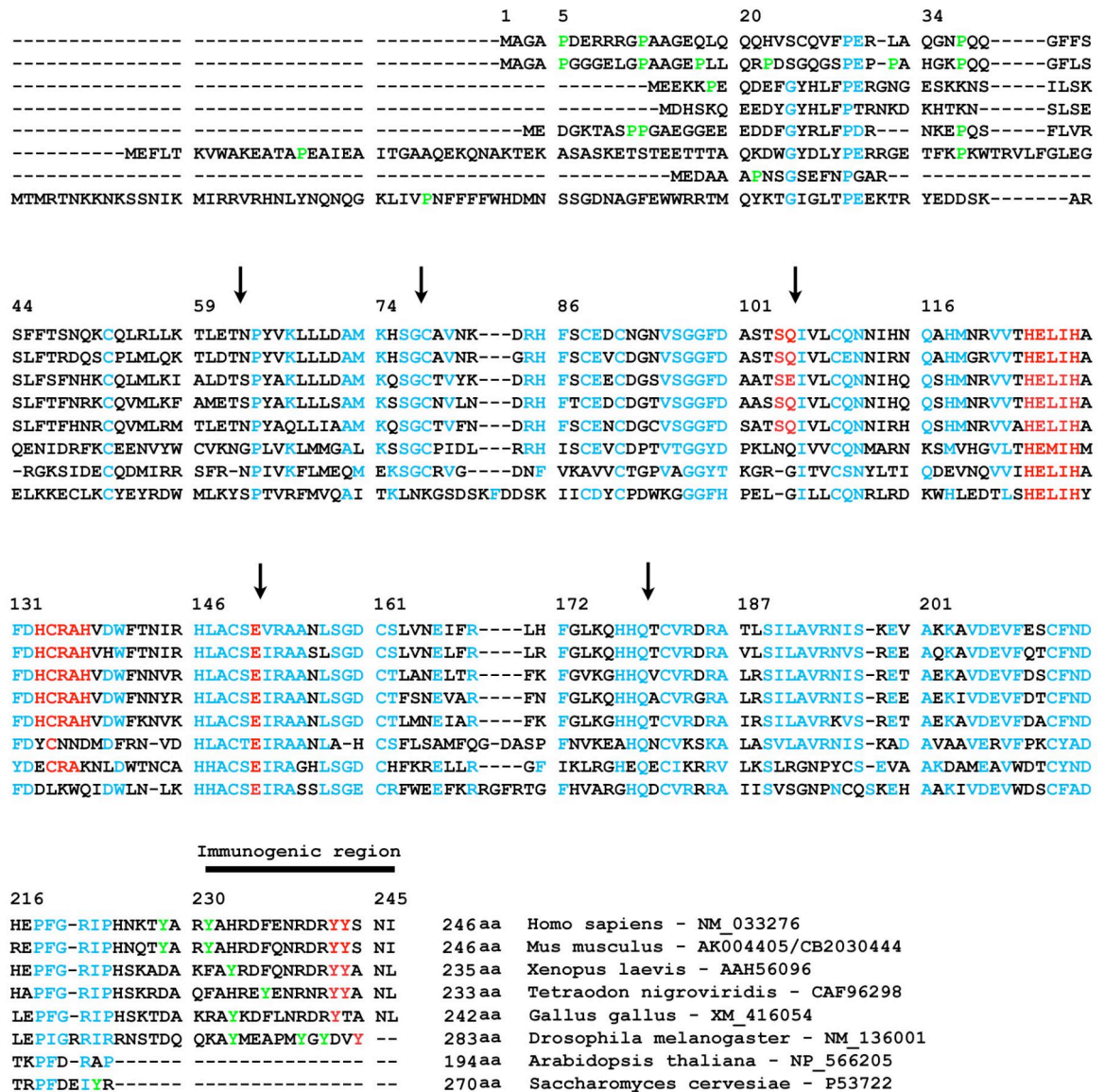


Figure 17. Alignment of Kub3 orthologs

Kub3 protein orthologs from the indicated organisms were aligned using ClustalW 1.8 X. Respective length of protein in aa and Genbank entries are shown. The colors highlight highly conserved amino acid residues of putative (red) or unknown function (blue). Green color depicts amino acid residues with low conservation of the position but typical for the N-terminus and C-terminus, respectively. The arrows mark the splice sites of the corresponding human Kub3 cDNA. Also shown is the human Kub3 C-terminal immunogenic region which was used for the anti-Kub3 antibody.

Especially the HEXXH motif was conserved from yeast to human. In contrast, the HCRAH motif was not found in yeast, drosophila and arabidopsis. Because these non-vertebrate organisms have Ku70/Ku80 orthologs but no DNA-PKcs ortholog, it is tempting to speculate that the HCRAH motif represents an adaption to the evolution of DNA-PKcs. Since Kub3 is a putative interaction partner of DNA-PKcs we also searched

for potential DNA-PKcs phosphorylation sites like pairs of serine/glutamine (SQ) or threonine/glutamine (TQ) residues. Indeed, at position 104 of human Kub3 we found a single SQ site, which is conserved only in the organisms with DNA-PKcs orthologs (Fig. 17). One explanation for the specific conservation of the HCRAH motif and the SQ site is that Kub3 is regulated by DNA-PKcs phosphorylation and has adapted its function to NHEJ involving DNA-PKcs.

We also looked at the conservation of other metalloprotease features. Of the before mentioned glutamic acid residues downstream of HEXXH only the one at position 151 (E151) is conserved in all species. It is located in the middle of a seven amino acid residue stretch that is identical in all orthologs (Fig. 17). This high degree of conservation implies that E151 is important for Kub3 function and also supports the idea that Kub3 is a “gluzincin” metalloprotease.

Because proteases can digest a large variety of proteins, their activity needs to be tightly regulated within the cell. That is why, for example, the members of the matrix metalloproteinase family have upstream of the catalytic site an inhibitory cysteine residue (cysteine switch), which interferes with zinc binding and renders the enzyme inactive (Springman et al., 1990). Upon cleavage of this pro-protease the cysteine is removed and the protease is enzymatically active (Van Wart and Birkedal-Hansen, 1990). Interestingly, we found several highly conserved cysteine residues upstream of the putative catalytic domain, which could constitute such a cysteine switch (Fig. 17).

Another interesting feature of all Kub3 orthologs is the existence of several tyrosine residues at the C-terminus (Fig. 17). Especially in vertebrates, the tyrosine residue five positions from the C-terminal end is conserved. Usually, C-terminal tyrosines are a common feature of oncoproteins like src, which are regulated by receptor tyrosine kinases (Bromann et al., 2004). They are also critical residues for DNA processing enzymes like topoisomerases and tyrosine integrases (Esposito and Scocca, 1997; Yu et al., 2004). Despite the low homology to known integrases the conservation at the C-terminus indicates that Kub3 might have such an activity. Another conserved characteristic of Kub3 is the existence of a few interspersed proline residues in the N-terminal region. Their abundance at the overall lowly conserved N-terminus suggests that they may be important for Kub3 function.

It has been suggested that functional protein domains are mostly embedded within one exon, allowing the process of “domain shuffling” during evolution (Liu and Grigoriev, 2004). To test if this is true for Kub3, we determined the exon/intron boundaries for the human 741 bp Kub3 transcript (Fig. 17). This also addressed the question which functional domains would be affected by the alternative splicing described by Fischer and colleagues (Fischer et al., 2001). To do so we used human genomic data from the Celera database and data from the ACEVIEW resource at NCBI. Surprisingly, we were not able to find the GAS16 sequence in the 1.7 kb intronic sequence supplied by ACEVIEW. Apart from that we found that the highly conserved region containing the putative metalloprotease domain resides entirely in exon four. This also includes the

conserved glutamic acid at position 151, which is another strong indication that this whole region of the protein is important.

We further deduced that the integration of the GAS16 sequence described by Fischer and colleagues would occur between the exons four and five. Because exon four contains the metalloprotease domain, we conclude that such a splice variant of Kub3 could have enzymatic activity.

In summary, we are confident that we have identified the correct reading frame of human Kub3 which is a protein composed of 247 amino acid residues. Furthermore, we have characterized a zinc-metalloprotease domain which is highly conserved among species. Additionally we found indications that Kub3 is a member of the “gluzincin” metalloprotease family and might be regulated by a cysteine switch.

4.2.2. A polyclonal antibody against the Kub3 C-terminus recognizes a 29 kD protein and variants of similar size

In order to study Kub3 in vivo we raised a polyclonal rabbit antibody against human Kub3. As immunogenic region we chose the C-terminal 16 amino acid residues (YAH RDFENRDRYY SNI) of the reading frame that we had previously identified as Kub3 (Fig. 17). As a positive control for the anti-Kub3 antibody we stably overexpressed human C-terminal myc-tagged Kub3 (mycKub3) in HeLa cells using a retroviral vector under puromycin selection (referred to as HeLa.mycKub3 cells). HeLa.GFP cells, which express GFP under puromycin selection, served as negative control. By using the online protein prediction tool Compute pI/Mw we predicted the molecular weight for Kub3 (28.1 kD) and mycKub3 (29.6 kD). Accordingly, the mycKub3 protein, which was resolved at approximately 30 kD, was readily detectable using an anti-myc antibody in both whole cell lysates and nuclear extracts from HeLa.mycKub3 cells (Fig. 18A, upper panel).

Next we tested if the polyclonal anti-Kub3 antibody could also detect mycKub3. After affinity purification the antibody recognized overexpressed mycKub3 of approximately 30 kD and endogenous Kub3 of approximately 28 kD (Fig. 18A, lower panel). We also observed that the signal in whole cell lysates was somewhat stronger than in nuclear extracts. Using a gel with higher resolution for the bands around 30 kD, we found two forms of endogenous Kub3 in whole cell lysates of HeLa.GFP cells (Fig. 18B). To our surprise in HeLa.mycKub3 cells we found four forms of Kub3 (Fig. 18B). Remarkably, the two bands supposedly representing endogenous Kub3 were also much stronger when mycKub3 was overexpressed. We also noticed several bands of higher molecular weight of approximately 50, 70, 80, 200 and 250 kD, respectively (Fig. 18A, lower panel). Considering the fact that our antibody bound to the C-terminus of Kub3, it was possible that these larger bands represented larger splice variants of Kub3, like the reported 220 kD/300 kD bands or the alternatively spliced product (Fischer et al., 2001; Yang et al., 1999a).

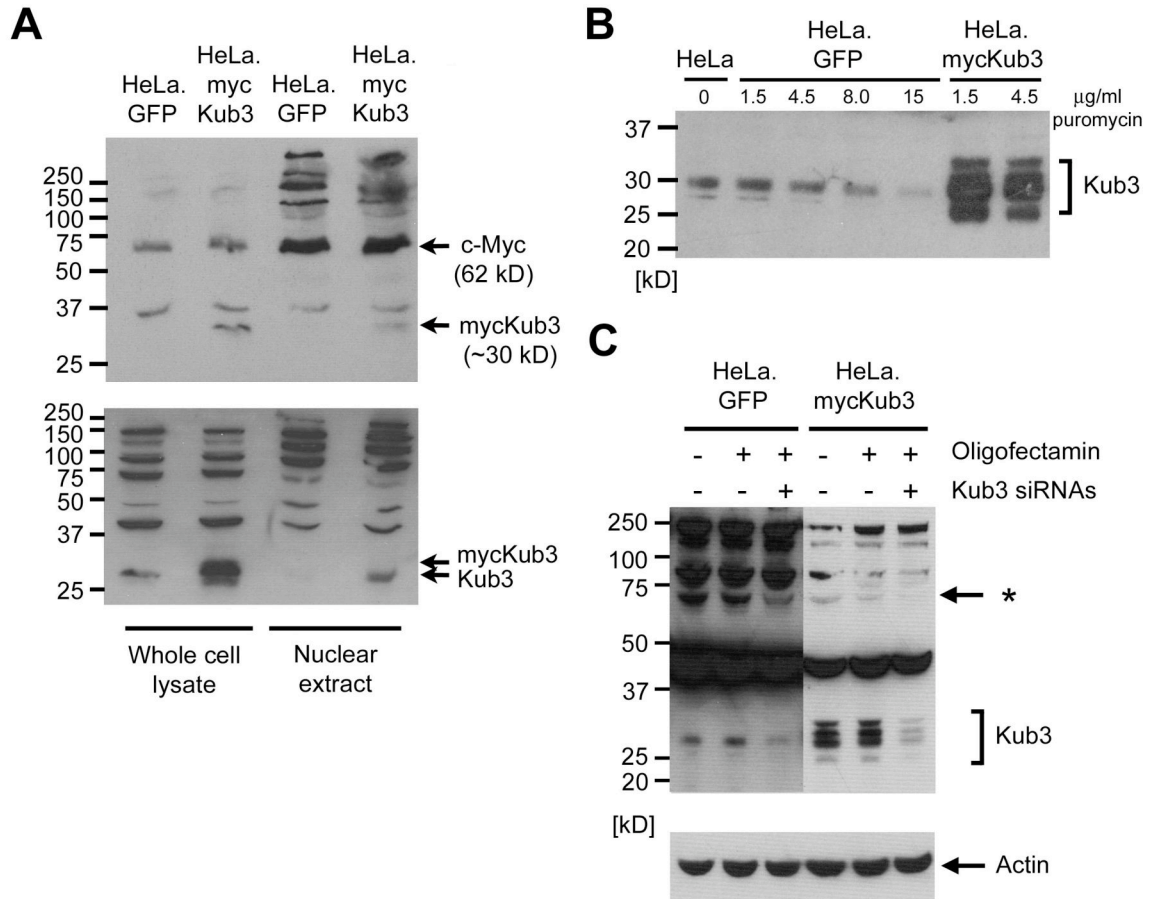


Figure 18. Polyclonal antibody against Kub3

(A) Western blotting of whole cell lysates (35 µg) and nuclear extracts (40 µg) of HeLa cells overexpressing either GFP or mycKub3. After SDS-PAGE (10% gel) the extracts were transferred to a membrane by wet electroblotting and probed with anti-myc antibody (1:200 dilution) (upper panel) or anti-Kub3 antibody (1:100 dilution) (lower panel). For (A), (B) and (C) goat anti-rabbit antibody coupled to HRP (Southern Biotech) was used in a 1:2500 dilution as secondary antibody. (B) Western blotting of whole cell lysates (30 µg) from HeLa.GFP and HeLa.mycKub3 cells grown for seven days under various puromycin concentrations as shown. For (B) and (C) cell lysates were separated on a pre-cast 4-12% NuPAGE® Bis-Tris Gel (Invitrogen) by SDS-PAGE and transferred on a membrane and probed with anti-Kub3 antibody (1:100) and anti-actin antibody (1:400) (loading control). (C) RNAi of HeLa.GFP and HeLa.mycKub3 cells. Cells were treated with Kub3 specific siRNAs and Oligofectamine transfection reagent as indicated. Whole cell lysates (70 µg) were then analyzed by Western blotting. The left side of the membrane was exposed longer to make the endogenous Kub3 visible. * putative long form of Kub3.

To investigate which bands are in fact variants of Kub3, we knocked down Kub3 in HeLa.mycKub3 and HeLa.GFP cells by transfecting a mixture of five different Kub3 specific siRNAs (Fig. 18C). The results showed that the two endogenous forms in HeLa.GFP and the four forms in HeLa.mycKub3 were affected by RNAi, confirming that they all represent Kub3. Interestingly, a band migrating at approximately 70 kD also seemed to be affected by Kub3 specific RNAi (Fig. 18C). As mentioned before, this could represent a larger splice variant of Kub3. However, we found no evidence for other Kub3 isoforms with a molecular weight of 220 or 300 kD.

There are several possible explanations for the multiple Kub3 bands. One possibility is that the two largest bands represent mycKub3 and the lower two bands represent endogenous Kub3. Furthermore, the respective two forms of Kub3 and mycKub3 could differ in their phosphorylation state and therefore would migrate differently. Because we found a potential DNA-PKcs phosphorylation site in Kub3, it is conceivable that this putative phosphorylation is mediated by DNA-PKcs and is therefore linked to DNA damage. To test this hypothesis, we treated whole cell lysates from undamaged and damaged (20 Gy) HeLa.mycKub3 and HeLa.GFP cells with λ protein phosphatase (λ -PPase) (Fig. 19). As positive control we used a phospho-specific antibody against ATM pS1981, which gets phosphorylated after IR (Bakkenist and Kastan, 2003). We could detect ATM S1981 phosphorylation 2 hr after 20 Gy and this phosphorylation was sensitive to λ -PPase treatment. This was not the case when we combined λ -PPase with EDTA at inhibitory concentrations. In fact, the ATM pS1981 signal was much stronger when EDTA was added (Fig. 19). In contrast, none of the Kub3 specific bands showed any difference between undamaged and damaged samples and none of the bands was sensitive towards λ -PPase treatment alone or in combination with EDTA. This rules out that that DNA damage dependent phosphorylation accounts for these bands.

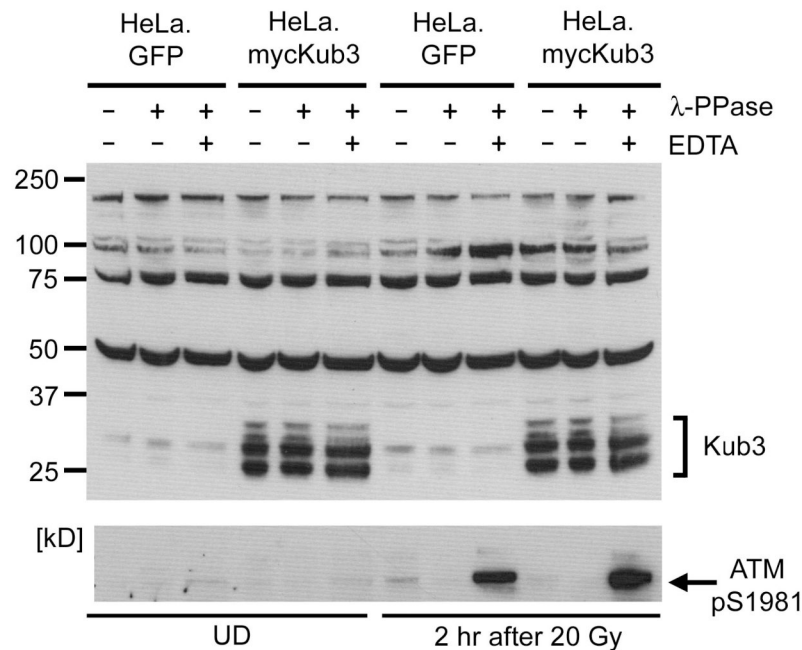


Figure 19. λ protein phosphatase (λ -PPase) treatment of Kub3

Whole cell lysates (60 μ g) of undamaged (UD) and damaged (2 hr after 20 Gy) HeLa.GFP and HeLa.mycKub3 cells were either mock treated or treated with λ -PPase (400 U for 1 hr at 30°C) with or without EDTA (50mM). Half of this reaction (30 μ g protein) was separated on a pre-cast 4-12% NuPAGE® Bis-Tris Gel (Invitrogen) by SDS-PAGE. After wet electrotransfer to a nitrocellulose membrane, the membrane was incubated with anti-Kub3 antibody (1:100 dilution) (upper panel) or anti-pS1981 ATM antibody (1:500 dilution) (lower panel). As secondary antibody, goat anti-rabbit antibody coupled to HRP (Southern Biotech) was used in a 1:2500 dilution.

4.2.3. Kub3 is localized in the nucleus

Most DNA repair proteins, like DNA-PKcs or Ku, are localized in the nucleus (Graeme C.M. Smith, 1999). Under the fluorescence microscope they show an even distribution in undamaged cells (Fig. 20). To determine if Kub3 is localized in the nucleus, we tested the polyclonal Kub3 antibody in immunofluorescence experiments on HeLa cells expressing either GFP or mycKub3. After staining with the Kub3 antibody we observed a strong nuclear signal in both cell types (Fig. 20). Most importantly, HeLa.mycKub3 cells showed a much stronger nuclear signal than HeLa.GFP cells, which indicates that the polyclonal antibody is specific for Kub3 when used in immunofluorescence. Staining with pre-immune serum, or the secondary antibody alone, showed an evenly distributed background signal only (Fig. 20). Therefore we conclude that Kub3 is a nuclear protein just like DNA-PKcs.

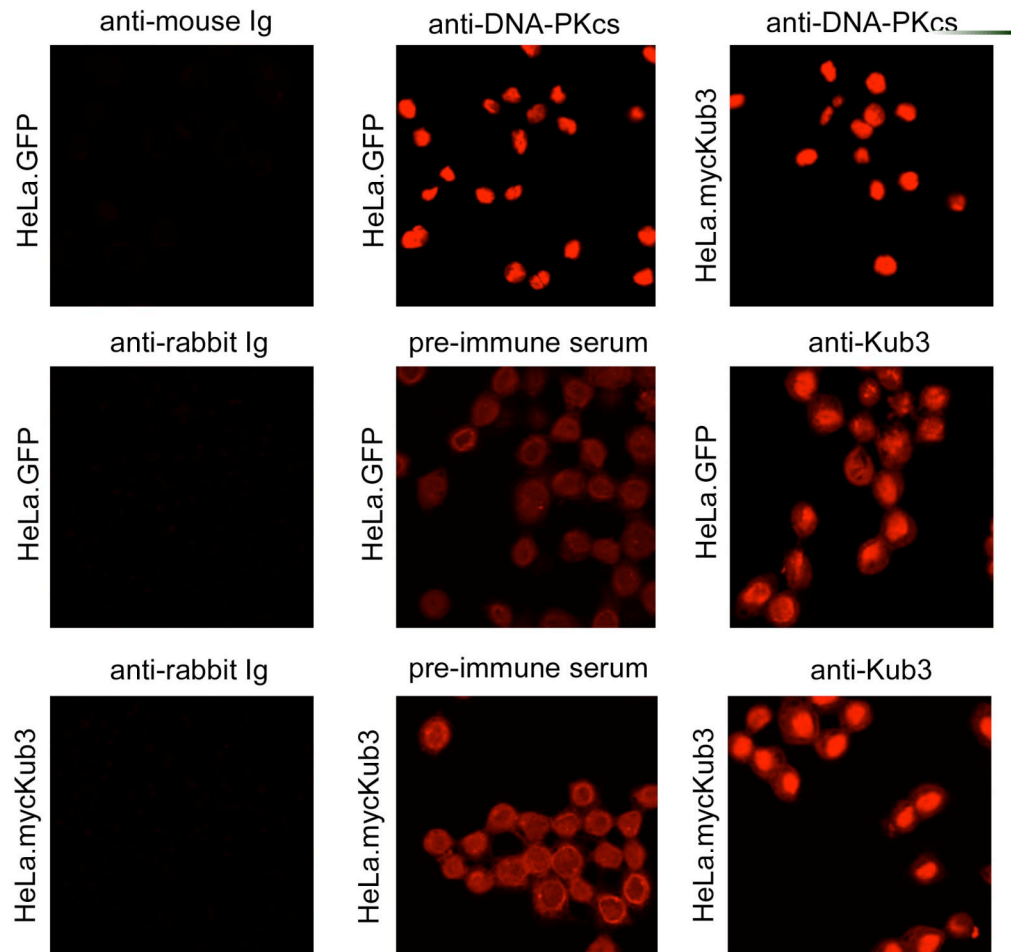


Figure 20. Cellular localization of Kub3

Confocal microscopy of HeLa.GFP and HeLa.mycKub3 cells. Cells were fixed with icecold methanol and stained with either secondary antibody only, rabbit pre-immune serum, mouse anti-DNA-PKcs antibody 25-4 or rabbit anti-Kub3 antibody. Secondary antibodies were either rabbit anti-mouse Ig rhodamin coupled or goat anti-rabbit Ig texas-red coupled.

4.2.4. Kub3 co-precipitates with DNA-PKcs

Because DNA-PKcs and Kub3 are both nuclear proteins and could interact in the yeast two-hybrid screen, we tried to validate this interaction by co-immunoprecipitation experiments in HeLa cells. The following experiments were carried out in conjunction with Sandra Fickenscher (Diplomarbeit "Kub3 als Co-Faktor der DNA-abhängigen Proteinkinase DNA-PK"). In order to verify the DNA-PKcs/Kub3 interaction we first pulled down DNA-PKcs from HeLa.GFP and HeLa.mycKub3 cells using the mouse monoclonal antibody 25-4, and stained the precipitates for DNA-PKcs (data not shown) and Kub3 (Fig. 21). While in the HeLa.GFP cells co-precipitation of Kub3 with DNA-PKcs did not occur, we saw two bands at approximately 30 kD after precipitates were stained with the antibody to Kub3 (Fig. 21, right panel, lane 3). The position of these bands was the same size as for Kub3 in the whole cell lysate and as for Kub3 pulled down directly with the anti-Kub3 antibody. The negative controls (beads only and unspecific IgG1 antibody) did not produce any bands at this size (Fig. 21, right panel, lane 1 and 2). Therefore we conclude that, when overexpressed, Kub3 can be co-precipitated with DNA-PKcs in HeLa cells. For this reason we used HeLa.mycKub3 cells in the experiments that followed. To investigate if antibodies binding to different regions of DNA-PKcs can pull down Kub3, we used the following mouse monoclonal DNA-PKcs antibodies: 18-2, which binds somewhere in the first 2700 aa of DNA-PKcs; 25-4, which binds to the N-terminus of DNA-PKcs; and 4F10C5, which binds to the C-terminus of DNA-PKcs.

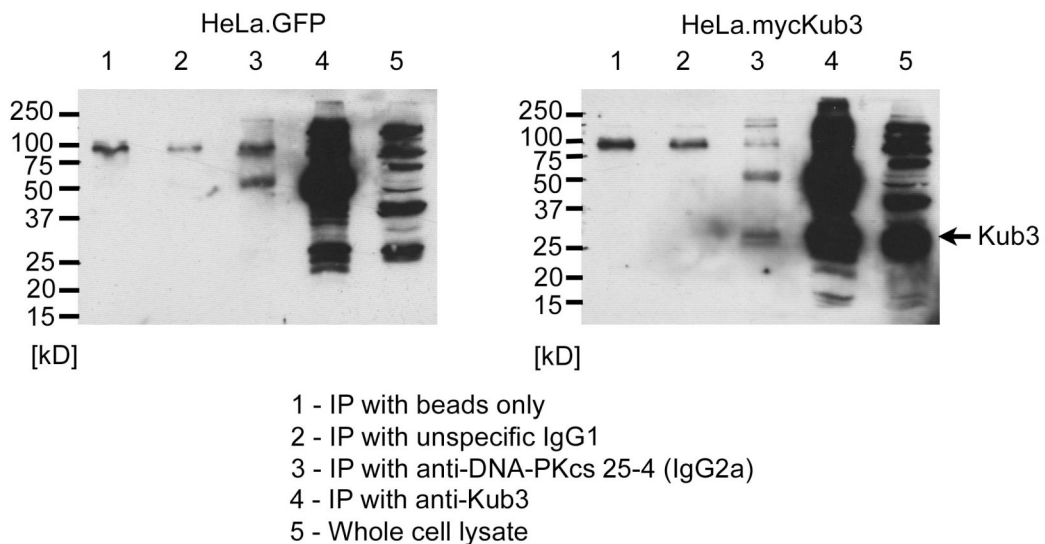


Figure 21. Kub3 Co-immunoprecipitation with DNA-PKcs

Western blotting of co-immunoprecipitates (lanes 1-4) and whole cell lysates (lane 5) from undamaged HeLa.GFP and HeLa.mycKub3 cells. Membranes were stained with anti-Kub3 antibody. Pull down antibodies are shown with Ig isotype if possible. Negative controls were protein G coupled sepharose beads alone (lane 1) and non-specific IgG1 antibody (lane 2).

We also included unspecific IgG1 and IgG2a antibody controls and pre-immune rabbit serum from the animal that produced the anti-Kub3 antibody. While all anti-DNA-PKcs antibodies successfully pulled down Kub3 (Fig. 22A, upper panel, lanes 5-7), the unspecific IgG2a antibody also pulled down a small amount of Kub3 (Fig. 22A, upper panel, lane 8). Although also small amounts of DNA-PKcs were detectable in this sample (Fig. 22A, lower panel, lane 8) and the Kub3 bands were much weaker than for the three DNA-PKcs pull downs, we decided to extend our IgG2a controls. Therefore, for the next experiments we included another unspecific IgG2a antibody and a mouse monoclonal anti-ATM IgG2a antibody (Fig. 22B, lane 3). This also served as a control against the non-specific stickiness of large PI-3 like kinases such as DNA-PKcs, ATM and ATR. Additionally we carried out two experimental sets with pull down incubation times of 1 hr and 3 hr. Interestingly, we found that Kub3 co-precipitated with DNA-PKcs only up to 1 hr (Fig. 22B) but not up to 3 hr (data not shown). One explanation for this is that the interaction between the two proteins is very fragile and can be disrupted by longer incubation times. We did not see any bands in the negative controls (Fig. 22B, lanes 3-5).

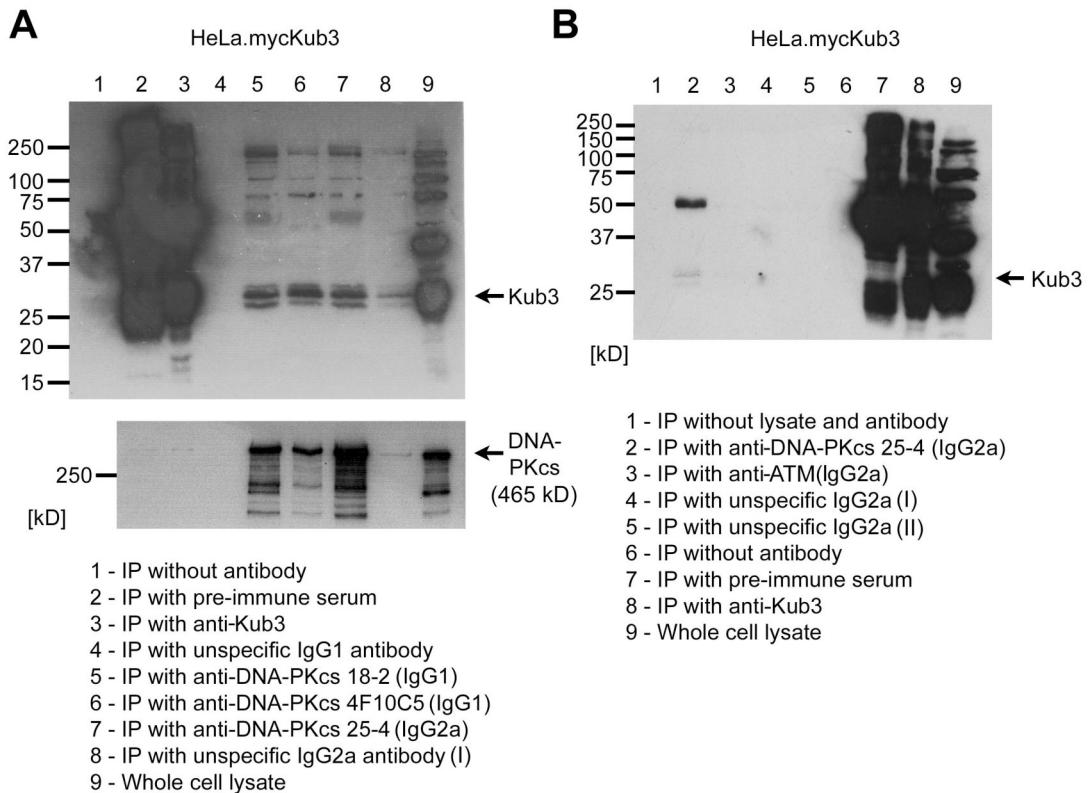


Figure 22. Kub3 Co-immunoprecipitation with DNA-PKcs

Western blotting of co-immunoprecipitates (lanes 1-8) and whole cell lysates (lane 9) from undamaged HeLa.mycKub3 cells. (A) Upper panel stained with Kub3 antibody. Lower panel stained with anti-DNA-PKcs antibody 18-2. Pull down antibodies are shown with Ig isotype if possible. The position of Kub3 is indicated. (B) Pull down antibodies are shown with Ig isotype if possible. The position of Kub3 is indicated. Membranes were stained with anti-Kub3 antibody and exposed until the putative Kub3 bands were visible. Therefore the lanes with the pre-immune serum IP, the Kub3 IP and the whole cell lysate appear overexposed.

However, the Kub3 signal was very weak, and so it is hard to tell if non-specific bands with the previous IgG2a control would be visible under these conditions. It is important to note, that it was not possible to co-precipitate DNA-PKcs with the Kub3 antibody. This may be due to the size of DNA-PKcs: with 465 kD it is more than fifteen times bigger than the bait protein Kub3 with 29 kD.

In summary, we have found strong indications that Kub3 and DNA-PKcs interact in HeLa cells, but further studies need to be done to confirm this connection.

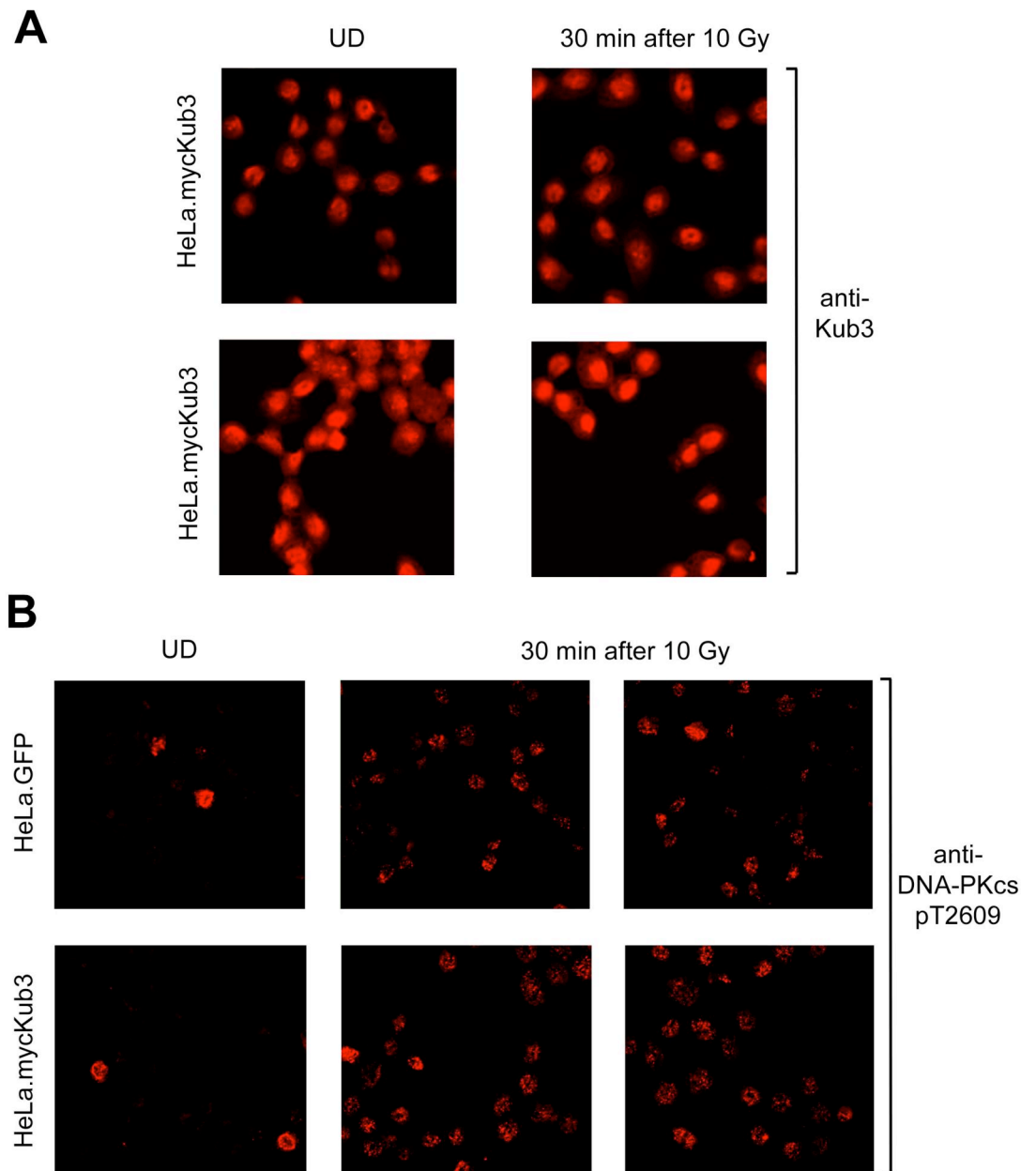


Figure 23. Cellular localization of Kub3 and pT2690 foci formation after DNA damage

Confocal microscopy of methanol fixed HeLa.GFP and HeLa.mycKub3 cells. (A) Undamaged (UD) or irradiated cells (30 min after 10 Gy) were stained with anti-Kub3 antibody as indicated. (B) Undamaged (UD) or irradiated cells were stained with anti-DNA-PKcs pT2690 antibody as indicated.

4.2.5. Kub3 does not redistribute after DNA damage

After confirming that DNA-PKcs can interact with Kub3 we next wanted to investigate the role of Kub3 in DSB repair. Upon DNA damage several DNA repair proteins, like H2AX or 53BP1, change their distribution in the nucleus and form so-called damage foci (Chan et al., 2002).

To test if either is the case for Kub3, we stained undamaged and irradiated cells (10 Gy) with anti-Kub3 antibody (Fig. 23A). After 30 min we did not see any redistribution of Kub3 in the nucleus. However, other DSB repair proteins form damage foci only after phosphorylation. Because our antibody recognizes total Kub3, the redistribution of such a Kub3 subpopulation might remain undetected.

4.2.6. Kub3 overexpression leads to increased DNA-PKcs pT2609 phosphorylation

To learn more about the function of Kub3 we investigated whether or not the overexpression of mycKub3 has an effect on DSB repair. Based on the hypothesis that Kub3 is a negative regulator of NHEJ, we would expect a decrease in DNA-PKcs activity when Kub3 is overexpressed. DNA-PKcs activity can be readily determined by its ability to autophosphorylate and to form pT2609 foci. Therefore, we checked if DNA-PKcs pT2609 foci formation was decreased in HeLa.mycKub3 cells versus HeLa.GFP cells and found that both cell types were indistinguishable with respect to pT2609 foci formation (Fig. 23B).

Although we found no evidence for altered DNA-PKcs T2609 foci formation under the fluorescence microscope when Kub3 is overexpressed, we decided to test the kinetics of pT2609 phosphorylation by Western blotting: we irradiated HeLa.GFP and HeLa.mycKub3 cells with 20 Gy, prepared nuclear extracts at different timepoints and stained them with a polyclonal anti-pT2609 antibody (Fig. 24A). We found in several experiments that when mycKub3 was overexpressed DNA-PKcs T2609 phosphorylation was increased even in the degradation products of DNA-PKcs. In previous experiments we had determined that in HeLa cells, DNA-PKcs T2609 phosphorylation peaked around 9 hr (data not shown). Therefore, we followed pT2609 phosphorylation by western blotting over up to 12 hr after IR. As expected, in the control HeLa.GFP cells phosphorylation peaked after 9 hr followed by a decline after 12 hr (Fig. 24B). In contrast, after 12 hr the pT2609 phosphorylation signal was still very strong in the HeLa.mycKub3 cells (Fig. 24B). But other DNA damage markers, like DNA-PKcs pS2056 (Chen et al., 2005) and ATM pS1981 (Bakkenist and Kastan, 2003) phosphorylation showed no differences in the same lysates (data not shown). This rules out that the increase of DNA-PKcs pT2609 phosphorylation is due to additional DNA damage caused by Kub3 overexpression.

We conclude that Kub3 overexpression leads to DNA-PKcs pT2609 hyperphosphorylation after IR compared to controls. This effect of Kub3 overexpression seems to be specific for DNA-PKcs and suggests a role for Kub3 in the regulation of NHEJ.

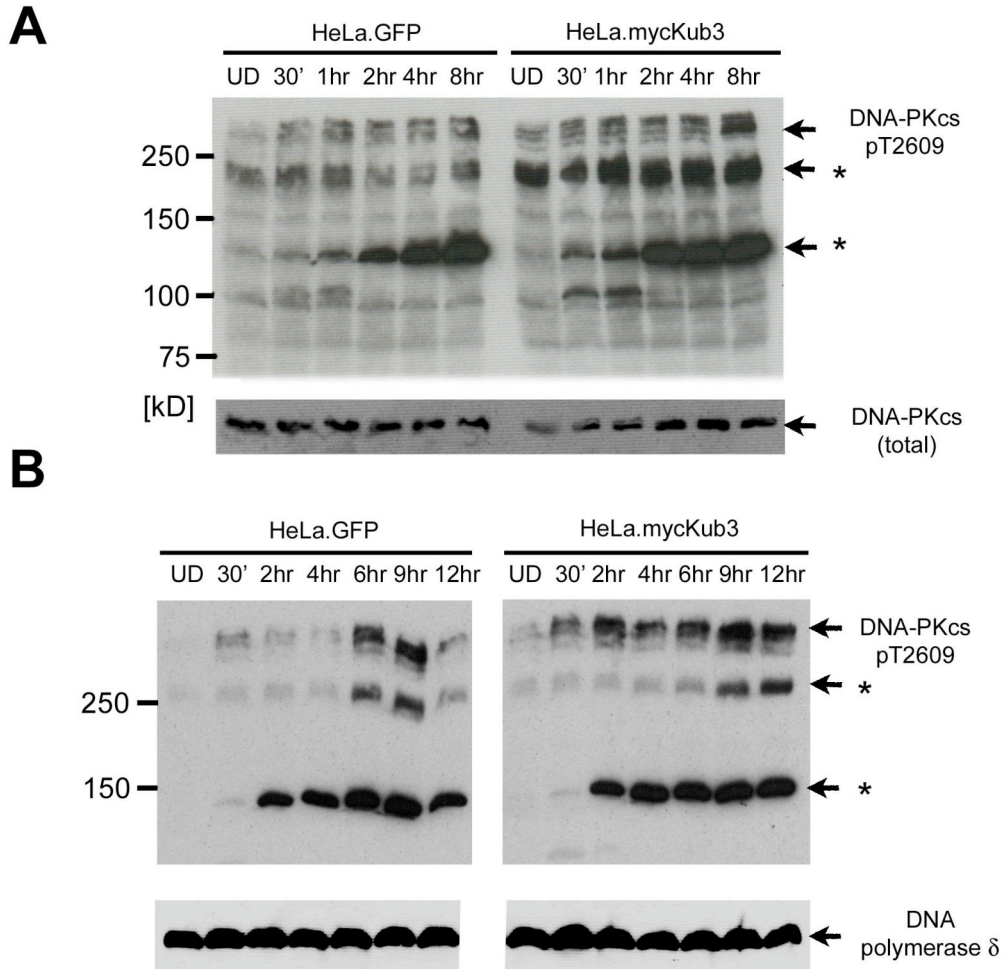


Figure 24. DNA-PK pT2609 phosphorylation

Western blotting of nuclear extracts (70 μ g) from HeLa.GFP and HeLa.mycKub3 cells. After SDS-PAGE (6 % gel) the extracts were transferred to a membrane by wet electroblotting and probed with anti-DNA-PKcs pT2609 (1:300 dilution) and anti-DNA-PKcs (total) (1:100) or anti-DNA-polymerase δ (1:300 dilution) (lower panel). For (A) and (B) goat anti-rabbit antibody coupled to HRP (Southern Biotech) was used in a 1:2500 dilution as secondary antibody. (A) Lysates were prepared from undamaged (UD) or irradiated cells (20 Gy) after the indicated time points. (B) Cells were treated under identical conditions as in (A), but tested at different time points after DNA damage. * and ** denote phosphorylated DNA-PKcs degradation products.

4.2.7. RNAi and double-strand break repair in *Drosophila melanogaster*

Drosophila melanogaster is an emerging organism of investigation with respect to DNA damage repair pathways. One reason is the fact that single and double mutants of drosophila can be created with ease (Adams and Sekelsky, 2002). Another reason is that in drosophila cell lines like S2, genes can be effectively knocked down by RNAi (Clemens et al., 2000). RNAi knock down in drosophila is carried out by incubation of S2 cells with dsRNA of about 500 bp in length. Without the need for transfection reagents the cells actively take up the dsRNA and appear to spread the effect to other cells in culture (Clemens et al., 2000). Hereby, the efficiency and duration of the RNAi effect in drosophila is superior to the effect in mammals.

Very conveniently, most of the DNA repair pathways in drosophila are highly homologous to their mammalian counterparts (Sekelsky et al., 2000). Furthermore, genetic mobile elements, like the P-element, provide powerful tools to study DSB repair (Rio, 1991). DSB repair after P-element excision is carried out predominantly by synthesis-dependent strand annealing (SDSA) (Adams et al., 2003). SDSA is a homology directed DSB repair pathway which relies on the invasion of single-stranded DNA into the donor locus and subsequent DNA synthesis using the donor DNA strand as template (Nassif et al., 1994). A protein involved in SDSA is the ortholog of the mammalian Blm protein, which is encoded by the Mus309 locus. Flies bearing a mutation in Mus309 have increased sensitivity towards MMS, IR and UV light (Min et al., 2004). Recent data indicates that Blm is involved in the dissociation of the invading strand from the complementary strand (McVey et al., 2004b). That is why Blm mutants exhibit large deletions flanking a P-element excision site (McVey et al., 2004b).

Another protein involved in drosophila DSB repair is the Rad54 ortholog encoded by the okra locus (Kooistra et al., 1997). Like its mammalian counterpart, it is essential for the repair of double-strand breaks by HR involving Holliday junctions (Essers et al., 1997). Rad54 mutant flies show higher radiation sensitivity than Mus309/Blm mutant flies, while double mutants show an additive effect (Kooistra et al., 1999).

Drosophila Ku70, also called inverted repeat binding protein (IRBP), and its interaction partner Ku80 play a role in NHEJ just as in mammalian cells (Beall et al., 1994). While the function of Ku70 has been studied using NHEJ specific P-element insertion (Min et al., 2004), it is not known to which degree the Ku heterodimer contributes to DSB repair after ionizing irradiation in drosophila. And it is important to note that in spite of reports about DNA-PKcs homologs in *Anopheles gambiae*, there is no evidence for a DNA-PKcs homolog in drosophila (Dore et al., 2004). For the following experiments all proteins mentioned besides GFP refer to their drosophila orthologs.

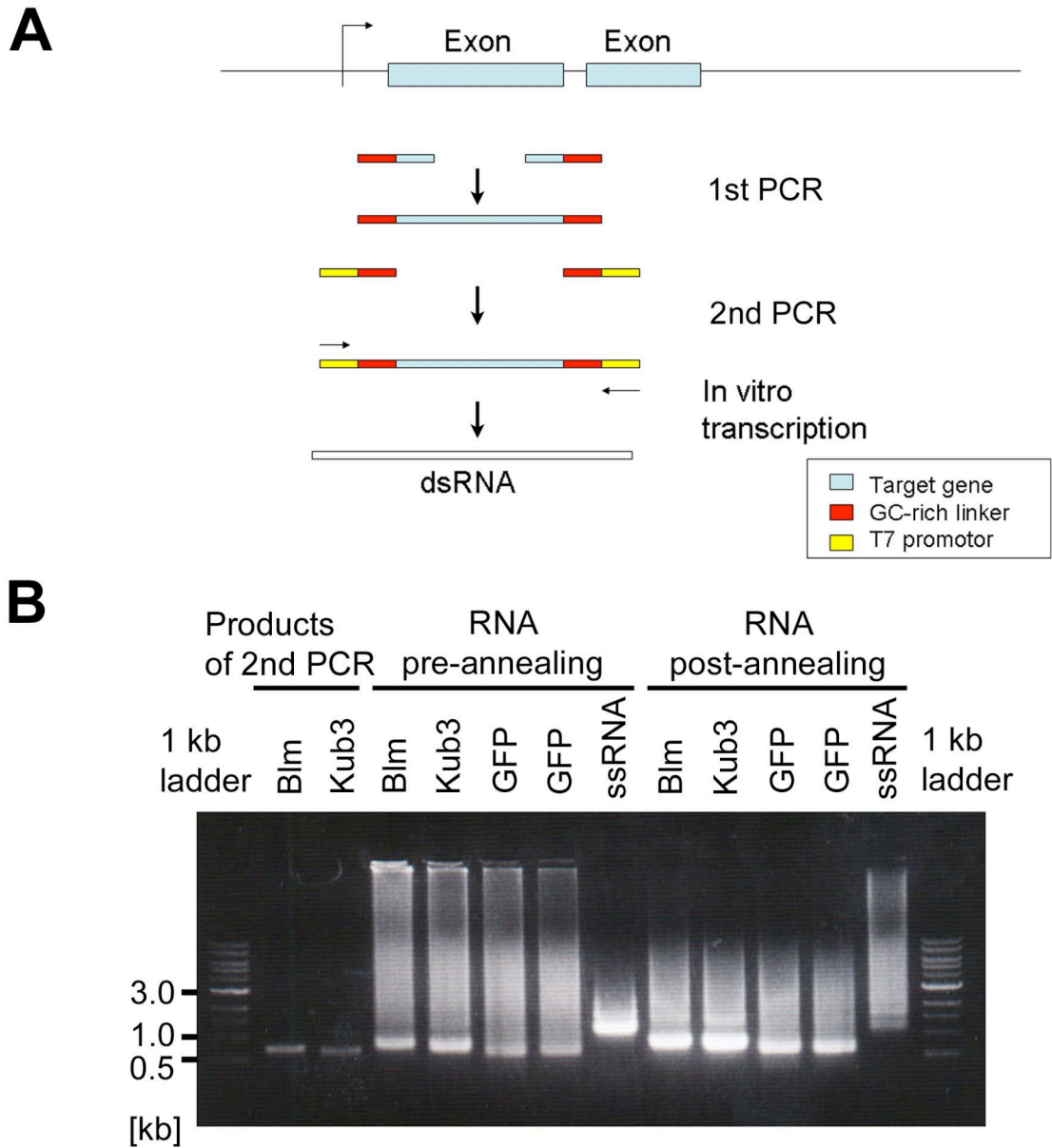


Figure 25. Production of dsRNA for RNAi in drosophila S2-cells

(A) Primers with a GC-rich linker were used to amplify about 500 bp of genomic DNA within one exon. The second PCR step generates the template for bi-directional in vitro transcription by adding the T7 promoter. (B) DNA and dsRNA samples were analyzed using a 1.5 % agarose gel and a 1 kb ladder as standard. The purified PCR product containing the T7 promoter is shown for Blm and Kub3. Some of the in vitro transcribed RNAs shown for Blm, Kub3 and GFP are double-stranded before annealing. After the annealing step most of the RNA is double-stranded. The lane depicted as ssRNA represents a 1.1 kb product (pGEM®) used as positive control for the in vitro transcription reaction.

4.2.8. RNAi of DSB repair proteins in drosophila S2 cells

Since we have shown that Kub3 is highly conserved among species, it should be possible to study Kub3 function in drosophila by RNAi. By accessing Flybase, a database holding genomic data of drosophila, we were able to identify the cDNA sequence and exon/intron structure of Kub3 (CG5131 or NM_136001). In order to use them as positive controls with respect to DSB repair defects, we also determined the drosophila sequences of several conserved components of NHEJ (Ku70 and Ku80), SDSA (Blm) and HR (Rad54). Based on these sequences, we designed oligos to amplify about 500 bp of coding DNA within one exon, using S2 genomic DNA as template. The amplification primers contained a GC-rich linker sequence, which was used in a second PCR to add the complete T7 promoter to both ends of the PCR product. In the next step bi-directional in vitro transcription generated long ssRNA (Fig. 25A). After the annealing step dsRNA could be visualized on an agarose gel (Fig. 25B). Subsequently, the dsRNA was purified, the concentration was determined by spectroscopy and 30 μ g of dsRNA were used for the following experiments.

To study overall efficiency of RNAi, we used S2 cells with a copper-inducible GFP gene (S2-IGFP) (Rogers et al., 2003). Induction of these cells with 50 μ M CuSO₄ induced GFP expression in about 25% of the cells with a mean fluorescence of 793 in the GFP positive quadrant (Fig. 26A). Application of GFP specific dsRNA led to a 56% decrease of GFP positive cells after four days; and the cells that still expressed GFP showed a 76% decrease in fluorescence (Fig. 26A). While the knock down effects were stable for several days when left in the same medium, change of the medium caused GFP expression to increase again up to about 50% after two days (data not shown).

For the following experiments we used S2 wildtype cells to knock-down Kub3 and known drosophila DSB repair proteins. GFP specific dsRNA served as negative control. Because there were no antibodies available for Kub3 and Rad54, we used quantitative RT-PCR (Taqman) to measure the expression levels of these proteins after RNAi. The data was normalized to drosophila actin homolog dmAct5C (isoform B) expression (Wagner et al., 2002). Using the two target sequences Kub3 (1) and Kub3 (2) the mRNA expression of Kub3 was knocked down to about 10% of the control levels (Fig. 26B). The levels of Rad54 mRNA were reduced by 50% compared to untreated cells and by 70% compared to GFP dsRNA treated cells (Fig. 26B). Therefore we conclude that RNAi is effective for both genes, Rad54 and Kub3. Because GFP dsRNA treatment also caused an increase in Rad54 mRNA levels, it is possible that nonspecific dsRNA might be able to induce expression of Rad54 in S2 cells.

The efficiency of the Blm RNAi was measured by Western blotting using an anti-Blm antibody (provided by Dr. Donald C. Rio). The antibody bound to several bands that were smaller than the expected size of 166 kD for Blm protein (Fig. 26C; upper panel). However, all these bands were highly sensitive to Blm specific RNAi but not to RNAi control. These bands probably represented degradation products of Blm, and so we concluded that the Blm RNAi worked.

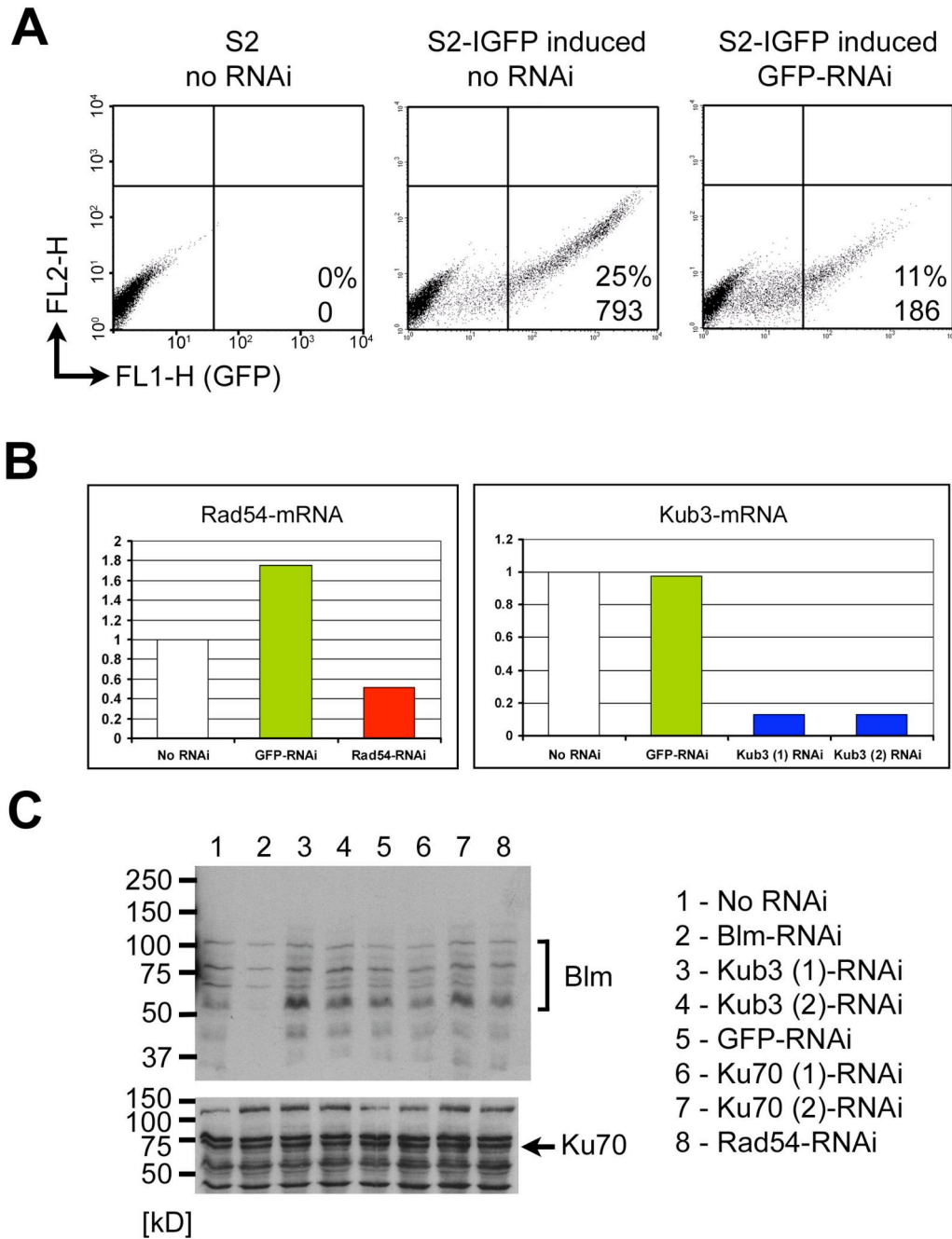


Figure 26. Efficiency of RNAi in Drosophila S2 cells

(A) S2 and S2-IGFP cells were analyzed for GFP by flow cytometry. Wildtype S2 cells express no GFP, while in S2-IGFP cells GFP expression was induced by 50 μ M CuSO₄. Induced S2-IGFP cells were treated with GFP specific dsRNA. The percentage of GFP positive cells (lower right quadrant) in the FL1-H channel is given for each sample. The number below depicts the average relative GFP expression level of cells in the lower right quadrant. (B) Quantitative RT-PCR to determine the expression levels of Rad54 and Kub3 after indicated RNAi treatment. Kub3 (1) and (2) represent two different, overlapping target sites within exon 1 of the Kub3 gene. The data was normalized to dmAct5C (isoform B) and set to 1.0 for untreated S2 cells. (C) Whole cell lysates (50 μ g) of S2 cells after RNAi as indicated were analyzed by Western blotting. Upper panel, staining with anti-Blm antibody; lower panel, staining with anti-Ku70 antibody. The putative Blm and Ku70 bands are marked. Ku70 (1) and (2) (Min et al. 2004) represent two different target sites within the Ku70 exons 1 and 2, respectively.

On the other hand our attempts to detect a knock down of Ku70 and Ku80 were not successful. Using antibodies raised against drosophila Ku70 (Fig. 26C, lower panel) and Ku80 (data not shown) we were not able to detect any RNAi effects with two Ku70 specific and one Ku80 specific dsRNAs (Min et al., 2004). While we designed the Ku70 (1) sequence ourselves, the Ku70 (2) and the Ku80 sequence were recently published to mediate Ku70/80 RNAi very efficiently in S2 cells (Min et al., 2004). We assume that the poor quality of the used antibodies accounts for this discrepancy (Fig. 26C).

For our knock-down experiments it is important to note that for all RNAis tested the S2 cells showed no increase in cell death or defects in cell division. By cell counting we verified that the generation time of all dsRNA treated cells was identical to that of 12 hr for wildtype S2 cells (data not shown). In summary, we were able to efficiently knock down four (GFP, Blm, Rad54 and Kub3) out of six target genes and also showed that a substantial reduction of Kub3 is not lethal for S2 cells.

4.2.9. Decreased expression of Blm and Rad54 but not of Kub3 increases radiation sensitivity in S2 cells

To our knowledge S2 cells have not been studied before with respect to radiation sensitivity. But if Kub3 is a functional component of NHEJ, a reduction in its expression, for example by RNAi, should lead to a increased radiation sensitivity phenotype in these cells. Since flies deficient in Rad54 and Blm are more sensitive to IR (Kooistra et al., 1999), we decided to use Rad54 and Blm RNAi as positive controls for our experiments. Although we could not detect a knock-down of Ku70 protein with the used antibodies, we still included the Ku70 specific dsRNA for the following experiments.

Because S2 cells are only semi-adhesive, we used the flow cytometry based survival assay described earlier (Wechsler et al., 2004). To do this, we irradiated untreated wildtype S2 cells with various γ -ray dosages and determined the percentage of viable cells after 72 hr by gating in the FSC/SSC (Fig. 27A). The data indicated that S2 cells were fairly resistant up to a dose of 10 Gy, while the lethal dose lied between 30 and 40 Gy (Fig. 27B). Apparently, in our assay a survival of 40% after 72 hr indicated a lethal dose. We conclude this from the observation that a higher dose of 50 Gy does not further decrease the number of viable cells (Fig. 27B). Therefore we decided to use for the following experiments a dose around 20 Gy, which would it still make possible to detect increase radiation sensitivity. To do so we first irradiated S2 cells with 18 Gy four days after the application of dsRNA of either GFP, Rad54, Kub3, Ku70 or no dsRNA. Treatment with control GFP dsRNA had no effect and these cells were indistinguishable from untreated cells after IR. In contrast, Blm RNAi cells showed a mild increase in radiation sensitivity, while Rad54 RNAi cells showed a stronger phenotype (Fig. 27C). Indeed, for cells treated with Rad54 dsRNA a dose of 18 Gy seemed to have the same effect as a dose of 40 Gy for wildtype cells in the previous experiment (Fig. 27B). Surprisingly, cells treated with either Ku70 or Kub3 dsRNA were no different from controls.

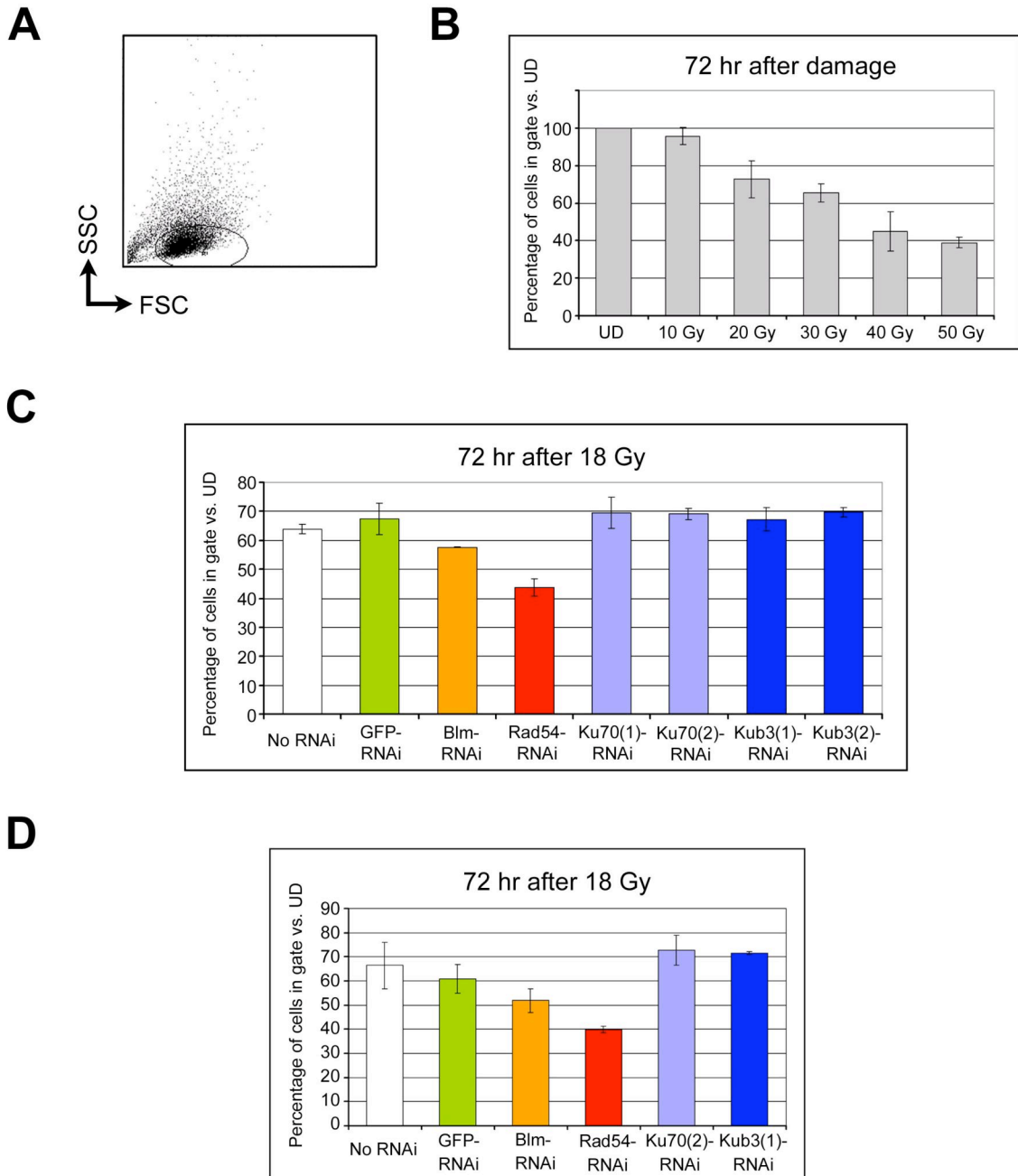


Figure 27. Survival of single RNAi S2 cells after ionizing irradiation

(A) S2 cells in the FSC/SSC of a flow cytometer. The oval gate depicts the cells considered to be viable and has been used for all following survival experiments. (B) S2 cells were irradiated with the indicated dose, seeded in triplicates and analyzed 72 hr afterwards for survival in the FSC/SSC. The percentage of viable cells versus the undamaged (UD) control (which is set to 100%) is shown. (C) Irradiation survival of S2 cells measured as in (A), while here the UD control is not shown. S2 cells were either left untreated (No RNAi) or treated once with the indicated dsRNA four days before irradiation (18 Gy). (D) Irradiation survival of S2 cells like in (C). S2 cells were either left untreated (No RNAi) or treated three times in three day intervals with the indicated dsRNA four days before irradiation (18 Gy).

Next, to further increase the RNAi efficiency, we applied the dsRNAs three times in three day intervals and assayed the radiation sensitivity (Fig. 27D). While untreated cells showed similar sensitivity as in the experiments before, control GFP dsRNA had a minor effect. Blm and Rad54 RNAi cells both showed a somewhat stronger phenotype than in the previous experiments, while Ku70 and Kub3 RNAi cells again showed no phenotype at all.

We conclude that in S2 cells both Blm and Rad54 contribute to DSB repair after ionizing irradiation. However, the contribution of Blm seems to be much lower than that of Rad54. Since the Ku70 RNAi did not seem to reduce Ku70 expression levels, the respective experimental sets can be considered additional negative controls. From these experiments it is clear that a reduction in Kub3 expression clearly has no effect on the survival of S2 cells after ionizing irradiation. This is inconsistent with the earlier proposed hypothesis that Kub3 is essential for DSB repair by NHEJ.

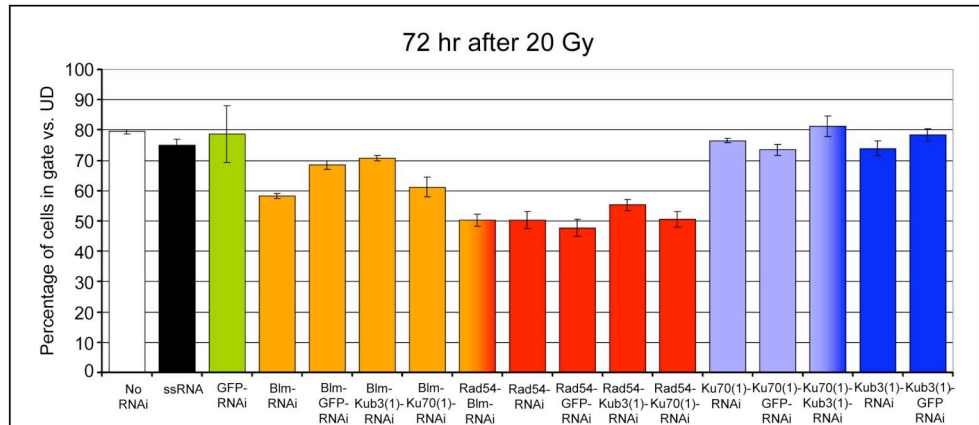
4.2.10. Decreased expression of Kub3 can not suppress the knock-down of homology directed DSB repair proteins in S2 cells

To test the other proposed hypothesis that Kub3 is a negative regulator of NHEJ, we have to assume that NHEJ and HR are competing DSB repair pathways which can compensate for each other. According to this model, decreased expression of Kub3 by RNAi should be able to partly reduce the effect of RNAi of either of the HR protein Rad54 or the SDSA protein Blm. In this case, the upregulated NHEJ pathway would compensate more efficiently for the loss of the homology directed DSB repair pathway. To address this question we applied two dsRNAs together at the same time and tested the S2 cells for survival after ionizing irradiation (Fig. 28A).

Consistent with our hypothesis, cells treated with both, Rad54 and Kub3 dsRNA, showed a slightly better survival than the ones treated with Rad54 dsRNA alone, or in combination with GFP dsRNA (Fig. 28A). On the other hand both, GFP dsRNA and Kub3 dsRNA, could suppress the decreased survival caused by Blm dsRNA (Fig. 28A). This raises the concern that these observations are caused by competition between the two co-applied dsRNAs, which non-specifically led to a lower knock-down efficiency of Blm. This could also explain why the double knock-down of Blm and Rad54 did not have an additive effect with respect to increased radiation sensitivity, as expected from data in experiments with whole fly embryo irradiation (Kooistra et al., 1999).

To avoid this artifact, we decided to give Rad54 and Blm RNAi a “head start”. If the expression of these proteins is already decreased before we apply Kub3 and control GFP dsRNAs, competition effects should be minimized. Accordingly, three days after two single applications of Rad54 or Blm dsRNA we co-applied GFP or Kub3 dsRNA and analyzed the cells as done previously (Fig. 28B, left panel). When we compared Blm RNAi to Blm/Kub3 double RNAi, there was no difference with respect to cell survival, while the co-application of Blm/GFP dsRNAs had a minor effect. This indicates that the previously observed effects were a technical artifact of the double knock-down strategy.

A



B

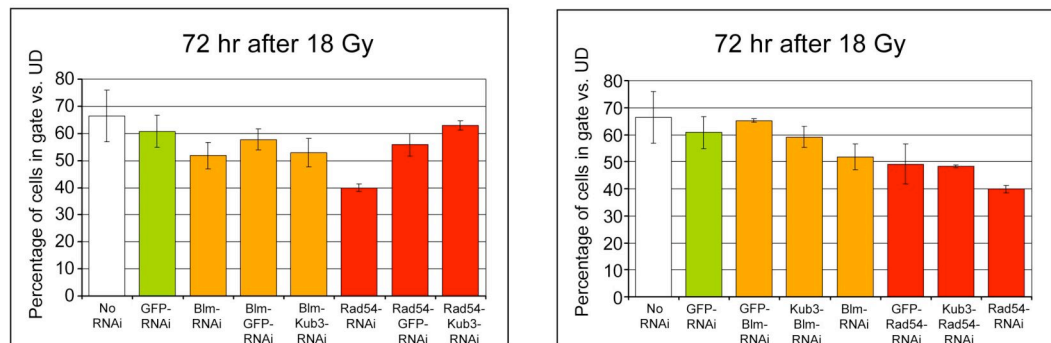


Figure 28. Survival of double RNAi S2 cells after ionizing irradiation

(A) Survival of S2 cells 72 hr after the indicated dose of irradiation (versus UD controls). Cells were treated once with the one or the two indicated dsRNAs at the same time four days before irradiation and seeding in triplicates 72 hr later. (B) Survival of S2 cells as in (A). S2 were treated once with the first indicated dsRNA alone before three days later they were treated a second time with both indicated dsRNAs. Four more days later they were irradiated with the indicated dose and analyzed 72 hr after that.

Also in Rad54 RNAi cells, this time both GFP and Kub3 dsRNA were able to improve the survival, pointing to the same conclusion as with Blm RNAi cells (Fig. 28B, left panel). When Kub3 RNAi and control GFP RNAi were given head starts and were subsequently co-depleted of Rad54 and Blm, there was also no indication for a suppressive effect of Kub3 RNAi versus GFP (Fig. 28B, right panel).

In summary, in all experiments described in this section we found no evidence that Kub3 RNAi can counteract the decreased expression of proteins involved in the HR or the SDSA repair pathways. This data does not support the hypothesis that Kub3 is a negative regulator of NHEJ. However, we can not rule it out either.

5. Discussion

5.1. DNA-PKcs function specifically regulated by protein phosphatase 5 (PP5)

5.1.1. Interaction of PP5 with DNA-PKcs

We were able to show that fragments of DNA-PKcs and PP5 can interact in yeast and based on this data suggested that the TPR region of PP5 is critical for this protein-protein interaction. Consistent with this we were able to show that GST-tagged DNA-PKcs fragments can pull down the TPR region of PP5 in vitro (Wechsler et al., 2004). However, we were not able to co-immunoprecipitate both proteins from HeLa extracts, even when PP5 was overexpressed.

Here we propose two possible explanations for the failed co-immunoprecipitation which are not mutual exclusive. In both cases activation of DNA-PKcs and its kinase activity lead to a destabilization of the DNA-PKcs/PP5 complex which makes it difficult to detect this interaction.

In the first case, autophosphorylation of DNA-PKcs disrupts the DNA-PKcs/PP5 complex. In GST pull down experiments we observed that a DNA-PKcs fragment carrying a phospho-mimetic mutation at T2609 (T2609D) could not bind the TPR region of PP5 as efficiently as a wildtype DNA-PKcs fragment (Wechsler et al., 2004). This indicates that PP5 binds to dephosphorylated DNA-PKcs rather than to phosphorylated DNA-PKcs. Although our co-immunoprecipitation experiments were carried out under undamaged conditions, it is possible that in the course of the incubation DNA-PKcs came in touch with fragmented cellular genomic DNA which triggered its activity and autophosphorylation. Indeed, we found evidence for such background activation of DNA-PKcs in nuclear extracts from undamaged cells (data not shown). In summary, if nonphosphorylated DNA-PKcs is needed for efficient PP5 pull down and DNA-PKcs autophosphorylation already occurs under undamaged conditions due to the extraction method it is difficult to isolate stable DNA-PKcs/PP5 complexes.

Interestingly, the same is true for ATM and its phosphatase PP2A (Goodarzi et al., 2004). Recently, it could be shown that irradiation induced ATM phosphorylation abolishes its interaction with PP2A. When ATM autophosphorylation was inhibited by the PI-3 like kinase inhibitor wortmannin, the ATM/PP2A complex was more stable (Goodarzi et al., 2004).

Another possibility, how DNA-PKcs activation can destroy its complex with PP5 is by phosphorylation of PP5. This could occur either by an unknown kinase or by DNA-PKcs itself, which could target one of five potential SQ/TQ DNA-PKcs phosphorylation sites in PP5 (data not shown). According to this model, phosphorylated PP5 dissociates from DNA-PKcs, is dephosphorylated by another phosphatase and can then target a different DNA-PKcs molecule for dephosphorylation. In this scenario, both, DNA-PKcs and PP5 could be recycled for multiple cycles of DNA damage repair.

5.1.2. A cell cycle checkpoint role for DNA-PKcs

After confirming the interaction of PP5 and DNA-PKcs *in vitro*, we overexpressed wildtype PP5 and dominant negative PP5.GFP in HeLa cells to investigate the function of this interaction. We found that cells overexpressing PP5 had a lower and cells expressing PP5.GFP had a higher level of DNA-PKcs phosphorylation at T2609. When we measured the radiation sensitivity in these cells we found that both hypo and hyper-phosphorylation correlate with increased radiation sensitivity. At first, it was surprising that also PP5 overexpression lead to this phenotype, because it was reported that PP5 can protect cells against apoptosis after oxidative stress by dephosphorylating ASK1 (Morita et al., 2001). On the other hand this might represent a completely different pathway and the induction of DSB might ablate this protective effect. Because we could rule out that defective NHEJ accounts for the increased radiation sensitivity, we consider other factors which could contribute to the observed phenotype:

First, it appears that PP5 can also regulate ATM function even though not by direct dephosphorylation (Ali et al., 2004; Goodarzi et al., 2004). This function of PP5, which is discussed in more detail in the following chapter, could contribute to the observed phenotype. Second, DNA-PKcs and ATM independent pleiotropic effects might play a role as well. So could aberrant expression of PP5 decrease the viability of the cells due to functions of PP5 unrelated to DSB repair. Although under undamaged conditions the subclones overexpressing PP5 and dominant negative PP5.GFP appeared to be normal with respect to cell division and cell survival, the additional strain of DNA damage might lower their viability beyond repair. One putative PP5 function that could have such an effect is the regulation of the cell cycle by interaction with CDC16/27 of the anaphase promoting complex (Das et al., 1998). Third, there have been reports about a subtle checkpoint role of DNA-PKcs. So could be shown that in DNA-PKcs deficient backgrounds the recovery from damage induced replication arrest was impaired (Guan et al., 2000). More recently, it could be shown that DNA-PKcs interacts with the checkpoint protein Chk2 and phosphorylates it at the functional phosphorylation site T68 (Li and Stern, 2005). This checkpoint function of DNA-PKcs might be affected by abnormal DNA-PKcs phosphorylation and as a consequence this might lead to either failed cell arrest, or alternatively, to a permanent cell cycle arrest. Evidence for the first case comes from a recent report that overexpression of dominant negative PP5 causes a mild radiationresistant DNA synthesis (RDS) phenotype (Ali et al., 2004). The occurrence of the RDS phenotype indicates a failure to halt the cell cycle at the S-phase checkpoint.

5.1.3. Regulation of DNA-PKcs and ATM by protein phosphatases

When we compared phosphorylation levels of DNA-PKcs T2609 and S2056 in HeLa cells overexpressing PP5 to wildtype HeLa cells the differences were much more pronounced for pT2609 than for pS2056. Nevertheless, more evidence for PP5 being the only phosphatase that can dephosphorylate both DNA-PKcs T2609 and S2056 comes from experiments where PP5 was knocked down in HeLa cells by transfection of

specific siRNAs (Wechsler et al., 2004). When HeLa cells treated with PP5 siRNAs were compared to mock treated cells without siRNAs, already a mild reduction of PP5 protein expression caused an increase of DNA-PKcs S2056 phosphorylation under undamaged and damaged conditions (Wechsler et al., 2004). The same was true for DNA-PKcs T2609 phosphorylation (Wechsler et al., 2004)

While this points out that PP5 regulates both S2056 and T2609, the effects of overexpression of wildtype and dominant negative PP5.GFP were weaker for the S2056 site. These differences can be explained by the different mechanisms of RNAi and dominant negative effects and may underscore the importance of nuclear import of PP5 for its regulation. Considering the multitude of PP5 substrates, it is possible that more efficient elimination of the enzyme cannot be achieved without arresting or killing the cells. Thus, selection against efficient siRNA treatment may occur in the cultures. At any rate, we conclude that PP5 cannot be replaced completely by another phosphatase at both DNA-PKcs at T2609 and S2056.

Because it is known that DNA-PKcs T2609 phosphorylation can also occur by ATM, we wanted to rule out that PP5 dephosphorylates ATM rather than DNA-PKcs (Chan et al., 2002). Therefore we looked at the only known ATM phosphorylation site at S1981 and observed no difference between wildtype HeLa cells and cells overexpressing PP5. However, a recent report claims that ATM S1981 and thus ATM kinase activity is regulated by PP5 (Ali et al., 2004). The authors show that both proteins interact *in vivo* and claim that PP5 also binds to Rad17 and ATR (Ali et al., 2004; unpublished result). Surprisingly, when they knocked down PP5 by RNAi the phosphorylation of downstream targets of ATM was decreased, implying that PP5 somehow activates ATM. Even so, when they overexpressed PP5, they observed a ATM S1981 phosphorylation increase rather than the expected decrease. Expression of a dominant negative form of PP5 caused the opposite effect (Ali et al., 2004). Although we have no explanation for the discrepancy between their data and ours regarding ATM phosphorylation at S1981, it is clear that PP5 does not dephosphorylate ATM at this site (Bakkenist and Kastan, 2004).

There is another indication that PP5 directly targets DNA-PKcs and not ATM. If PP5 overexpression leads to increased ATM kinase activity, one would also expect increased DNA-PKcs pT2609 phosphorylation, which is not the case. One explanation is that the PP5 dephosphorylation of this DNA-PKcs site is so effective that it masks any opposite effects due to ATM. Another explanation is that ATM does not significantly phosphorylate DNA-PKcs at T2609 and this is mainly an autophosphorylation site.

Interestingly, a recent report showed that protein phosphatase 2A (PP2A) interacts with ATM as well (Goodarzi et al., 2004). Furthermore, PP2A specific inhibition, but not of PP5, could increase spontaneous S1981 phosphorylation without activating ATM kinase activity. Expression of a dominant negative form of PP2A led to increased S1981 phosphorylation. However, the authors did not address the question whether overexpression of PP2A results in more efficient dephosphorylation of S1981 after DNA damage. It is important to note that PP5 and PP2A also interact (Lubert et al., 2001),

which makes this relationship between ATM, DNA-PKcs, PP2A and PP5 even more complex. In summary, the authors suggest that PP2A might prevent leaky ATM autophosphorylation in the absence of damage (Goodarzi et al., 2004).

This is consistent with our own model of PP5 regulation of DNA-PKcs. Because under undamaged conditions expression of dominant negative PP5.GFP caused hyperphosphorylation of T2609 we propose a model where spontaneous DNA-PKcs autophosphorylation occurs at this site and that PP5 dephosphorylates DNA-PKcs under these circumstances (Fig. 29). This ensures that a unphosphorylated population of DNA-PKcs is always present and ready to be activated by open DNA ends. After the DNA repair process has been successfully completed, DNA-PKcs gets hyperphosphorylated and dissociates from DNA (Fig. 29). Even though we can not rule out that some phosphorylated DNA-PKcs molecules are degraded at this point, we were able to show that PP5 can dephosphorylate at least two functional sites of DNA-PKcs after damage (Wechsler et al., 2004). Also, other DNA-PKcs phosphorylation sites may be targeted by other yet to be identified protein phosphatases (Fig. 29).

Such a mechanism would allow the cell to recycle DNA-PKcs protein and would help to sustain a high number of DNA-PKcs molecules at all times. This is an important prerequisite for the function of DNA-PKcs in DNA double strand break repair and aging.

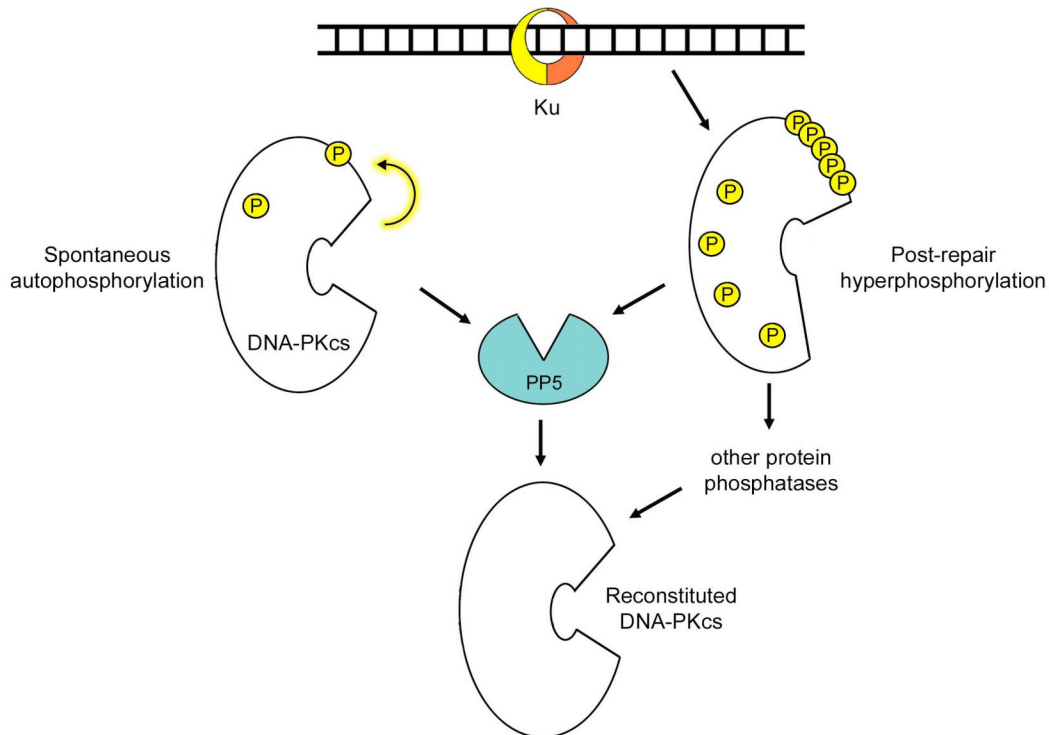


Figure 29. Model for DNA-PKcs dephosphorylation by PP5

Spontaneous autophosphorylation of DNA-PKcs at T2609 or S2056 can be reversed by PP5. After completed DSB repair the Ku protein remains on the DNA while hyperphosphorylated DNA-PKcs dissociates from the DNA. Next to other unknown protein phosphatases, PP5 contributes to a complete dephosphorylation of DNA-PKcs. This reconstitutes DNA-PKcs which can be activated by DSB breaks again and fulfill its function in NHEJ.

5.2. Ku70 binding protein 3 (Kub3) is a putative metalloprotease and interacts with DNA-PKcs

5.2.1. Characterization of Kub3 protein

Kub3 has been initially described as a 220 or 300 kD protein (Yang et al., 1999b). Here we presented evidence that human Kub3 is a 247 aa protein with a molecular weight of 29 kD. This reading frame of Kub3 was highly conserved among species with respect to both protein length and protein homology. The fact that a polyclonal antibody against the C-terminus of Kub3 recognized a band of the predicted size is another strong indication that Kub3 is indeed a 29 kD protein. Apart from this band, we found in whole cell lysates from HeLa cells one additional smaller band of approximately 27 kD, which was specific for Kub3. Even more puzzling, we observed altogether four Kub3 bands when we overexpressed mycKub3 in HeLa cells. Because we were able to rule out that phosphorylation accounts for these differences in size, we propose the following possible explanations:

1) Endogeneous Kub3 has at least two splice variants.

Because we observed two Kub3 proteins of similar size in HeLa cell extracts, it is possible that they represent Kub3 splice variants and both share the C-terminus which is recognized by the anti-Kub3 antibody. This explanation is supported by the fact that several Kub3 splice variants termed A, B, C, D, E and F have been posted at the ACEVIEW resource at NCBI. But although the Kub3 splice version F with a predicted size of 27 kD could account for the smaller endogenous Kub3 band, more experiments are necessary to confirm the existence of these Kub3 splice variants in vivo.

2) Overexpression of ectopic mycKub3 induces expression of endogenous Kub3.

Assuming that the two top bands represent mycKub3 and the two smaller bands represent endogenous Kub3, one could conclude that expression of mycKub3 leads to increased expression of endogenous Kub3 by an unknown mechanism.

One model for this mechanism suggests that Kub3 overexpression causes increased DNA damage which in turn triggers its own expression. However, when we looked at known DNA double-strand break markers we found that Kub3 overexpression only led to increased DNA-PKcs T2609 phosphorylation while other markers like DNA-PKcs pS2056 and ATM pS1981 were unaffected. Therefore we conclude that Kub3 can not induce DNA damage. Because we also showed that IR can not induce Kub3 expression in HeLa cells, we can certainly rule out this model.

It is also possible that Kub3 itself can act as a transcription factor and therefore regulate its own expression and the expression of other genes. However, this is unlikely because we found no protein homology in Kub3 which could facilitate DNA binding. Nevertheless, it is also possible that Kub3 indirectly triggers its own expression or increases its protein stability. Both would result in increased levels of Kub3 protein after mycKub3 overexpression.

3) The multiple Kub3 bands are due to proteolytic cleavage of mycKub3.

Because only one band was recognized by the anti-myc antibody when we overexpressed mycKub3, it is possible that only the top band represents full length mycKub3. If N-terminal proteolytic cleavage occurs, the myc-tag is removed, and this leads to one or several shorter Kub3 polypeptides. Because the anti-Kub3 antibody binding domain is on the C-terminus, these polypeptides would be still visible when this antibody is used. This explanation is consistent with the existence of several conserved cysteine residues on the N-terminus of the Kub3 protein. These cysteines could represent potential cleavage sites for a zymogen activation of the metalloprotease Kub3. This would account for the two endogenous Kub3 bands and the four bands when mycKub3 is overexpressed. This model could also explain why we failed to detect a recombinant GFP-Kub3 fusion protein which was expressed under puromycin selection. Instant cleavage at the N-terminus could destroy such a fusion protein. However, we were unable to detect cleavage products using anti-GFP and anti-Kub3 antibodies by Western blotting (data not shown).

5.2.2. Interaction of Kub3 with DNA-PKcs

Because Kub3 could interact in yeast with Ku70 and DNA-PKcs fragments as bait, we had strong indications that Kub3 binds to the DNA-PK complex (Yang et al., 1999b). To verify the interaction of Kub3 with DNA-PKcs *in vivo*, we performed co-immunoprecipitation experiments and could co-precipitate overexpressed mycKub3 with three different anti-DNA-PKcs pull down antibodies. This is remarkable considering the fact that these antibodies bind to completely different regions of DNA-PKcs. Ku70 for instance can only be co-precipitated with DNA-PKcs when the 25-4 antibody is used, while other anti-DNA-PKcs antibodies presumably compete with Ku70 for DNA-PKcs binding (Benjamin P. C. Chen, personal communication). It is possible though, that this is not the case for the much smaller protein Kub3. Also, Kub3 did interact in the yeast two-hybrid screen with two different not adjacent fragments of DNA-PKcs, which could mean that Kub3 binds to several domains of the DNA-PKcs protein *in vivo*. This would also allow the Kub3 protein to bind to DNA-PKcs irrespective of the DNA-PKcs pull down antibody.

Unfortunately, one of the five unspecific pull down antibodies we have used as negative controls in our experiments did also precipitate small amounts of mycKub3. It is important to note that we observed this only one time and not when the experiment was repeated. Also, the negative control showed a much weaker pull down signal when compared to the respective co-immunoprecipitations with anti-DNA-PKcs antibodies. Because the sample in question also showed small amounts of unspecific DNA-PKcs pull down, we conclude that in this sample we had a higher overall background signal. This could be due to unspecific protein precipitates, which occur when high protein concentrations and long incubation times are used.

Remarkably, when we used an antibody against ATM, a DNA-PKcs related PI-3 like kinase of similar size, we observed no co-immunoprecipitation of Kub3. This shows that the stickiness of such large proteins is insufficient to pull down Kub3. In parallel co-precipitation experiments with HeLa cells expressing Kub3 wildtype levels and cells overexpressing mycKub3/Kub3 we were only able to pull down Kub3 with DNA-PKcs when it was overexpressed. Because Kub3 seems to be expressed to a much lower degree than DNA-PKcs, it is conceivable that we had to overexpress mycKub3/Kub3 to gain a sufficient amount of DNA-PKcs/Kub3 complexes which we could detect by Western blotting.

Another interesting question is why in side by side experiments we were able to co-precipitate Kub3 after one hour but not after three hours of incubation. One explanation is that the DNA-PKcs/Kub3 complex is fragile and might become increasingly unstable while under the co-immunoprecipitation conditions. Because it is known that hyperphosphorylated DNA-PKcs dissociates from DNA and Ku70 (Merkle et al., 2002), the phosphorylation status of DNA-PKcs might be also critical for its interaction with Kub3. Therefore we consider the following two possibilities:

In the first case, hyperphosphorylation of DNA-PKcs could interfere with Kub3 binding. This seems likely, because Kub3 interacted in yeast with DNA-PKcs fragments which were presumably not phosphorylated. Interestingly, also another DNA-PKcs yeast-two hybrid hit, PP5, binds only to dephosphorylated DNA-PKcs and recent data showed the same situation for ATM and its phosphatase PP2A (Goodarzi et al., 2004). As mentioned before, genomic DNA in the co-precipitation sample may lead to DNA-PKcs autophosphorylation and subsequent disruption of the DNA-PKcs/Kub3 complex.

In the alternative case, only hyperphosphorylated DNA-PKcs binds to Kub3. This would be consistent with a role of Kub3 in dissociating the DNA-PK complex after the repair process has been finished. It is possible that in our immunoprecipitation experiments DNA-PKcs comes in contact with unspecific protein phosphatases which are usually in other compartments of the cell. Thus, DNA-PKcs phosphorylation and Kub3 binding would be decreased. For future experiments we therefore recommend the use of potent PI-3 like kinase inhibitors like wortmannin to prevent DNA-PKcs autophosphorylation or protein phosphatase inhibitors to prevent the opposite.

5.2.3. Function of Kub3 in DSB repair

Assuming that Kub3 binds to the DNA-PK complex, we presented two hypotheses for a role of Kub3 in DSB repair by NHEJ.

The first hypothesis states that Kub3 is essential for the function of the DNA-PK complex and is therefore needed for efficient NHEJ. To address this question we knocked down the Kub3 ortholog in drosophila S2 cells by RNAi and measured the radiation sensitivity of these cells. While we observed increased radiation sensitivity when we decrease the expression of the drosophila orthologs of the HR repair protein Rad54 and the SDSA protein Blm, we found no phenotype in cells with decreased Kub3

expression. Therefore we concluded that Kub3 does not contribute to DSB repair in S2 cells after IR.

To measure the contribution of NHEJ to DSB repair after IR in these cells, we attempted to knock down Ku70 and Ku80 using published dsRNA sequences (Min et al., 2004). To our surprise the cells treated with Ku70 and Ku80 specific dsRNA did not show increased radiation sensitivity. This could be explained by inefficient RNAi of Ku70 and Ku80, but unfortunately, the provided anti-Ku70 and anti-Ku80 immunosera were of such poor quality that were not able to conclusively determine the extent of the knock-down of both proteins.

However, for the following reasons we speculate that both knock-downs worked: First, the dsRNA sequences we used have been published before to efficiently mediate RNAi of Ku70 and Ku80 in S2 cells (Min et al., 2004). It is important to note, that apart from the published Ku70 dsRNA sequence (Ku70(1)), we have also designed and used one more Ku70 specific RNA (Ku70 (2)). Second, when we attempted to knock-down the four proteins Rad54, Blm, GFP and Kub3 we observed a strong reduction in the expression of these target genes. For Kub3 this was even the case for two different dsRNAs (Kub3 (1) and (2)). While these results are consistent with the reported high efficiency of RNAi in insect cells, only the three attempts to knock-down Ku70/Ku80 seemed to fail.

Assuming that we successfully knocked-down Ku70 and Ku80, we could conclude that NHEJ does not contribute to DSB repair after IR in S2 cells. This would be somewhat surprising because drosophila larvae deficient in Ku70 show a much lower survival rate after IR than their wildtype counterparts. On the other hand, our experiments took place in S2 cells and it is possible that developmental functions of Ku70 in larvae contribute to the increased radiation sensitivity in this system.

Another indication for a minor role of NHEJ in S2 cells after IR is the extremely high radiation sensitivity in cells with decreased Rad54 expression. The lethal dose for S2 cells was reduced from about 40 Gy to about 20 Gy when Rad54 mRNA was reduced to 50% of wildtype levels. Apparently, in this case NHEJ is not able to compensate for the loss of HR proteins. The contribution of the Blm protein and presumably that of the SDSA pathway is smaller than that of the HR pathway but can still be measured by our method.

The competition model for DSB pathways suggests that depending on the cell cycle, developmental stage and tissue specificity either homology based pathways or end joining pathways are chosen. Consistent with this model the preference in S2 cells for a certain pathway could be rooted either in the origin or the cell cycle stage of the cells. During our experiments we have used only unsynchronized S2 cells, which are constantly replicating and dividing. Therefore the majority of these cells is in the G2-phase and would prefer homology based repair pathways (Weinert et al., 2005).

In summary, we found indications that in unsynchronized S2 cells predominantly the HR and SDSA pathway contribute to DSB repair after IR. If this is the case, it is difficult to

determine the role of Kub3 in NHEJ using this system. Therefore we propose radiation sensitivity experiments with G1 arrested S2 cells or Kub3 RNAi experiments in mammalian cells lacking HR activity like Rad54 knock-out cells.

The second hypothesis proposes that Kub3 is a negative regulator of NHEJ. We also tried to find evidence for this hypothesis in RNAi knock-down experiments in drosophila cells. According to the model of competitive DSB repair pathways, we reasoned that if we decrease the efficiency of homology directed repair by either Rad54 or Blm RNAi and knock-down the putative NHEJ inhibitor Kub3 at the same time, the increased activation of the NHEJ pathway would compensate for the loss of the other pathway. Unfortunately, we found no evidence that Kub3 RNAi can suppress the knock down of Rad54 or Blm. This might be due to the discussed predominance of homology based repair in the S2 cells. At least we could rule out that this preference for homology directed repair is upheld by Kub3 and we therefore propose other factors that efficiently suppress NHEJ at times.

We also overexpressed mycKub3 in HeLa cells and measured irradiation sensitivity and DNA-PKcs pT2609 foci formation. We found that overexpression of mycKub3 did not lead to increased irradiation sensitivity and DNA-PKcs pT2609 foci formation appeared normal as well. However, we found that the level of T2609 phosphorylation was clearly increased when mycKub3 was overexpressed. There are two explanations for this phenotype. First, overexpression of mycKub3 could interfere with NHEJ and therefore delay the dephosphorylation of DNA-PKcs at T2609. If this is the case, this delay has no effect on the survival of the cells, because we observed no increased radiation sensitivity in these cells (data not shown). The second explanation is that Kub3 competes with a phosphatase which dephosphorylates DNA-PKcs. Because we have shown that it is the phosphatase PP5 which dephosphorylates DNA-PKcs at T2609, future experiments will determine if Kub3 and PP5 indeed compete for DNA-PKcs binding.

5.2.4. Alternative functions of Kub3

Because we couldn't find clear evidence for a Kub3 function in DSB repair, the question remains: "What does Kub3 do?"

Although Kub3 seems to be expressed in all tissues, in our DNA-PKcs yeast two-hybrid screen we isolated Kub3 from mouse 18-81 cells, which are of B-cell origin. It is therefore possible that Kub3 might be expressed to a higher degree in those cells and thus has a function with respect to DSB repair specifically in B-cell specific processes like V(D)J rearrangement and immunoglobulin class switch. Genatlas expression data also indicate a higher Kub3 expression in cells of lymphopoietic origin (data not shown). Consistent with this hypothesis, Mazumder and colleagues have presented data that links DSB repair to Kub3 in hemopoietic cells. The authors showed that the G1-phase specific cyclin E can be cleaved by caspase 3 upon apoptosis induction (Mazumder et al., 2002). The resulting fragment, termed p18-cyclin E, could further radiosensitize cells of hemopoietic origin (Mazumder et al., 2002). Using this fragment as a bait in a yeast

two-hybrid screen the authors identified Ku70 and Kub3 as putative interaction partners and further stated that p18-cyclin E expression interferes with DSB repair. Therefore it would be interesting to study cells of non-hemopoietic origin with respect to p18-cyclin E generation and further determine the Kub3 requirement for the increased radiation sensitivity.

Recently the Ku heterodimer has been implicated in the regulation of cell adhesion molecules and cell-cell interactions. This completely new function of the Ku protein could theoretically also involve DNA-PKcs or Kub3. In human cancer cell lines, like the T-cell line MLA144 or HL-60, it was possible to show that the Ku protein can not only be found in both nuclear and cytoplasmic fractions but also in a membrane associated fraction on the cell surface (Dalziel et al., 1992). Moreover, it could be shown that this fraction has a function in promoting cell-cell adhesion (Monferran et al., 2004b). Furthermore, Ku70 and Ku80 could be found on the surface of human primary macrophages together with matrix metalloproteinase MMP-9 (Monferran et al., 2004a). All three proteins interacted with each other and were necessary for collagen matrix invasion, which points to a DSB repair independent function of Ku (Monferran et al., 2004a). Even though DNA-PKcs was not found on the cell surface in these studies, there is data that DNA-PKcs is associated with lipid rafts on the inside of the cell membrane (Lucero et al., 2003). In this context it is interesting that we found in the original DNA-PKcs yeast two-hybrid screen the factors epsin and Hrs which are both involved in a clathrin independent endocytosis pathway with lipid rafts (Chen et al., 1998a; Raiborg et al., 2001; Sigismund et al., 2005). Because we are confident that Kub3 interacts with DNA-PKcs and possesses metalloprotease activity like MMP-9, it is possible that Kub3 works in this pathway as well. However, in our experiments we localized Kub3 predominantly in the nucleus of HeLa cells. Further studies on other cell types are necessary to implicate Kub3 in proteolysis on the cell surface.

6. Materials and Methods

6.1. Cell lines, cell culture and irradiation treatments

For our experiments we used human S2 cells, HeLa cells and the Chinese hamster ovary (CHO) cell line V3 (DNA-PKcs mutant) transfected with empty expression vector (V3-JM) or vector with full length human DNA-PKcs (V3-F18), both under neomycin selection (Kurimasa et al., 1999). V3 cells were grown in 5% CO₂ at 37°C in α -DMEM medium supplemented with 10% fetal bovine serum (FBS), 1% Pen/Strep and 200 μ g/ml Neomycin for selection. HeLa cells were grown in DMEM medium supplemented with 10% FBS, 1% Pen/Strep and 1% Glutamax 1 (Invitrogen) in 5% CO₂ at 37°C. S2 cells were grown in Schneider's Medium supplemented with 10% FBS and 1% Pen/Strep at 25°C. Induction of GFP expression in S2-IGFP cells required addition of 50 μ M/ml CuSO₄ to the medium. For irradiation experiments cells were trypsinized, put into cell culture medium and placed in a γ -irradiator (288 rad/min). Afterwards the cells were recovered in the incubator for graded time periods and then lysed.

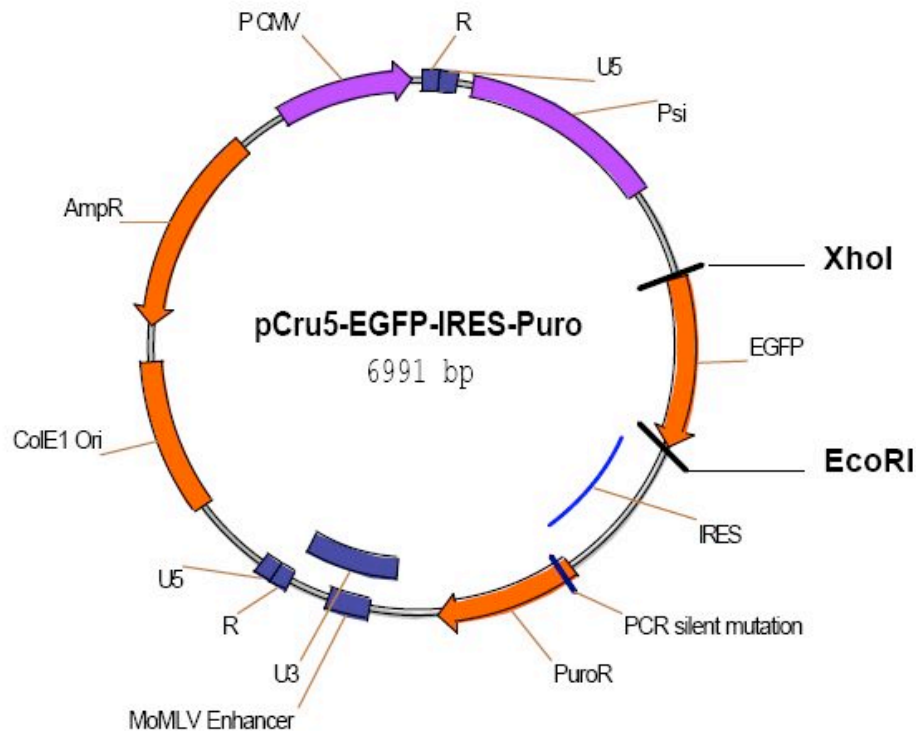


Figure 30. Map of Cru5-EGFP-IRES-PURO

The map depicts the structure of the retroviral plasmid Cru5-EGFP-IRES-PURO. Functional elements of the backbone plasmid are the origin of replication (ColE1 Ori), the ampicillin resistance gene (AmpR) and the Cytomegalovirus promoter (pCMV). The retroviral elements are flanking long terminal repeats like R/U5 and U5/R/U3, which overlaps with a Moloney murine leukemia virus promoter (MoMLV); a RNA packaging signal (Psi); an internal ribosomal entry site (IRES); enhanced green fluorescent protein (EGFP) and a puromycin resistance gene (PuroR). The restriction sites for Xho I and EcoR I can be used to replace EGFP by other genes.

6.2. Retroviral constructs and transduction

All used retroviral vectors share the backbone with plasmid Cru5-EGFP-IRES-PURO (Fig. 30). Full length human PP5 was cloned into the retroviral vector Cru5-IRES-EGFP. Dominant negative PP5.GFP human PP5, lacking the last 110 aa was contained in Cru5-PP5.GFP. Full length Kub3 ORF was amplified by RT-PCR from the activated B-cell library used for the yeast two-hybrid screen and then cloned into vector Cru5-myc-IRES-PURO. Amphotropic Phoenix packaging cells were transfected with 2 µg plasmid DNA by using Eugene 6 transfection reagent (Roche). After two days cultural supernatant containing the retrovirus were used to infect HeLa cells by spin-infection at 300 g 1hr with 5 µg/ml polybrene® (1,5-dimethyl-1,5-diazaundecamethylene polymethobromide, hexadimethrine bromide) (Sigma). For PP5, after three days HeLa cells were sorted for GFP positive subclones by FACS. Subclones were grown up and tested for stable GFP expression by flow cytometry. Expression of PP5 and PP5.GFP fusion protein was confirmed by Western blotting of whole cell lysates and nuclear extracts. To select for stable mycKub3 expression, cells were grown three days after infection with cell medium containing 1.5 µg/ml puromycin.

6.3. Whole cell lysates

To prepare whole cell lysates the cells were first harvested by trypsination. After counting, 1×10^7 cells were spun down and the pellet was washed three times with cold PBS. After the last washing step, the pellet was incubated with lysis buffer (150 mM NaCl, 0.5% Triton X, 50 mM Tris (pH 7.4), 5 mM EDTA and protease inhibitors) for 45 min on ice. Then the sample was spun down in a cold microcentrifuge at maximal speed for 20 min. The protein concentration of the supernatant was determined by the Bradford method. 1×10^7 HeLa cells lysed in a 1 ml volume yielded approximately 1 mg of total protein.

6.4. Nuclear extracts

Nuclear extracts (P10 fraction) were prepared as described (Lees-Miller et al., 1990).

6.5. Western blotting

Protein concentration was measured by the Bradford method, and equal protein amounts (20-80 µg) were separated by SDS-PAGE. The acrylamide gels were either pre-cast 4-12% NuPAGE® Bis-Tris Gels (Invitrogen) or were freshly poured. For regular acrylamide gels (6-10 %) an acrylamide/bisacrylamide ratio of 19:1 (Fisher scientific) was used. To ensure complete transfer of the 465 kD DNA-PKcs protein during Western blotting, an acrylamide/bisacrylamide ratio of 112.5:1 was used for DNA-PKcs gels (9%). The proteins were transferred by wet electrotransfer (1 mA/cm² at 4°C) onto a nitrocellulose membrane (Hybond-C super/Amersham pharmacia), blocked for 1 hr in TBS-T with 5 % dry milk powder and then incubated with the following primary antibodies: antibody 18-2 to DNA-PKcs (Neomarkers); antibody 25-4 to DNA-PKcs (Neomarkers); antibody 4F10C5 to DNA-PKcs (BD transduction); antibody to DNA-PKcs

pT2609 (Chan et al., 2002); antibody to DNA-PKcs pS2056 (Chen et al., 2005); antibody to DNA polymerase δ (BD transduction); antibody to PP5 (BD transduction); antibody to myc-tag (Clontech); antibody to actin (calbiochem) or antibody to ATM pS1981 (Rockland). Polyclonal rabbit antibody against Kub3 was generated by the company AnaSpec Inc. The keyhole limpet hemocyanin (KLH) coupled peptide YAHRDFENRDRYYSNI was used to immunize a rabbit three times before serum was tested by ELISA for immunoglobulin titers. After affinity purification the antibody was used for Western blotting, co-immunoprecipitation and immunofluorescence experiments. Antibodies against the *Drosophila melanogaster* orthologs of Blm, Ku70 and Ku80 were provided by Dr. Donald Rio (Min et al., 2004). Secondary antibodies were horseradish peroxidase (HRP)-conjugated rabbit anti-mouse and goat anti-rabbit antibodies, respectively (Southern Biotech). For detection a ECL-detection kit was used (Amersham pharmacia). For re-probing of nitrocellulose membranes with different antibodies, the membranes were first stripped off the antibodies used for the first staining. To do so, the membrane was incubated for 60 min at 60°C in stripping buffer (100 mM β -Mercaptoethanol, 2% SDS, 62.5 mM Tris-HCl pH 6.7). Afterwards the membrane was blocked again and incubated with the respective antibodies as before.

6.6. Co-Immunoprecipitation

For Co-immunoprecipitation whole cell lysates or nuclear extracts of HeLa wildtype cells or HeLa cells overexpressing GFP or mycKub3 were prepared. The protein concentration of the cell lysates was determined by the Bradford method and 0.5 - 2 mg of total protein were used in samples of 1 ml volume. At 4°C the lysates were pre-incubated for 1 hr with 4 μ g of pull-down antibody. After adding 30 μ l of equilibrated Rec protein G-Sepharose beads (Zymed) the samples were moved by a rotator at 4°C for 1-3 hr. Afterwards the sepharose beads were spun down by a short centrifugation step at maximal speed and then washed three times with 1 ml of lysis buffer for each 10 min on the rotator at 4°C. To remove contaminating protein precipitates during the washing steps, the sepharose beads were carefully transferred to a fresh tube. After the final centrifugation the beads were left in 30 μ l lysis buffer and mixed 15 μ l of 3x SDS sample buffer. After the sample were boiled at 95°C for 7 min, they were analyzed by Western blotting.

6.7. Immunofluorescence

To prepare HeLa cells for immunofluorescence analysis sterile round glass slides (12 mm) were coated with 1:10 diluted polylysine. The slides were transferred into a 24 well plate and 2×10^5 cells were seeded per well. After the cells were attached over night, they were washed three times with PBS and then fixed at -20°C with 200 μ l icecold methanol per well. Immediately after methanol removal 200 μ l icecold acetone was added for 20 sec and then washed three times with PBS. The slides then were incubated in blocking solution in 0.5 % FCS + 0.5 % BSA in PBS (300 μ l per well) for 30 min at room temperature. Then incubation with first antibody diluted 1:10 -1:100 in

blocking solution was carried out at room temperature for 2 hr. After one washing step in PBS the slides were washed three more times in PBS + 2.5 % NP 40 for 5 min each. Cells were blocked again and then incubated with secondary antibody diluted 1:100 in blocking solution for 1 hr at room temperature. The slides were washed three times 10 min in PBS and then transferred onto a microscope slide with 30 μ l of mounting buffer. The slides were sealed with nail polish and analyzed under the microscope.

6.8. λ protein phosphatase (λ -PPase) treatment

In a 50 μ l reaction 60 μ g of HeLa whole cell lysates were incubated with 400 U of λ -PPase (400 U/ μ l) in a 1x λ -PPase reaction buffer supplemented with 2 mM $MnCl_2$. To inhibit λ -PPase in some reactions, 50 mM Na_2EDTA was added. After incubation for 1 hr at 30°C, the reaction was stopped by heat inactivation at 65°C for 1hr.

6.9. Dik van Gent assay

The Dik van Gent assay was performed as described (Verkaik et al., 2002). In detail, 2 μ g of Eco47 III linearized plasmid pDVG94 were transfected into HeLa and V3 cells of 50% confluency in 6 well plates using 3 μ l Fugene 6 transfection reagent. The transfection efficiency was determined by transfection of plasmid CRU5-IRES-GFP and flow cytometry analysis after 3 days. Two days after transfection with pDVG94, plasmid DNA was recovered using a Qiagen Miniprep Kit (25 μ l elution volume). Then the region surrounding the Eco47 III site was PCR amplified using the primers pDVG94-back (5'-CTCCATTTAGC TTCCTTAGCTCCTG -3') and [γ -³²P] ATP end-labeled primer pDVG94-fwd (5'-TGCTTCCG GCTCGTATGTTGGTTGGAAT -3'). The end-labeling was performed in a 50 μ l reaction with 50 pmol primer, 50 pmol of [γ -³²P] ATP (5000 Ci/mmol) and 20 U of T4-PNK (Biolabs). Amplification was done with 1 μ l of V3 and 5 μ l of HeLa template DNA in 21 cycles of 1 min at 94°C, 1 min at 60°C and 1 min at 72°C. Afterwards the PCR product was purified using a Qiagen Qiaquick column (elution volume 25 μ l). Half of the purified PCR product was BstX I digested for 3 hr and separated along with undigested PCR product in a 6 % polyacrylamid gel in a TBE buffer system. The dried polyacrylamid gel was used to expose a phosphor screen for 24 hr which was analyzed in a phospho-Imager. The bands representing the undigested PCR product (180 bp) or cut (120 bp) and uncut (180 bp) PCR product after BstXI digestion were quantitated by phospho-imager software and compared.

6.10. Flow cytometry survival assay

100.000 cells each of various HeLa subclones were irradiated and immediately seeded in triplicates in 6-well plates. Irradiated cells were collected after 72 hr and 120 hr and undamaged cells after 96 hr. For this the supernatant, presumably containing the less viable or dead cells, the PBS wash fraction and the trypsinized adherent cells were pooled and spun down. Then they were resuspended in PBS containing 1% FBS and analyzed by flow cytometry. The protocol was slightly modified for S2-cells by plating 200.000 cells and analysis after 72 hr.

6.11. siRNA inhibition in HeLa cells

siRNA duplexes were synthesized by Dharmacon. For Kub3, a mixture of five different unknown siRNAs specific for human Kub3 was purchased from Dharmacon. Transfection of HeLa with siRNA duplexes was carried out by using Oligofectamine (Invitrogen) according to manufacturer's instruction. 48 hr after initial transfection, the HeLa cells were divided into two cultures and subjected to 10 Gy irradiation or mock treatment at 72 hr. The HeLa cells were harvested 30 min after irradiation for Western blotting analysis.

6.12. DsRNA inhibition in drosophila S2 cells

a) dsRNA production

The following primers were designed to amplify 400-600 bp within the indicated exon of the target gene. All oligonucleotides were synthesized at a 100 nmol scale by Integrated DNA Technologies:

Kub3 (1); exon 1:

Fwd: 5'- GGGCGGGTGTTCCTGACTAAAGTGTGGGC -3'

Back: 5'- GGGCGGGTCTTGACATTAAATGGCGAGGC -3'

Kub3 (2); exon 1:

Fwd: 5'- GGGCGGGTGTTCCTGACTAAAGTGTGGGC -3'

Back: 5'- GGGCGGGTGCAGGAGAACATTGATCGTTTC -3'

Ku70 (1); exon 1:

Fwd: 5'- GGGCGGGTGTGGACCTGCTGTCTGGGTCCG -3'

Back: 5'- GGGCGGGTCTCCTTGCCCTCCAGATCGCTGG -3'

Ku70 (2); exon 2 (Min et al., 2004):

Fwd: 5'- GGGCGGGTGCTTCAAGCATCGATCCTCTC -3'

Back: 5'- GGGCGGGTTGGATCGTTGATGAGATTCCG -3'

Ku80; exon 5 (Min et al., 2004):

Fwd: 5'- GGGCGGGTGCCGCCGTGAAGCTGGACGCT -3'

Back: 5'- GGGCGGGTTGGCACTCGCCAGAATACAT -3'

Blm; exon 2:

Fwd: 5'- GGGCGGGTCCATTAGTTAGCAACAATCTGGC -3'

Back: 5'- GGGCGGGTGATTTCTTGAACTTTTGGCAGG -3'

Rad54; exon 2:

Fwd: 5'- GGGCGGGTGCAGGAACTGGAGCGAGAGCAAG -3'

Back: 5'- GGGCGGGTGGAGAACTGCTCGAGTGCTCGG -3'

EGFP:

Fwd: 5'- GGGCGGGTGGAGCTGGACGGCGACGTAAAC -3'

Back: 5'- GGGCGGGTGGTGTCTGCTGGTAGTGGTCG -3'

The template was genomic DNA extracted from *Drosophila melanogaster* S2-cells using a DNeasy kit (Qiagen). The primers all share the T7 promotor sequence GGGCGGGT at the 5' end as a linker for the second PCR with the primer 5'- TAATACGACTCA CTATAGGGAGACCACGGGCGGGT -3' to complete the T7 promotor. Depending on the amplified gene, the annealing temperature was 55°C for the 1st PCR and 58°C for all second PCR reactions. Amplified DNA from the 1st PCR was diluted 1:10 to serve as template for the second PCR. To concentrate DNA from the second PCR, 50 µl reactions were carried out in triplicates, pooled and purified using a Qiaquick column (Qiagen) (elution volume 30 µl). This resulted in a DNA concentration of about 1 µg/µl. For In Vitro Transcription the RiboMAX kit (Promega) was used. For a 40 µl reaction 10 µl of template DNA were diluted with 6 µl RNase free water and mixed with 12 µl rNTPs (25mM), 8 µl 5x T7 buffer and 4 µl T7-reaction mix and incubated for 4 hr at 37°C. Afterwards, template DNA was degraded by incubation with 4 U of DNase for 1 hr at 37°C. For annealing, RNA was denatured at 70°C for 5 min and cooled down at room temperature for 20 min. dsRNA was purified by RNeasy kit (Qiagen) and eluted in 80 µl of RNase free water. The dsRNA was analyzed by agarose gel electrophoresis (with 1 µl of the eluate on a 0.5% gel) and by spectroscopy at 260 nm (conversion factor: OD₂₆₀ = 1.0 equals 40 µg RNA /ml). It was stored at -20°C.

b) dsRNA application

Before dsRNA application S2 cells were grown to about 5x10⁶ cells/ml, washed with PBS and starved in serum free Schneider's Medium for 30-45 min. Afterwards, cells were counted and 0.5x10⁶ cells in 2 ml full medium were plated in 6-well plates. 30 µg of dsRNA were added to the cultures and incubated for 3-4 days without splitting.

6.13. Quantitative RT-PCR (Taqman)

Expression of drosophila Rad54, Kub3 and Act5C (isoform B) were measured using quantitative RT-PCR (Taqman). Total RNA was extracted from S2 cells which were left either untreated or were treated with dsRNAs. Then 2 µg of total RNA were reversely transcribed by Superscript II (Invitrogen) using an oligo dT primer. The synthesized cDNA was diluted 1:10 and 5µl were used in a 25 µl PCR reaction with 0.625 µl Fwd primer (20 mM), 0.625 µl, back primer (20 mM) and 0.3125 µl dual labeled probe (20 mM) together with TaqMan® One-Step RT-PCR Master Mix Reagents Kit (Applied Biosystems). PCR was performed in triplicates using the ABI PRISM® 7700 machine (Applied Biosystems). Drosophila Rad54 and Kub3 expression was normalized to the amount of expressed Act5C (isoform B).

The following PCR primers and dual-labeled probes were synthesized at 100 nmol scale (primers) or 250 nmol scale (probes) by Integrated DNA Technologies. To prevent

amplification of contaminating chromosomal DNA, the PCR primers were designed to bind to different adjacent exons as indicated.

dmAct5C (isoform B):

Fwd 5'- CAGTCATTCCTTTCAAACCGTGCGG -3' ; exon 1

Back 5'- CAGAGCAGCAACTTCTTCGTACAC -3' ; exon 2

Probe 5'- [6-FAM]-TAGCTCAGCCTCGCCACTTGCCTTTACAGTAGTTTTTCACG - [TAMRA]-3';

dmKub3:

Fwd 5'- CAAACCTGGCGCATTGCTCCTTC -3' ; exon 1

Back 5'- CTAGGGCTTTGGACTTGACGCAG -3' ; exon 2

Probe 5'- [6-FAM]-AGCGCCATGTTCCAAGGAGATGCCTCGCCATTTAATGTC - [TAMRA]-3';

dmRAD54:

Fwd 5'- AACACGAGTCGGCCGAGAAGC -3' ; exon 5

Back 5'- CCTCGGGCGGTGGCTTCATTT -3' ; exon 6

Probe 5'- [6-FAM]-CACCCGCGACGATCTGAAGGACTTGTTCATTTGATGCGAACA- [TAMRA]-3';

6.14. Bioinformatics resources

Aceview: <http://www.ncbi.nlm.nih.gov/AceView/>

BCM Search Launcher/Multiple Sequence Alignments:

<http://searchlauncher.bcm.tmc.edu/multi-align/multi-align.html>

ExpASY - Translate tool: <http://us.expasy.org/tools/dna.html>

Flybase: <http://www.flybase.net>

NCBI home page: <http://www.ncbi.nlm.nih.gov/>

Oligonucleotide Properties Calculator: <http://www.basic.nwu.edu/biotools/oligocalc.html>

Protein size prediction tool Compute pI/Mw : http://us.expasy.org/tools/pi_tool.html

6.15. Instruments

PCR machines:	MJ research / PTC-100, PTC-200
Table top centrifuge:	Sorvall instruments / TechnoSpin R
Photometer:	Biorad / SmartSpec 3000
Microcentrifuge:	Eppendorf / 5415C
SDS-PAGE chamber:	Biorad / Miniprotean 3
Confocal microscope:	Biorad / 1024 MP/Nikon TE300 confocal
Flow cytometry:	BD / FACScalibur
Flow cytometry software:	BD / Cellquest V.1.0
Tissue culture incubator:	Heraeus / B5060-EK-CO ₂ (5% and 10% CO ₂)
Quantitative PCR machine:	Applied Biosystems / ABI PRISM® 7700 machine

7. Acknowledgments

First, I want to thank Dr. Elisabeth Weiss and the Biology faculty of the LMU University Munich for supervising and correcting my thesis and making this all possible.

I also want to thank all the great members of the Wabl lab: Cliff for being such a good friend and such a superb source of ideas and advice over the years (C-dub out); Sandra for the awesome spirit and work she showed on her way to a high-speed swedish wedding. Christoph for being part of the “dodge couple” and all the laughs we had, Ryan for all the great sailing trips, Desiree for watering my flower, Tobias for advice on “good deals”, Freia for upholding the ideals of the socialistic worker, Claudia for liking franconians and Jamie and Joachim for fresh ideas.

Because collaboration is such an integral part of science I would like to thank my collaborators and scientific friends: David and Benjamin Chen for their great work on PP5, Hans-Martin Jaeck for support in all kinds of situations and all members of the Ganem lab for their help and, more importantly, for their “Jaegermeister” party spirit.

For funding my thesis I would like to thank the Boehringer-Ingelheim foundation.

Undoubtedly the best thing that happened to me in San Francisco (sorry, Today) was to run into my beloved Erin. Over the last two years she was always there for me and I will do my best to return the favor during her thesis. LU

For his support and friendship I would like to thank Bob McCormick, who made the Hillpoint Guest House a home for many young scientists.

My dear sister Elke always managed to provide me (apart from moral support) with the right equipment when I needed it most. Therefore thanks very much for the Polo, the laser printers and the apartment !

Thanks to my parents and my brother Michael I always had a sanctuary in Spalt to resort to when I was back home. I am also very grateful for the support of my parents over the course of my studies and I hope they will enjoy London just like San Francisco. Thanks also to my uncle Hans-Joerg, who was always a good host when I was in Munich.

I would like to thank my friends Armin, Carsten, Florian und Jens which I left behind in Germany but who suffered to come over to visit me and distract me from science.

Last but not least, I would like to thank Matthias Wabl for altogether fantastic five years in his lab. He was always an amazing mentor with the greatest interest in teaching and educating his students. Although I can not hope to step in his footsteps, I will be inspired by his enthusiasm and his ability to focus on the important things.

8. Literature

- Abraham, R. T. (2001). Cell cycle checkpoint signaling through the ATM and ATR kinases. *Genes Dev* 15, 2177-2196.
- Adams, M. D., McVey, M., and Sekelsky, J. J. (2003). *Drosophila* BLM in double-strand break repair by synthesis-dependent strand annealing. *Science* 299, 265-267.
- Adams, M. D., and Sekelsky, J. J. (2002). From sequence to phenotype: reverse genetics in *Drosophila melanogaster*. *Nat Rev Genet* 3, 189-198.
- Ali, A., Zhang, J., Bao, S., Liu, I., Otterness, D., Dean, N. M., Abraham, R. T., and Wang, X. F. (2004). Requirement of protein phosphatase 5 in DNA-damage-induced ATM activation. *Genes Dev* 18, 249-254.
- Allen, C., Kurimasa, A., Brenneman, M. A., Chen, D. J., and Nickoloff, J. A. (2002). DNA-dependent protein kinase suppresses double-strand break-induced and spontaneous homologous recombination. *Proc Natl Acad Sci U S A* 99, 3758-3763.
- Andreeva, A. V., and Kutuzov, M. A. (1999). RdgC/PP5-related phosphatases: novel components in signal transduction. *Cell Signal* 11, 555-562.
- Bakkenist, C. J., and Kastan, M. B. (2003). DNA damage activates ATM through intermolecular autophosphorylation and dimer dissociation. *Nature* 421, 499-506.
- Bakkenist, C. J., and Kastan, M. B. (2004). Phosphatases join kinases in DNA-damage response pathways. *Trends Cell Biol* 14, 339-341.
- Baumann, P., Benson, F. E., and West, S. C. (1996). Human Rad51 protein promotes ATP-dependent homologous pairing and strand transfer reactions in vitro. *Cell* 87, 757-766.
- Beall, E. L., Admon, A., and Rio, D. C. (1994). A *Drosophila* protein homologous to the human p70 Ku autoimmune antigen interacts with the P transposable element inverted repeats. *Proc Natl Acad Sci U S A* 91, 12681-12685.
- Benson, F. E., Baumann, P., and West, S. C. (1998). Synergistic actions of Rad51 and Rad52 in recombination and DNA repair. *Nature* 391, 401-404.

Blunt, T., Finnie, N. J., Taccioli, G. E., Smith, G. C., Demengeot, J., Gottlieb, T. M., Mizuta, R., Varghese, A. J., Alt, F. W., Jeggo, P. A., and et al. (1995). Defective DNA-dependent protein kinase activity is linked to V(D)J recombination and DNA repair defects associated with the murine scid mutation. *Cell* 80, 813-823.

Bode, W., Gomis-Ruth, F. X., and Stockler, W. (1993). Astacins, serralytins, snake venom and matrix metalloproteinases exhibit identical zinc-binding environments (HEXXHXXGXXH and Met-turn) and topologies and should be grouped into a common family, the 'metzincins'. *FEBS Lett* 331, 134-140.

Borthwick, E. B., Zeke, T., Prescott, A. R., and Cohen, P. T. (2001). Nuclear localization of protein phosphatase 5 is dependent on the carboxy-terminal region. *FEBS Lett* 491, 279-284.

Boskovic, J., Rivera-Calzada, A., Maman, J. D., Chacon, P., Willison, K. R., Pearl, L. H., and Llorca, O. (2003). Visualization of DNA-induced conformational changes in the DNA repair kinase DNA-PKcs. *Embo J* 22, 5875-5882.

Bosma, G. C., Kim, J., Urich, T., Fath, D. M., Cotticelli, M. G., Ruetsch, N. R., Radic, M. Z., and Bosma, M. J. (2002). DNA-dependent protein kinase activity is not required for immunoglobulin class switching. *J Exp Med* 196, 1483-1495.

Boyd, J. B., and Harris, P. V. (1981). Mutants partially defective in excision repair at five autosomal loci in *Drosophila melanogaster*. *Chromosoma* 82, 249-257.

Brandt, R., Hundelt, M., and Shahani, N. (2005). Tau alteration and neuronal degeneration in tauopathies: mechanisms and models. *Biochim Biophys Acta* 1739, 331-354.

Bromann, P. A., Korkaya, H., and Courtneidge, S. A. (2004). The interplay between Src family kinases and receptor tyrosine kinases. *Oncogene* 23, 7957-7968.

Burrows, P. D., Beck, G. B., and Wabl, M. R. (1981). Expression of mu and gamma immunoglobulin heavy chains in different cells of a cloned mouse lymphoid line. *Proc Natl Acad Sci U S A* 78, 564-568.

Casellas, R., Nussenzweig, A., Wuerffel, R., Pelanda, R., Reichlin, A., Suh, H., Qin, X. F., Besmer, E., Kenter, A., Rajewsky, K., and Nussenzweig, M. C. (1998). Ku80 is required for immunoglobulin isotype switching. *Embo J* 17, 2404-2411.

Chan, D. W., Chen, B. P., Prithivirajasingh, S., Kurimasa, A., Story, M. D., Qin, J., and Chen, D. J. (2002). Autophosphorylation of the DNA-dependent protein kinase catalytic subunit is required for rejoining of DNA double-strand breaks. *Genes Dev* 16, 2333-2338.

Chappell, C., Hanakahi, L. A., Karimi-Busheri, F., Weinfeld, M., and West, S. C. (2002). Involvement of human polynucleotide kinase in double-strand break repair by non-homologous end joining. *Embo J* 21, 2827-2832.

Chen, B. P., Chan, D. W., Kobayashi, J., Burma, S., Asaithamby, A., Morotomi-Yano, K., Botvinick, E., Qin, J., and Chen, D. J. (2005). Cell cycle dependence of DNA-PK phosphorylation in response to DNA double strand breaks. *J Biol Chem*.

Chen, H., Fre, S., Slepnev, V. I., Capua, M. R., Takei, K., Butler, M. H., Di Fiore, P. P., and De Camilli, P. (1998a). Epsin is an EH-domain-binding protein implicated in clathrin-mediated endocytosis. *Nature* 394, 793-797.

Chen, J., Silver, D. P., Walpita, D., Cantor, S. B., Gazdar, A. F., Tomlinson, G., Couch, F. J., Weber, B. L., Ashley, T., Livingston, D. M., and Scully, R. (1998b). Stable interaction between the products of the BRCA1 and BRCA2 tumor suppressor genes in mitotic and meiotic cells. *Mol Cell* 2, 317-328.

Chen, M. S., Silverstein, A. M., Pratt, W. B., and Chinkers, M. (1996). The tetratricopeptide repeat domain of protein phosphatase 5 mediates binding to glucocorticoid receptor heterocomplexes and acts as a dominant negative mutant. *J Biol Chem* 271, 32315-32320.

Chen, M. X., McPartlin, A. E., Brown, L., Chen, Y. H., Barker, H. M., and Cohen, P. T. (1994). A novel human protein serine/threonine phosphatase, which possesses four tetratricopeptide repeat motifs and localizes to the nucleus. *Embo J* 13, 4278-4290.

Chinkers, M. (2001). Protein phosphatase 5 in signal transduction. *Trends Endocrinol Metab* 12, 28-32.

- Clemens, J. C., Worby, C. A., Simonson-Leff, N., Muda, M., Maehama, T., Hemmings, B. A., and Dixon, J. E. (2000). Use of double-stranded RNA interference in *Drosophila* cell lines to dissect signal transduction pathways. *Proc Natl Acad Sci U S A* 97, 6499-6503.
- Dalziel, R. G., Mendelson, S. C., and Quinn, J. P. (1992). The nuclear autoimmune antigen Ku is also present on the cell surface. *Autoimmunity* 13, 265-267.
- Das, A. K., Cohen, P. W., and Barford, D. (1998). The structure of the tetratricopeptide repeats of protein phosphatase 5: implications for TPR-mediated protein-protein interactions. *Embo J* 17, 1192-1199.
- Ding, Q., Reddy, Y. V., Wang, W., Woods, T., Douglas, P., Ramsden, D. A., Lees-Miller, S. P., and Meek, K. (2003). Autophosphorylation of the catalytic subunit of the DNA-dependent protein kinase is required for efficient end processing during DNA double-strand break repair. *Mol Cell Biol* 23, 5836-5848.
- Dore, A. S., Drake, A. C., Brewerton, S. C., and Blundell, T. L. (2004). Identification of DNA-PK in the arthropods. Evidence for the ancient ancestry of vertebrate non-homologous end-joining. *DNA Repair (Amst)* 3, 33-41.
- Douglas, P., Moorhead, G. B., Ye, R., and Lees-Miller, S. P. (2001). Protein phosphatases regulate DNA-dependent protein kinase activity. *J Biol Chem* 276, 18992-18998.
- Douglas, P., Sapkota, G. P., Morrice, N., Yu, Y., Goodarzi, A. A., Merkle, D., Meek, K., Alessi, D. R., and Lees-Miller, S. P. (2002). Identification of in vitro and in vivo phosphorylation sites in the catalytic subunit of the DNA-dependent protein kinase. *Biochem J* 368, 243-251.
- Downs, J. A., and Jackson, S. P. (2004). A means to a DNA end: the many roles of Ku. *Nat Rev Mol Cell Biol* 5, 367-378.
- Durocher, D., and Jackson, S. P. (2001). DNA-PK, ATM and ATR as sensors of DNA damage: variations on a theme? *Curr Opin Cell Biol* 13, 225-231.
- Errami, A., Smider, V., Rathmell, W. K., He, D. M., Hendrickson, E. A., Zdzienicka, M. Z., and Chu, G. (1996). Ku86 defines the genetic defect and restores X-ray resistance

and V(D)J recombination to complementation group 5 hamster cell mutants. *Mol Cell Biol* 16, 1519-1526.

Esposito, D., and Scocca, J. J. (1997). The integrase family of tyrosine recombinases: evolution of a conserved active site domain. *Nucleic Acids Res* 25, 3605-3614.

Essers, J., Hendriks, R. W., Swagemakers, S. M., Troelstra, C., de Wit, J., Bootsma, D., Hoeijmakers, J. H., and Kanaar, R. (1997). Disruption of mouse RAD54 reduces ionizing radiation resistance and homologous recombination. *Cell* 89, 195-204.

Feldmann, E., Schmiemann, V., Goedecke, W., Reichenberger, S., and Pfeiffer, P. (2000). DNA double-strand break repair in cell-free extracts from Ku80-deficient cells: implications for Ku serving as an alignment factor in non-homologous DNA end joining. *Nucleic Acids Res* 28, 2585-2596.

Fernandez-Capetillo, O., Lee, A., Nussenzweig, M., and Nussenzweig, A. (2004). H2AX: the histone guardian of the genome. *DNA Repair (Amst)* 3, 959-967.

Fischer, U., Hemmer, D., Heckel, D., Michel, A., Feiden, W., Steudel, W. I., Hulsebos, T., and Meese, E. (2001). KUB3 amplification and overexpression in human gliomas. *Glia* 36, 1-10.

Frank, K. M., Sekiguchi, J. M., Seidl, K. J., Swat, W., Rathbun, G. A., Cheng, H. L., Davidson, L., Kangaloo, L., and Alt, F. W. (1998). Late embryonic lethality and impaired V(D)J recombination in mice lacking DNA ligase IV. *Nature* 396, 173-177.

Fulop, G. M., and Phillips, R. A. (1990). The scid mutation in mice causes a general defect in DNA repair. *Nature* 347, 479-482.

Garcia-Higuera, I., Taniguchi, T., Ganesan, S., Meyn, M. S., Timmers, C., Hejna, J., Grompe, M., and D'Andrea, A. D. (2001). Interaction of the Fanconi anemia proteins and BRCA1 in a common pathway. *Mol Cell* 7, 249-262.

Goodarzi, A. A., Jonnalagadda, J. C., Douglas, P., Young, D., Ye, R., Moorhead, G. B., Lees-Miller, S. P., and Khanna, K. K. (2004). Autophosphorylation of ataxia-telangiectasia mutated is regulated by protein phosphatase 2A. *Embo J* 23, 4451-4461.

Literature

Gottlich, B., Reichenberger, S., Feldmann, E., and Pfeiffer, P. (1998). Rejoining of DNA double-strand breaks in vitro by single-strand annealing. *Eur J Biochem* 258, 387-395.

Graeme C.M. Smith, a. S. P. J. (1999). The DNA-dependent protein kinase. *Genes & Development Vol. 13*, pp. 916-934.

Grawunder, U., Wilm, M., Wu, X., Kulesza, P., Wilson, T. E., Mann, M., and Lieber, M. R. (1997). Activity of DNA ligase IV stimulated by complex formation with XRCC4 protein in mammalian cells. *Nature* 388, 492-495.

Grawunder, U., Zimmer, D., Fugmann, S., Schwarz, K., and Lieber, M. R. (1998). DNA ligase IV is essential for V(D)J recombination and DNA double-strand break repair in human precursor lymphocytes. *Mol Cell* 2, 477-484.

Gu, Y., Seidl, K. J., Rathbun, G. A., Zhu, C., Manis, J. P., van der Stoep, N., Davidson, L., Cheng, H. L., Sekiguchi, J. M., Frank, K., *et al.* (1997). Growth retardation and leaky SCID phenotype of Ku70-deficient mice. *Immunity* 7, 653-665.

Gu, Y., Sekiguchi, J., Gao, Y., Dikkes, P., Frank, K., Ferguson, D., Hasty, P., Chun, J., and Alt, F. W. (2000). Defective embryonic neurogenesis in Ku-deficient but not DNA-dependent protein kinase catalytic subunit-deficient mice. *Proc Natl Acad Sci U S A* 97, 2668-2673.

Guan, J., DiBiase, S., and Iliakis, G. (2000). The catalytic subunit DNA-dependent protein kinase (DNA-PKcs) facilitates recovery from radiation-induced inhibition of DNA replication. *Nucleic Acids Res* 28, 1183-1192.

Hooper, N. M. (1994). Families of zinc metalloproteases. *FEBS Lett* 354, 1-6.

Ivanov, E. L., Sugawara, N., Fishman-Lobell, J., and Haber, J. E. (1996). Genetic requirements for the single-strand annealing pathway of double-strand break repair in *Saccharomyces cerevisiae*. *Genetics* 142, 693-704.

Junop, M. S., Modesti, M., Guarne, A., Ghirlando, R., Gellert, M., and Yang, W. (2000). Crystal structure of the Xrcc4 DNA repair protein and implications for end joining. *Embo J* 19, 5962-5970.

Literature

- Kabotyanski, E. B., Gomelsky, L., Han, J. O., Stamato, T. D., and Roth, D. B. (1998). Double-strand break repair in Ku86- and XRCC4-deficient cells. *Nucleic Acids Res* *26*, 5333-5342.
- Kastan, M. B., and Lim, D. S. (2000). The many substrates and functions of ATM. *Nat Rev Mol Cell Biol* *1*, 179-186.
- Kasten, U., Borgmann, K., Burgmann, P., Li, G., and Dikomey, E. (1999). Overexpression of human Ku70/Ku80 in rat cells resulting in reduced DSB repair capacity with appropriate increase in cell radiosensitivity but with no effect on cell recovery. *Radiat Res* *151*, 532-539.
- Kooistra, R., Pastink, A., Zonneveld, J. B., Lohman, P. H., and Eeken, J. C. (1999). The *Drosophila melanogaster* DmRAD54 gene plays a crucial role in double-strand break repair after P-element excision and acts synergistically with Ku70 in the repair of X-ray damage. *Mol Cell Biol* *19*, 6269-6275.
- Kooistra, R., Vreeken, K., Zonneveld, J. B., de Jong, A., Eeken, J. C., Osgood, C. J., Buerstedde, J. M., Lohman, P. H., and Pastink, A. (1997). The *Drosophila melanogaster* RAD54 homolog, DmRAD54, is involved in the repair of radiation damage and recombination. *Mol Cell Biol* *17*, 6097-6104.
- Kurimasa, A., Kumano, S., Boubnov, N. V., Story, M. D., Tung, C. S., Peterson, S. R., and Chen, D. J. (1999). Requirement for the kinase activity of human DNA-dependent protein kinase catalytic subunit in DNA strand break rejoining. *Mol Cell Biol* *19*, 3877-3884.
- Kusano, K., Johnson-Schlitz, D. M., and Engels, W. R. (2001). Sterility of *Drosophila* with mutations in the Bloom syndrome gene--complementation by Ku70. *Science* *291*, 2600-2602.
- Lees-Miller, S. P., Chen, Y. R., and Anderson, C. W. (1990). Human cells contain a DNA-activated protein kinase that phosphorylates simian virus 40 T antigen, mouse p53, and the human Ku autoantigen. *Mol Cell Biol* *10*, 6472-6481.
- Li, B., and Comai, L. (2002). Displacement of DNA-PKcs from DNA ends by the Werner syndrome protein. *Nucleic Acids Res* *30*, 3653-3661.

Li, J., and Stern, D. F. (2005). Regulation of CHK2 by DNA-dependent Protein Kinase. *J Biol Chem* 280, 12041-12050.

Lieber, M. R., Hesse, J. E., Lewis, S., Bosma, G. C., Rosenberg, N., Mizuuchi, K., Bosma, M. J., and Gellert, M. (1988). The defect in murine severe combined immune deficiency: joining of signal sequences but not coding segments in V(D)J recombination. *Cell* 55, 7-16.

Lieber, M. R., Ma, Y., Pannicke, U., and Schwarz, K. (2003). Mechanism and regulation of human non-homologous DNA end-joining. *Nat Rev Mol Cell Biol* 4, 712-720.

Lieber, M. R., Ma, Y., Pannicke, U., and Schwarz, K. (2004). The mechanism of vertebrate nonhomologous DNA end joining and its role in V(D)J recombination. *DNA Repair (Amst)* 3, 817-826.

Lin, F. L., Sperle, K., and Sternberg, N. (1984). Model for homologous recombination during transfer of DNA into mouse L cells: role for DNA ends in the recombination process. *Mol Cell Biol* 4, 1020-1034.

Liu, F., Zaidi, T., Iqbal, K., Grundke-Iqbal, I., and Gong, C. X. (2002). Aberrant glycosylation modulates phosphorylation of tau by protein kinase A and dephosphorylation of tau by protein phosphatase 2A and 5. *Neuroscience* 115, 829-837.

Liu, M., and Grigoriev, A. (2004). Protein domains correlate strongly with exons in multiple eukaryotic genomes--evidence of exon shuffling? *Trends Genet* 20, 399-403.

Liu, Y., Masson, J. Y., Shah, R., O'Regan, P., and West, S. C. (2004). RAD51C is required for Holliday junction processing in mammalian cells. *Science* 303, 243-246.

Lubert, E. J., Hong, Y., and Sarge, K. D. (2001). Interaction between protein phosphatase 5 and the A subunit of protein phosphatase 2A: evidence for a heterotrimeric form of protein phosphatase 5. *J Biol Chem* 276, 38582-38587.

Lucero, H., Gae, D., and Taccioli, G. E. (2003). Novel localization of the DNA-PK complex in lipid rafts: a putative role in the signal transduction pathway of the ionizing radiation response. *J Biol Chem* 278, 22136-22143.

Ma, Y., Pannicke, U., Schwarz, K., and Lieber, M. R. (2002). Hairpin opening and overhang processing by an Artemis/DNA-dependent protein kinase complex in nonhomologous end joining and V(D)J recombination. *Cell* 108, 781-794.

Mahajan, K. N., Nick McElhinny, S. A., Mitchell, B. S., and Ramsden, D. A. (2002). Association of DNA polymerase mu (pol mu) with Ku and ligase IV: role for pol mu in end-joining double-strand break repair. *Mol Cell Biol* 22, 5194-5202.

Manis, J. P., Dudley, D., Kaylor, L., and Alt, F. W. (2002). IgH class switch recombination to IgG1 in DNA-PKcs-deficient B cells. *Immunity* 16, 607-617.

Manis, J. P., Gu, Y., Lansford, R., Sonoda, E., Ferrini, R., Davidson, L., Rajewsky, K., and Alt, F. W. (1998). Ku70 is required for late B cell development and immunoglobulin heavy chain class switching. *J Exp Med* 187, 2081-2089.

Mazumder, S., Gong, B., Chen, Q., Drazba, J. A., Buchsbaum, J. C., and Almasan, A. (2002). Proteolytic cleavage of cyclin E leads to inactivation of associated kinase activity and amplification of apoptosis in hematopoietic cells. *Mol Cell Biol* 22, 2398-2409.

McBlane, J. F., van Gent, D. C., Ramsden, D. A., Romeo, C., Cuomo, C. A., Gellert, M., and Oettinger, M. A. (1995). Cleavage at a V(D)J recombination signal requires only RAG1 and RAG2 proteins and occurs in two steps. *Cell* 83, 387-395.

McVey, M., Adams, M., Staeva-Vieira, E., and Sekelsky, J. J. (2004a). Evidence for multiple cycles of strand invasion during repair of double-strand gaps in *Drosophila*. *Genetics* 167, 699-705.

McVey, M., Larocque, J. R., Adams, M. D., and Sekelsky, J. J. (2004b). Formation of deletions during double-strand break repair in *Drosophila* DmBlm mutants occurs after strand invasion. *Proc Natl Acad Sci U S A* 101, 15694-15699.

Merkle, D., Douglas, P., Moorhead, G. B., Leonenko, Z., Yu, Y., Cramb, D., Bazett-Jones, D. P., and Lees-Miller, S. P. (2002). The DNA-dependent protein kinase interacts with DNA to form a protein-DNA complex that is disrupted by phosphorylation. *Biochemistry* 41, 12706-12714.

Mimori, T., and Hardin, J. A. (1986). Mechanism of interaction between Ku protein and DNA. *J Biol Chem* 261, 10375-10379.

Min, B., Weinert, B. T., and Rio, D. C. (2004). Interplay between *Drosophila* Bloom's syndrome helicase and Ku autoantigen during nonhomologous end joining repair of P element-induced DNA breaks. *Proc Natl Acad Sci U S A* 101, 8906-8911.

Monferran, S., Muller, C., Mourey, L., Frit, P., and Salles, B. (2004a). The Membrane-associated form of the DNA repair protein Ku is involved in cell adhesion to fibronectin. *J Mol Biol* 337, 503-511.

Monferran, S., Paupert, J., Dauvillier, S., Salles, B., and Muller, C. (2004b). The membrane form of the DNA repair protein Ku interacts at the cell surface with metalloproteinase 9. *Embo J* 23, 3758-3768.

Morita, K., Saitoh, M., Tobiume, K., Matsuura, H., Enomoto, S., Nishitoh, H., and Ichijo, H. (2001). Negative feedback regulation of ASK1 by protein phosphatase 5 (PP5) in response to oxidative stress. *Embo J* 20, 6028-6036.

Nassif, N., Penney, J., Pal, S., Engels, W. R., and Gloor, G. B. (1994). Efficient copying of nonhomologous sequences from ectopic sites via P-element-induced gap repair. *Mol Cell Biol* 14, 1613-1625.

Noordzij, J. G., Verkaik, N. S., van der Burg, M., van Veelen, L. R., de Bruin-Versteeg, S., Wiegant, W., Vossen, J. M., Weemaes, C. M., de Groot, R., Zdzienicka, M. Z., *et al.* (2003). Radiosensitive SCID patients with Artemis gene mutations show a complete B-cell differentiation arrest at the pre-B-cell receptor checkpoint in bone marrow. *Blood* 101, 1446-1452.

Nussenzweig, A., Chen, C., da Costa Soares, V., Sanchez, M., Sokol, K., Nussenzweig, M. C., and Li, G. C. (1996). Requirement for Ku80 in growth and immunoglobulin V(D)J recombination. *Nature* 382, 551-555.

O'Driscoll, M., Gennery, A. R., Seidel, J., Concannon, P., and Jeggo, P. A. (2004). An overview of three new disorders associated with genetic instability: LIG4 syndrome, RS-SCID and ATR-Seckel syndrome. *DNA Repair (Amst)* 3, 1227-1235.

Ollendorff, V., and Donoghue, D. J. (1997). The serine/threonine phosphatase PP5 interacts with CDC16 and CDC27, two tetratricopeptide repeat-containing subunits of the anaphase-promoting complex. *J Biol Chem* 272, 32011-32018.

Pan-Hammarstrom, Q., Jones, A. M., Lahdesmaki, A., Zhou, W., Gatti, R. A., Hammarstrom, L., Gennery, A. R., and Ehrenstein, M. R. (2005). Impact of DNA ligase IV on nonhomologous end joining pathways during class switch recombination in human cells. *J Exp Med* 201, 189-194.

Paques, F., and Haber, J. E. (1999). Multiple pathways of recombination induced by double-strand breaks in *Saccharomyces cerevisiae*. *Microbiol Mol Biol Rev* 63, 349-404.

Petukhova, G., Van Komen, S., Vergano, S., Klein, H., and Sung, P. (1999). Yeast Rad54 promotes Rad51-dependent homologous DNA pairing via ATP hydrolysis-driven change in DNA double helix conformation. *J Biol Chem* 274, 29453-29462.

Pospiech, H., Rytönen, A. K., and Syväoja, J. E. (2001). The role of DNA polymerase activity in human non-homologous end joining. *Nucleic Acids Res* 29, 3277-3288.

Preston, C. R., Engels, W., and Flores, C. (2002). Efficient repair of DNA breaks in *Drosophila*: evidence for single-strand annealing and competition with other repair pathways. *Genetics* 161, 711-720.

Raiborg, C., Bache, K. G., Mehlum, A., Stang, E., and Stenmark, H. (2001). Hrs recruits clathrin to early endosomes. *Embo J* 20, 5008-5021.

Reddy, Y. V., Ding, Q., Lees-Miller, S. P., Meek, K., and Ramsden, D. A. (2004). Non-homologous end joining requires that the DNA-PK complex undergo an autophosphorylation-dependent rearrangement at DNA ends. *J Biol Chem* 279, 39408-39413.

Rio, D. C. (1991). Regulation of *Drosophila* P element transposition. *Trends Genet* 7, 282-287.

Rivera-Calzada, A., Maman, J. P., Spagnolo, L., Pearl, L. H., and Llorca, O. (2005). Three-dimensional structure and regulation of the DNA-dependent protein kinase catalytic subunit (DNA-PKcs). *Structure (Camb)* 13, 243-255.

Rogers, S. L., Wiedemann, U., Stuurman, N., and Vale, R. D. (2003). Molecular requirements for actin-based lamella formation in *Drosophila* S2 cells. *J Cell Biol* 162, 1079-1088.

Literature

Rooney, S., Sekiguchi, J., Zhu, C., Cheng, H. L., Manis, J., Whitlow, S., DeVido, J., Foy, D., Chaudhuri, J., Lombard, D., and Alt, F. W. (2002). Leaky Scid phenotype associated with defective V(D)J coding end processing in Artemis-deficient mice. *Mol Cell* *10*, 1379-1390.

Sawada, M., Sun, W., Hayes, P., Leskov, K., Boothman, D. A., and Matsuyama, S. (2003). Ku70 suppresses the apoptotic translocation of Bax to mitochondria. *Nat Cell Biol* *5*, 320-329.

Schatz, D. G., Oettinger, M. A., and Baltimore, D. (1989). The V(D)J recombination activating gene, RAG-1. *Cell* *59*, 1035-1048.

Schlissel, M. S. (2002). Does artemis end the hunt for the hairpin-opening activity in V(D)J recombination? *Cell* *109*, 1-4.

Schuler, W., Weiler, I. J., Schuler, A., Phillips, R. A., Rosenberg, N., Mak, T. W., Kearney, J. F., Perry, R. P., and Bosma, M. J. (1986). Rearrangement of antigen receptor genes is defective in mice with severe combined immune deficiency. *Cell* *46*, 963-972.

Scully, R., Chen, J., Plug, A., Xiao, Y., Weaver, D., Feunteun, J., Ashley, T., and Livingston, D. M. (1997). Association of BRCA1 with Rad51 in mitotic and meiotic cells. *Cell* *88*, 265-275.

Sekelsky, J. J., Brodsky, M. H., and Burtis, K. C. (2000). DNA repair in *Drosophila*: insights from the *Drosophila* genome sequence. *J Cell Biol* *150*, F31-36.

Shao, J., Hartson, S. D., and Matts, R. L. (2002). Evidence that protein phosphatase 5 functions to negatively modulate the maturation of the Hsp90-dependent heme-regulated eIF2alpha kinase. *Biochemistry* *41*, 6770-6779.

Sigismund, S., Woelk, T., Puri, C., Maspero, E., Tacchetti, C., Transidico, P., Di Fiore, P. P., and Polo, S. (2005). From the Cover: Clathrin-independent endocytosis of ubiquitinated cargos. *Proc Natl Acad Sci U S A* *102*, 2760-2765.

Smith, G. C., and Jackson, S. P. (1999). The DNA-dependent protein kinase. *Genes Dev* *13*, 916-934.

Literature

Song, Q., Lees-Miller, S. P., Kumar, S., Zhang, Z., Chan, D. W., Smith, G. C., Jackson, S. P., Alnemri, E. S., Litwack, G., Khanna, K. K., and Lavin, M. F. (1996). DNA-dependent protein kinase catalytic subunit: a target for an ICE- like protease in apoptosis. *Embo J* 15, 3238-3246.

Springman, E. B., Angleton, E. L., Birkedal-Hansen, H., and Van Wart, H. E. (1990). Multiple modes of activation of latent human fibroblast collagenase: evidence for the role of a Cys73 active-site zinc complex in latency and a "cysteine switch" mechanism for activation. *Proc Natl Acad Sci U S A* 87, 364-368.

Stiff, T., O'Driscoll, M., Rief, N., Iwabuchi, K., Lobrich, M., and Jeggo, P. A. (2004). ATM and DNA-PK function redundantly to phosphorylate H2AX after exposure to ionizing radiation. *Cancer Res* 64, 2390-2396.

Sugawara, N., Ira, G., and Haber, J. E. (2000). DNA length dependence of the single-strand annealing pathway and the role of *Saccharomyces cerevisiae* RAD59 in double-strand break repair. *Mol Cell Biol* 20, 5300-5309.

Sung, P. (1994). Catalysis of ATP-dependent homologous DNA pairing and strand exchange by yeast RAD51 protein. *Science* 265, 1241-1243.

Sung, P. (1997). Function of yeast Rad52 protein as a mediator between replication protein A and the Rad51 recombinase. *J Biol Chem* 272, 28194-28197.

Szostak, J. W., Orr-Weaver, T. L., Rothstein, R. J., and Stahl, F. W. (1983). The double-strand-break repair model for recombination. *Cell* 33, 25-35.

van den Bosch, M., Bree, R. T., and Lowndes, N. F. (2003). The MRN complex: coordinating and mediating the response to broken chromosomes. *EMBO Rep* 4, 844-849.

Van Wart, H. E., and Birkedal-Hansen, H. (1990). The cysteine switch: a principle of regulation of metalloproteinase activity with potential applicability to the entire matrix metalloproteinase gene family. *Proc Natl Acad Sci U S A* 87, 5578-5582.

Verkaik, N. S., Esveldt-van Lange, R. E., van Heemst, D., Bruggenwirth, H. T., Hoeijmakers, J. H., Zdzienicka, M. Z., and van Gent, D. C. (2002). Different types of

V(D)J recombination and end-joining defects in DNA double-strand break repair mutant mammalian cells. *Eur J Immunol* 32, 701-709.

Wagner, C. R., Mahowald, A. P., and Miller, K. G. (2002). One of the two cytoplasmic actin isoforms in *Drosophila* is essential. *Proc Natl Acad Sci U S A* 99, 8037-8042.

Walker, J. R., Corpina, R. A., and Goldberg, J. (2001). Structure of the Ku heterodimer bound to DNA and its implications for double-strand break repair. *Nature* 412, 607-614.

Wang, C. L., and Wabl, M. (2004). DNA acrobats of the Ig class switch. *J Immunol* 172, 5815-5821.

Wang, H., Perrault, A. R., Takeda, Y., Qin, W., and Iliakis, G. (2003). Biochemical evidence for Ku-independent backup pathways of NHEJ. *Nucleic Acids Res* 31, 5377-5388.

Wang, H., Zeng, Z. C., Perrault, A. R., Cheng, X., Qin, W., and Iliakis, G. (2001). Genetic evidence for the involvement of DNA ligase IV in the DNA-PK-dependent pathway of non-homologous end joining in mammalian cells. *Nucleic Acids Res* 29, 1653-1660.

Wang, Y. G., Nnakwe, C., Lane, W. S., Modesti, M., and Frank, K. M. (2004). Phosphorylation and regulation of DNA ligase IV stability by DNA-dependent protein kinase. *J Biol Chem* 279, 37282-37290.

Wechsler, T., Chen, B. P., Harper, R., Morotomi-Yano, K., Huang, B. C., Meek, K., Cleaver, J. E., Chen, D. J., and Wabl, M. (2004). DNA-PKcs function regulated specifically by protein phosphatase 5. *Proc Natl Acad Sci U S A* 101, 1247-1252.

Weinert, B. T., Min, B., and Rio, D. C. (2005). P element excision and repair by non-homologous end joining occurs in both G1 and G2 of the cell cycle. *DNA Repair (Amst)* 4, 171-181.

West, S. C. (2003). Molecular views of recombination proteins and their control. *Nat Rev Mol Cell Biol* 4, 435-445.

Xiantuo Wu, M. R. L. (1997). Interaction between DNA-dependent protein kinase and a novel protein, KIP. *Mutation Research* 385, 13-20.

Literature

Yamaguchi, Y., Katoh, H., Mori, K., and Negishi, M. (2002). Galpha(12) and Galpha(13) interact with Ser/Thr protein phosphatase type 5 and stimulate its phosphatase activity. *Curr Biol* 12, 1353-1358.

Yang, C. R., Yeh, S., Leskov, K., Odegaard, E., Hsu, H. L., Chang, C., Kinsella, T. J., Chen, D. J., and Boothman, D. A. (1999a). Isolation of Ku70-binding proteins (KUBs). *Nucleic Acids Res* 27, 2165-2174.

Yang, C. R., Yeh, S., Leskov, K., Odegaard, E., Hsu, H. L., Chang, C., Kinsella, T. J., Chen, D. J., and Boothman, D. A. (1999b). Isolation of Ku70-binding proteins (KUBs). *Nucleic Acids Res* 27, 2165-2174.

Yannone, S. M., Roy, S., Chan, D. W., Murphy, M. B., Huang, S., Campisi, J., and Chen, D. J. (2001). Werner syndrome protein is regulated and phosphorylated by DNA-dependent protein kinase. *J Biol Chem* 276, 38242-38248.

Yu, D., Khan, E., Khaleque, M. A., Lee, J., Laco, G., Kohlhagen, G., Kharbanda, S., Cheng, Y. C., Pommier, Y., and Bharti, A. (2004). Phosphorylation of DNA topoisomerase I by the c-Abl tyrosine kinase confers camptothecin sensitivity. *J Biol Chem* 279, 51851-51861.

Zhao, S., and Sancar, A. (1997). Human blue-light photoreceptor hCRY2 specifically interacts with protein serine/threonine phosphatase 5 and modulates its activity. *Photochem Photobiol* 66, 727-731.

Zhou, B. B., and Elledge, S. J. (2000). The DNA damage response: putting checkpoints in perspective. *Nature* 408, 433-439.

Zuo, Z., Dean, N. M., and Honkanen, R. E. (1998). Serine/threonine protein phosphatase type 5 acts upstream of p53 to regulate the induction of p21(WAF1/Cip1) and mediate growth arrest. *J Biol Chem* 273, 12250-12258.

Curriculum vitae

Thomas Wechsler

Personal Information

Date of birth: 13.09.1974
Place of birth: Roth, Germany

Education

- 1995 -1998 Biology at the Friedrich-Alexander University, Erlangen-Nuremberg, Germany
- 1998 - 2001 Biology at the Ludwig-Maximilians University, Munich, Germany
- 1999 Internship in the lab of Dr. Matthias Wabl, Department of Microbiology and Immunology at the University of California, San Francisco, USA
- 2000 - 2001 Diploma thesis in the lab of Dr. Matthias Wabl, Department of Microbiology and Immunology at the University of California, San Francisco, USA. The thesis was supervised by Prof. Elisabeth Weiss from the Institute of Anthropology and Human Genetics, Ludwig-Maximilians University Munich, Germany
Identification of interaction partners of the repair protein DNA-PKcs by a yeast-two-hybrid screen
- 2001 Diploma in Biology
- 2002 Visiting scientist in the lab of Dr. Stephen P. Jackson at the Wellcome Trust/Cancer Research UK Gurdon Institute of Cancer and Developmental Biology, University of Cambridge, UK
- 2001 to 2005 Ph.D. thesis in the lab of Dr. Matthias Wabl, Department of Microbiology and Immunology at the University of California, San Francisco, USA. The thesis was supervised by Prof. Elisabeth Weiss from the Institute of Anthropology and Human Genetics, Ludwig-Maximilians University Munich, Germany.
Characterization of new interaction partners of the double-strand repair protein DNA-PKcs
- Ph.D. thesis submitted: 23.05.2004
Day of oral exam: 18.08.2005

Publications

Wechsler, T (2002).
Characterization of interaction partners of the repair protein DNA-PKcs
B.I.F. FUTURA 17, 165-166.

Wechsler, T., Chen, B. P., Harper, R., Morotomi-Yano, K., Huang, B. C., Meek, K., Cleaver, J. E., Chen, D. J., and Wabl, M. (2004).
DNA-PKcs function regulated specifically by protein phosphatase 5. Proc Natl Acad Sci U S A 101, 1247-1252.

Fellowship

2002-2005 Boehringer Ingelheim Fonds Ph.D. Scholarship for Biomedical Research

Presentations as invited speaker

2001

GSF - National Research Center for Environment and Health
Munich, Germany

Identification of interaction partners of the repair protein DNA-PKcs by a yeast-two-hybrid screen

Institute for Anthropology and Human Genetics, Munich, Germany

Identification of interaction partners of the repair protein DNA-PKcs by a yeast-two-hybrid screen

2002

B.I.F. Meeting, Woods Hole, USA

Characterization of interaction partners of the repair protein DNA-PKcs

2003

Nikolaus-Fiebiger Center
Division of Molecular Immunology, Erlangen, Germany

DNA double strand break repair and cell survival

2004

B.I.F. Meeting, Woods Hole, USA

DNA-PKcs function regulated by protein phosphatase 5